DIGITAL COMPUTER ANALYSIS OF POWER SYSTEM NETWORKS

A thesis presented for the degree of
Doctor of Philosophy in Electrical Engineering
in the University of Canterbury,
Christchurch, New Zealand.

by

R. PODMORE B.E.(Hons.)

1972

ACKNOWLEDGEMENTS

I am very grateful to Prof. J.H. Andreae and Dr J.M. Undrill for jointly supervising this project. I am especially indebted to Dr Undrill; his suggestions, criticisms and practical knowledge have been invaluable.

In chapter 2 the linked-list techniques for representing networks were developed in conjunction with fellow post-graduates P.M. Cashin and M.R. Mayson. I am grateful to them for sharing their substantial contributions.

I thank the General Manager, Mr E.B. Mackenzie, and staff of the New Zealand Electricity Department for their co-operation.

The financial support of the Canterbury Frozen Meat Company and the University Grants Committee Postgraduate Scholarships is gratefully acknowledged.

Also, I thank my wife Stella for her patience and encouragement in my work.

TABLE OF CONTENTS

		Page
CHAPTER 1:	INTRODUCTION	
1.1	Brief History of Power System Network Analysis	1.1
1.2	Reasons for the Continuing Development of Network Methods	1.2
1.3	Scope of Thesis and Approach to Problem	1.4
1.4	Outline of Thesis	1.5
1.5	Computer Programs	1.7
	References	1.8
CHAPTER 2:	LINKNET - A STRUCTURE FOR COMPUTER REPRESENTATION OF NETWORKS	
2.1	Introduction	2.1
2.2	The LINKNET Structure	2.2
2.3	Illustrative Application of LINKNET to forming Network Mesh Equations	2.7
2.4	Conclusions	2.13
	References	2.14
CHAPTER 3:	AN EFFICIENT PROGRAM FOR SOLVING NETWORK EQUATIONS	
3.1	Introduction	3.1
3.2	Triangular Decomposition of the Nodal Admittance Equations	3.2
3.3	Ordering Eliminations to Preserve Sparsity	3.5
3.4	Recording the Triangularization of the Y Matrix with LINKNET	3.7
3.5	Algorithm	3.9

		Page
3.6	Program Description	3.11
	3.6.1 Storage Requirements	3.11
	3.6.2 Operation Counts	3.11
	3.6.3 Timing Example	3.12
3.7	Conclusion	3.12
	References	3.13

CHAPTER 4: GENERAL METHOD FOR UNBALANCED FAULT ANALYSIS

4.1	Introduction	4.1
4.2	Theoretical Development	4.4
4.3	Implementation	4.11
	4.3.1 Network Partitioning	4.11
	4.3.2 Calculation of Mesh Equivalents of the Unbalanced Subnetworks	4.11
	4.3.3 Solution of the Balanced Subnetwork	4.14
	4.3.4 Sequence - Phase Transformations	4.15
	4.3.5 Node-Reference to Node-Node Transformation	4.16
	4.3.6 Summary of Procedure	4.18
4.4	Computational Results	4.19
4.5	Conclusion	4.21
	References	4.22

CHAPTER 5: MODIFIED NODAL ITERATIVE LOADFLOW ALGORITHM - IMPROVEMENT IN SPEED OF CONVERGENCE

5.1	Introduction	5.1
5.2	The Proposed Modification	5.1
	5.2.1 Qualitative Description	5.1
	5.2.2 Conventional Adjustment Formula	5.2
	5.2.3 Primary and Secondary Adjustment Formulas	5.2
	5.2.4 Voltage Controlled Buses	5.5

		Page
5.2.5	Acceleration Factors	5.5
5.3	Description of the Algorithm	5.5
5.4	Evaluation of the Proposed Algorithm	5.7
5.4.1	Test Systems	5.7
5.4.2	Convergence Characteristics	5.7
5.4.3	Comparison of Solution Times	5.10
5.4.4	Comparison of Mismatches	5.12
5.5	Conclusions	5.12
	References	5.13

CHAPTER 6: MODIFIED NODAL ITERATIVE LOADFLOW ALGORITHM - IMPROVEMENT IN RELIABILITY WITH SERIES CAPACITORS

6.1	Introduction	6.1
6.2	Network Equations	6.1
6.3	An Approximate Convergence Criterion	6.2
6.4	D.C. Loadflow Studies	6.3
6.5	A.C. Loadflow Studies	6.12
6.6	Conclusions	6.16
6.7	Appendix - Derivation of Transition Elements	6.16
	References	6.21

CHAPTER 7: A SIMPLIFIED AND IMPROVED METHOD FOR CALCULATING TRANSMISSION LOSS FORMULAS

7.1	Introduction	7.1
7.2	Loss Formula Development	7.3
7.2.1	Angle and Magnitude Dependent Losses	7.4
7.2.2	The Linearized D.C. Loadflow	7.6
7.2.3	The D.C. Loadflow Loss Formula	7.7
7.2.4	Versions of D.C. Loadflow Loss Formula	7.9

		Page
7.3	Algorithm	7.10
7.4	Evaluation	7.12
	7.4.1 Test Systems	7.12
	7.4.2 Calculation of Angle and Magnitude Dependent Losses	7.13
	7.4.3 D.C. Loadflow Loss Calculations	7.15
	7.4.4 Incremental Loss Calculations	7.19
	7.4.5 Loss Formula Selection	7.24
	7.4.6 Program Performance	7.29
7.5	Conclusions	7.30
	References	7.32

CHAPTER 8: ECONOMIC POWER DISPATCH WITH LINE SECURITY LIMITS

8.1	Introduction	8.1
8.2	Problem Formulation	8.2
	8.2.1 Unit Cost Characteristics	8.3
	8.2.2 Representation of System Losses	8.5
	8.2.3 Line Security Limits	8.5
	8.2.4 Mathematical Statement of Problem	8.7
	8.2.5 Transformation of the Demand Constraint	8.8
8.3	Implementation	8.9
	8.3.1 Calculation of Line Constraints	8.9
	8.3.2 The Dispatch Program	8.11
8.4	Evaluation	8.13
	8.4.1 Test Systems	8.13
	8.4.2 Convergence	8.17
	8.4.3 Illustrative Examples	8.21
	8.4.4 Computation Requirements	8.36
	8.4.5 Further Program Developments	8.38

Page

8.5 Conclusions 8.40

8.6 Appendix - The Gradient Projection Method 8.40

8.6.1 Geometrical Problem Formulation 8.41

8.6.2 Projection of the Gradient 8.41

8.6.3 Determination of Optimum Step Length 8.43

8.6.4 Conditions for an Optimum 8.45

8.6.5 The Gradient Projection Algorithm 8.47

References 8.49

CHAPTER 9: SUMMARY AND CONCLUSIONS 9.1

C H A P T E R 1

INTRODUCTION

1.1 BRIEF HISTORY OF POWER SYSTEM NETWORK ANALYSIS

Network analysis plays a vital role in the planning, design and operation of power systems. To meet the practical requirements of the industry a number of distinct methods of power system network analysis have evolved. They include loadflow, transient stability, short circuit analysis and loss formula calculation. The methods have been developed as engineering tools and are used extensively in the analysis of a number of major power system engineering problems:

i) Planning of generation and transmission system expansion.

In this area loadflow and transient stability studies form the basis of engineering decisions which have to meet high reliability standards and make full utilization of large capital investments.

ii) Design and operation of protection systems.

Short circuit studies are used for determining interrupting capacities of circuit breakers and for co-ordinating the operation of protective relays.

iii) Maintenance of secure and economic system operation.

Loadflow studies are used to test system operating policies to ensure that equipment is operated at safe levels. To obtain maximum operating economy transmission loss formulas are used in determining the dispatch of generation.

One of the earliest computational aids to be used for power system network analysis was the D.C. calculating board developed in 1920 for analyzing short circuits[1]. In 1929 a

major advance occurred with the development of the A.C. network analyzer[2,3]. This device provided power engineers with the ability to study in detail the voltages and power flows on practical systems. In the following years A.C. network analyzers received widespread use for loadflow, transient stability, short circuit analysis and loss formula calculation. In the mid 1950's there were 50 network analyzer installations in operation in Canada and the U.S.A.[4]

Digital computers were first applied to power system problems in the late 1940's[5], but it was not until the development of larger scale computers in the mid 1950's (e.g. IBM 704) that they became economically competitive with the network analyzer. From then on, however, the digital computer because of its greater flexibility and rapid development very quickly took over the role of the network analyzer[6-10]. Now, the digital computer plays a vital part in analysis of power system networks.

The theoretical foundation of power system network analysis has been largely laid by Gabriel Kron[11]. Kron's early work into the matrix-tensor representation of networks proved ideally suited to digital computer analysis. Many network methods have been and still are developed on the basis of his pioneering work.

1.2 REASONS FOR THE CONTINUING DEVELOPMENT OF NETWORK METHODS

The early digital methods for the solution of the loadflow, transient stability, short circuit and loss formula problems were developed about the mid 1950's[6-10]. However, even though there has been a substantial increase in the power of digital computers since this time, this alone has not been able to keep

pace with the increasing demands of network analysis. Consequently, there has been a continued and widespread effort into the development of more efficient network methods. The increase in the computer demands of network analysis has been due to several factors:

i) The increase in size of power system networks. Prior to 1960 a loadflow with several hundred buses was regarded as a fairly large problem whereas a recent survey[12] showed that a number of utilities now wished to make loadflow studies on systems with more than 2000 buses.

ii) The increasing size, cost and complexity of successive power system installations requires more thorough planning and design to ensure reliability and economy. Consequently, this requires more extensive use of engineering tools such as network analysis.

iii) There has been an increasing use of network analysis in system operations in order to match the more and more stringent requirements for secure system operation. In recent years there has been a trend towards the use of loadflow for the on-line assessment of transmission security[13-15]. In these applications there is an absolute necessity for highly efficient methods of analysis. Programs must be executed on a time shared basis within budgeted time limits. Further, on-line dispatch computers typically have only moderate amounts of core memory in comparison to the off-line scientific models.

1.3 SCOPE OF THESIS AND APPROACH TO PROBLEM

This thesis contributes to the evolutionary development and improvement of the network methods which are used for power system analysis. The thesis covers a wide range of power system network analysis and presents new and improved methods for:

i) Unbalanced fault analysis

ii) Loadflow

iii) Loss coefficient calculation

iv) Recognition of transmission security constraints within economic dispatch.

The methods which are developed represent positive steps towards meeting the increasing demands for power system network analysis described in section 1.2. Computer time and storage requirements are economized but at the same time practical simplicity is maintained within each method. In particular, the developments listed under ii), iii) and iv) are especially relevant to the problem of applying on-line dispatch computers to obtaining secure and economic system operation.

The development of the improved methods has been achieved by using two underlying approaches, sometimes simultaneously:

i) An improved method is obtained by closely matching a solution technique to exploit special characteristics of the problem. For example, the highly efficient sparse programming and ordered elimination techniques were developed by Tinney and co-workers[16] on the basis of this approach.

ii) The network behaviour is approximated so that the problem is simplified computationally but without the practical end result being significantly affected. A classical and highly

practical illustration of this approach is the use of an approximate loss formula[17] for the economic dispatch of generation.

1.4 OUTLINE OF THESIS

i) Computational Techniques for Network Representation and Solution.

The work in Chapters 2 and 3 provides basic computational tools which are used for the development and study of network methods in later chapters. Chapter 2 describes LINKNET a linked-list structure for the efficient computer representation of networks (see Acknowledgements). Chapter 3 describes an efficient program for the ordered reduction and solution of network equations.

ii) General Method for Unbalanced Fault Analysis.

In Chapter 4 a piecewise method for solving networks with general types unbalanced fault (e.g. simultaneous unbalances, line open unbalances, unbalanced impedances) is developed. The network is partitioned into a main balanced network and a number of small unbalanced subnetworks. The solutions of the separate balanced and unbalanced subnetworks are obtained in terms of sequence and phase co-ordinates respectively. The solutions of the subnetworks are then combined to obtain the solution of the original unpartitioned network. The piecewise method exploits the limited size of the unbalanced subnetworks and obtains the respective advantages of sequence and phase co-ordinates simultaneously. Computational savings are gained by the sequence solution of the main balanced subnetwork and the phase solution of the small unbalanced subnetworks allows very general types of fault to be treated.

iii) Improvement in Convergence of the Nodal Iterative Loadflow.

Chapters 5 and 6 describe a modification which improves the speed and reliability of the convergence of the nodal iterative loadflow. Typically, the modification has decreased the iterations for convergence by 65% and the solution time by 40% on a New Zealand 185 bus system. The modification has also greatly improved the reliability of the nodal iterative loadflow in the presence of series branches with low or capacitive impedance; such that under these conditions convergence is almost invariably obtained. The modification can be easily included in existing nodal iterative loadflow programs with little increase in complexity or memory.

iv) Simplified and Improved Methods for Economic Dispatch.

In Chapter 7 a very simplified method for calculating transmission loss coefficients directly from network admittances is developed. The method is based upon the linearized or D.C. loadflow approximation and does not require the usual assumptions of uniform load distribution or a certain generation P/Q relationship. Test studies have shown that the method usually calculates generator penalty factors to within 1% of values calculated by A.C. loadflow. The method requires a very low computation time and introduces the possibility of updating loss coefficients according to actual network status and load condition. As an illustration, the calculation of the loss coefficients for 17 generators in the IEEE 118 Bus Test System required 23s. IBM 360/44 execution time.

In Chapter 8 a method is developed for the economic dispatch of generation with the explicit recognition of line security limits. System losses are accounted for using the

loss formula developed in Chapter 7. The D.C. loadflow is again used to formulate the line security limits as linear inequality constraints on the generator outputs. The optimization problem is efficiently solved by the method of gradient projection. The method's low computation and system-state data requirements make it well suited for on-line dispatch. The method typically requires only several times the computation time of the classical method which is unable to treat line security limits. The extra system-state data is limited to the network status and the MW flow in the constrained lines, the method does not require individual load data.

The main contributions and conclusions of the thesis are summarized in Chapter 9.

References are given at the end of each chapter since they tend to divide according to the different network methods which are considered. The references which have also occurred in previous chapters are denoted by an asterisk.

1.5 COMPUTER PROGRAMS

This thesis has required an extensive use of the digital computer for the development and evaluation of the methods which are presented. The programs have been written in Fortran IV and executed on the University of Canterbury's IBM 360/44 computer. A total computation time of 90 hours was used and this was shared between the development and evaluation of the different methods as follows:

i)	Network representation and solution	10 hours
ii)	Piecewise method for unbalanced fault analysis	19 hours
iii)	Modified nodal iterative loadflow	28 hours
iv)	D.C. loadflow loss formula method	17 hours

v) Method for economic scheduling recognizing line security constraints 16 hours

Source listings of the programs are included in a separate report[18] (obtainable from the author or the Department of Electrical Engineering). The report includes:

i) Subroutines for the solution of large sets of network equations.

ii) Program for the solution of general types of unbalanced fault.

iii) Modified nodal iterative loadflow program.

iv) Linearized D.C. loadflow program.

v) Program for the calculation of D.C. loadflow loss coefficients.

vi) Program for the economic scheduling of generation with recognition of line security limits.

REFERENCES

1. W.W. Lewis, "A New Short-Circuit Calculating Table", General Electric Rev., 1920, p.669.

2. H.L. Hazen, O.R. Schurig, M.J. Gardner, "The M.I.T. Network Analyzer. Design and Application to Power System Problems", AIEE Trans., vol. 49, 1930, pp.1102-1114.

3. H.A. Travers, W.W. Parker, "An Alternating Current Calculating Board", Electric Journal, vol. 27, 1930, pp. 266-270.

4. E.T.B. Gross, "Network Analyzer Installations in Canada and the United States", Proc. Am. Power Conf., vol.21, 1959, pp.665-669.

5. L.A. Dunstan, "Machine Computation of Power Network Performance", AIEE Trans., vol.66, 1947, pp.610-624.

6. J.B. Ward, H.W. Hale, "Digital Computer Solution of Power-Flow Problems", AIEE Trans., vol.75, pt.III, 1956, pp.398-404.

7. A.F. Glimm, G.W. Stagg, "Automatic Calculation of Load-flows", AIEE Trans., vol. 76, Pt. III, 1957, pp.817-825.

8. D.L. Johnson, J.B. Ward, "The Solution of Power System Stability Problems by Means of Digital Computers", Trans. AIEE, vol. 75, Pt.III, pp.1321-1329, 1956.

9. L.W. Coombe, D.G. Lewis, "Digital Calculation of Short-Circuit Currents in Large Complex Impedance Networks", AIEE Trans., vol.75, Pt.III, 1956, pp.1394-1397.

10. L.K. Kirchmayer, Economic Operation of Power Systems, Wiley, New York, 1958.

11. G. Kron, Tensor Analysis of Networks, Wiley, New York, 1939. Reprinted Macdonald, London, 1965.

12. H.H. Happ, C.C. Young, "Tearing Algorithms for Large-Scale Network Programs", IEEE, PAS-90, 1971, pp.2639-2649.

13. J.M. Undrill, O.J. Denison, D. Hayward, "Dispatchers Loadflow for the REMVEC Dispatch Center", Presented at IEEE Summer Power Meeting, Dallas, Texas, 1969.

14. J.M. Undrill, "Power-system Dispatch-office Automation Functions", N.Z. Eng., 1972, pp.164-170.

15. F.J. Hubert, D.R. Hayes, "A Rapid Digital Computer Solution for Power System Network Loadflow", IEEE, PAS-90, 1971, pp.934-940.

16. W.F. Tinney, J.W. Walker, "Direct Solutions of Sparse Network Equations by Optimally Ordered Triangular Factorization", IEEE Proc., vol.55, 1967, pp.1801-1809.

17. E.E. George, "Intrasystem Transmission Losses", AIEE Trans., vol.62, 1943, pp.153-158.

18. R. Podmore, "Programs for the Analysis of Power System Networks", Departmental Memorandum, Department of Electrical Engineering, University of Canterbury, 1972.

C H A P T E R 2

LINKNET - A STRUCTURE FOR COMPUTER REPRESENTATION OF NETWORKS

2.1 INTRODUCTION

In the development of any algorithm which deals with a network, the programmer must decide on how the network information should be stored in computer memory. The decision is particularly important for the analysis of the large sparse networks which occur in power system studies. Often, it will largely determine the computer memory requirements and it may also significantly affect the processing efficiency of the algorithm.

In the past a wide variety of methods has been used to store power system network information. Examples of the more common methods are, single entry line tables[1], double entry line tables[2] and compressed storage of the node connection or node admittance matrices[3]. Most of the structures have been developed for particular types of network algorithm and have a limited range of application. However, for a wide variety of network problems there are a number of common features which are desirable in a storage structure. These can be summarized as:

i) Use of a small amount of computer memory.

ii) Processing of the network information should be facilitated; e.g. the branches and nodes connected to any given node should be easily scanned.

iii) The structure should easily reflect network changes; e.g. the addition or removal of branches.

iv) The structure should be basically simple and easy to program.

The LINKNET structure (see ref. 5 and Acknowledgements) has been designed as a general purpose structure for representing networks in a computer. It incorporates each of the desirable features which are listed in a balanced manner. The structure derives its name from linked-lists[4] which it applies to obtain some of these features. The usefulness of the LINKNET structure has been demonstrated by its application in the programming of a wide variety of network algorithms. It has proved to be a valuable tool for the programming of the power system network methods which have been studied and developed in this thesis. It has also been effectively applied to other diverse problems[5] such as game playing and minimum cost path finding.

In the first part of this chapter the LINKNET structure is described along with some of the basic functions for processing the network information. The application of the LINKNET structure is then demonstrated by an example in which the mesh equations of an electric network are formed.

2.2 THE LINKNET STRUCTURE

The LINKNET structure can be implemented either at machine language level to work as a linked addressing scheme or it can be implemented in a high level language, in which case it works as a linked indexing scheme[5]. Here the LINKNET structure and the ensuing network algorithms are described so that they can be directly related to a high level language such as Fortran IV.

We assume that the nodes and branches in the network are numbered, either manually or by the computer. Typically in a power system network the nodes are numbered manually but the

branch numbering is left to the computer. The properties of the network are divided into node properties, branch properties and topological properties. The node and branch properties are stored in a fairly standard fashion. For each node or branch property a one-dimensional array is allocated and each position in the array is identified with the node or branch having the corresponding number.

The topological properties of the network are represented by specifying the connections between the nodes and the branches. Firstly, we assume that the ends of each branch are numbered as follows; ends of branch 1 are numbered 1 and 2, ends of branch 2 are numbered 3 and 4 etc. Thus, the branch end numbers may be derived from a branch number as,

$$END = f(BRANCH)$$

$$= 2.BRANCH - 1$$

and,

$$END = g(BRANCH)$$

$$= 2.BRANCH$$

Conversely, a branch number may be derived from either of its end numbers using,

$$BRANCH = h(END)$$

$$= (END + 1)/2$$

In this relationship the integer round off is used to obtain the two to one mapping between branch ends and branches. The topology of the network can now be defined by constructing a linked-list of the branch ends which are connected to each node. This is illustrated in figure 2.1. For each node we define a pointer:

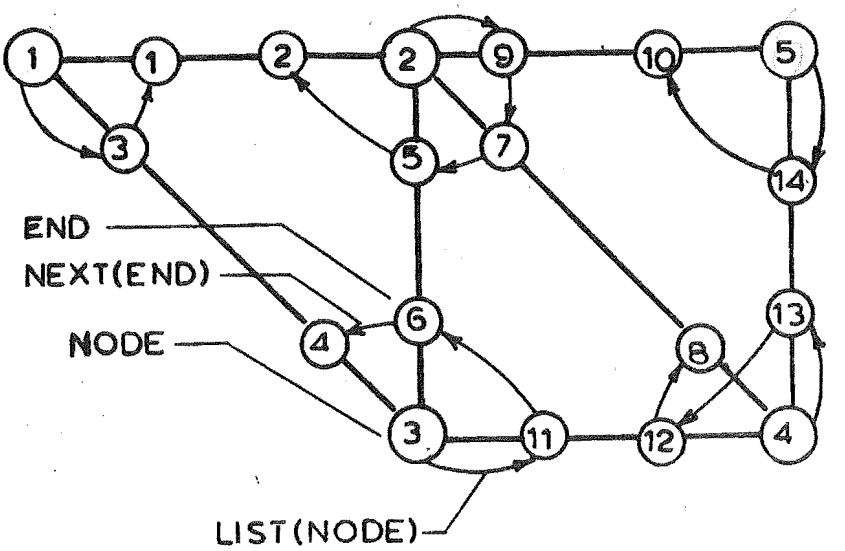

NODE	LIST(NODE)
1	3
2	9
3	11
4	13
5	14

arrows indicate the linked-list of branch ends connected to node 2

END	NEXT(END)
1	0
2	0
3	1
4	0
5	2
6	4
7	5
8	0
9	7
10	0
11	6
12	8
13	12
14	10

Figure 2.1: The LIST(NODE) and NEXT(END) Pointers

LIST(NODE) = The first branch end on the list from NODE. For each branch end we define a pointer, NEXT(END) = The next branch end on the list after END. The last branch end on the list for each node is indicated when NEXT(END) = 0. The LIST(NODE) and NEXT(END) pointers are sufficient to define the network topology uniquely. They allow the branches connected to any node to be directly obtained using the procedure:

Initialize, END = LIST(NODE)

then set, BRANCH = h(END)

and END = NEXT(END) until NEXT(END) = 0.

In network computations it is often necessary to obtain the nodes which are connected to a given node. This operation is facilitated by defining an additional pointer for each branch end:

FAR(END) = The node at the far or opposite end of the branch. The FAR(END) pointers are illustrated in figure 2.2. The nodes connected to any given node can now be obtained using the procedure:

Initialize, END = LIST(NODEA)

then set, NODEB = FAR(END)

and END = NEXT(END) until NEXT(END) = 0.

The successive values of NODEB will be the nodes which are connected to NODEA.

It may also be required to obtain the nodes at the ends of a given branch. These can be obtained as follows:

ENDA = f(BRANCH)

ENDB = g(BRANCH)

NODEA = FAR(ENDB)

NODEB = FAR(ENDA)

The pointers LIST(NODE), NEXT(END) and FAR(END) form the

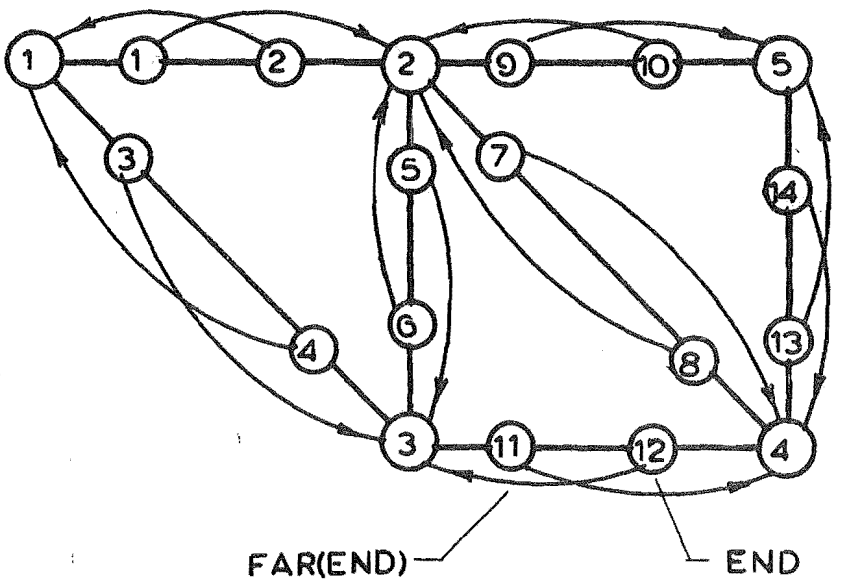

END	FAR(END)
1	2
2	1
3	3
4	1
5	3
6	2
7	4
8	2
9	5
10	2
11	4
12	3
13	5
14	4

Figure 2.2: The FAR(END) Pointers

framework of the LINKNET structure. As illustrated by the preceding examples they enable various network scanning operations to be performed very easily. Another important attribute of the LINKNET structure is the ease with which the structure can be modified to reflect the addition or removal of network branches. This is in fact one of the main features which distinguishes the LINKNET structure from more conventional structures such as double entry line tables. In figure 2.3 a flow diagram illustrates how the LINKNET structure can be built simply by adding each branch in turn to the network.

2.3 ILLUSTRATIVE APPLICATION OF LINKNET TO FORMING NETWORK MESH EQUATIONS

To illustrate the application of the LINKNET structure we consider the problem of forming the mesh equations; $V = Z\ I$, where V is a vector of mesh voltages, Z is the mesh impedance matrix and I is the vector of mesh currents. Previous methods presented in the literature[1,6,7] have generally been based upon implementation of a matrix transformation originally introduced by Kron[8]. The LINKNET structure represents the network information in such a way that the mesh equations can be automatically set up by direct inspection of the network meshes. The method is similar in principle to the manual method of mesh inspection which is commonly applied by engineers to establish the mesh equations of small uncomplicated networks directly.

The procedure of the method can be divided into three steps:

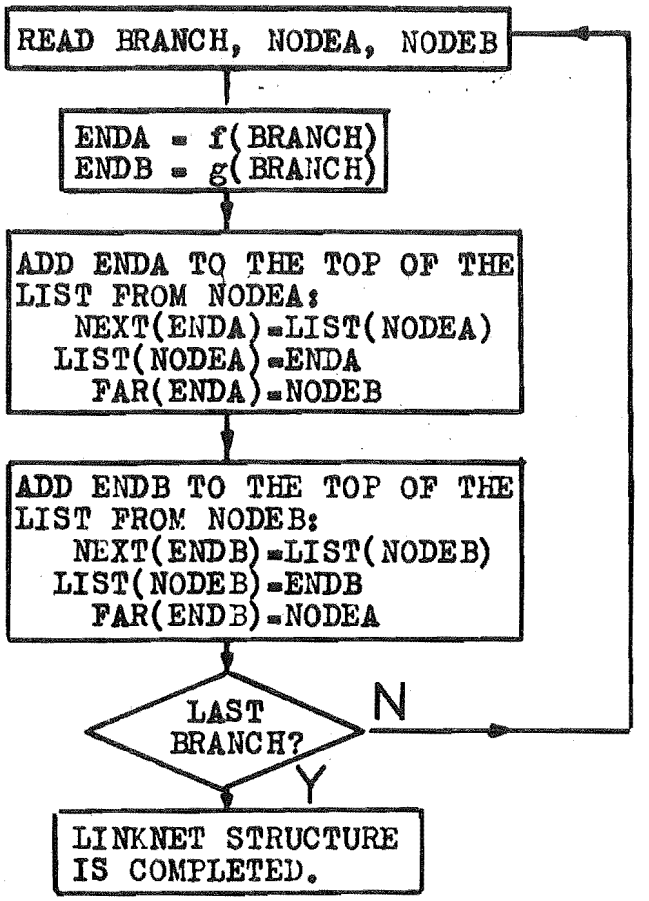

Figure 2.3: Construction of the LINKNET Structure

i) The set-up of the network information as a LINKNET structure within the computer.

ii) The specification of the network meshes within the LINKNET structure.

iii) Formation of the elements of the mesh impedance matrix and mesh voltage vector by inspection of the network meshes.

The network information is read in one branch at a time and stored within the LINKNET structure in the manner which was shown in figure 2.3.

The network meshes are selected by defining a network tree which is a subset of the network branches just sufficient in number to connect all the network nodes[1]. The branches in the tree are termed tree branches and the remaining branches are termed link branches or links. Each link branch in the network can be associated with a closed mesh. This closed mesh consists of the link branch itself and the single path of tree branches between the ends of the link branch.

To set up a tree within the LINKNET representation of the network the algorithm 'expands' out from a root node and labels the branches as 'tree branches' and the nodes at the ends of these branches as 'tree nodes'. Subsequent expansions occur from nodes that are members of the tree, and if any branch leads to a node already in the tree then this branch is labelled as a 'link branch' rather than a 'tree branch'. The algorithm terminates after all nodes have been expanded once. A flow diagram of the program to set up the tree within the LINKNET structure is shown in figure 2.4. As each node is added to the tree a special pointer TREE(NODE) is set up to indicate the tree branch which led to this node. It is in

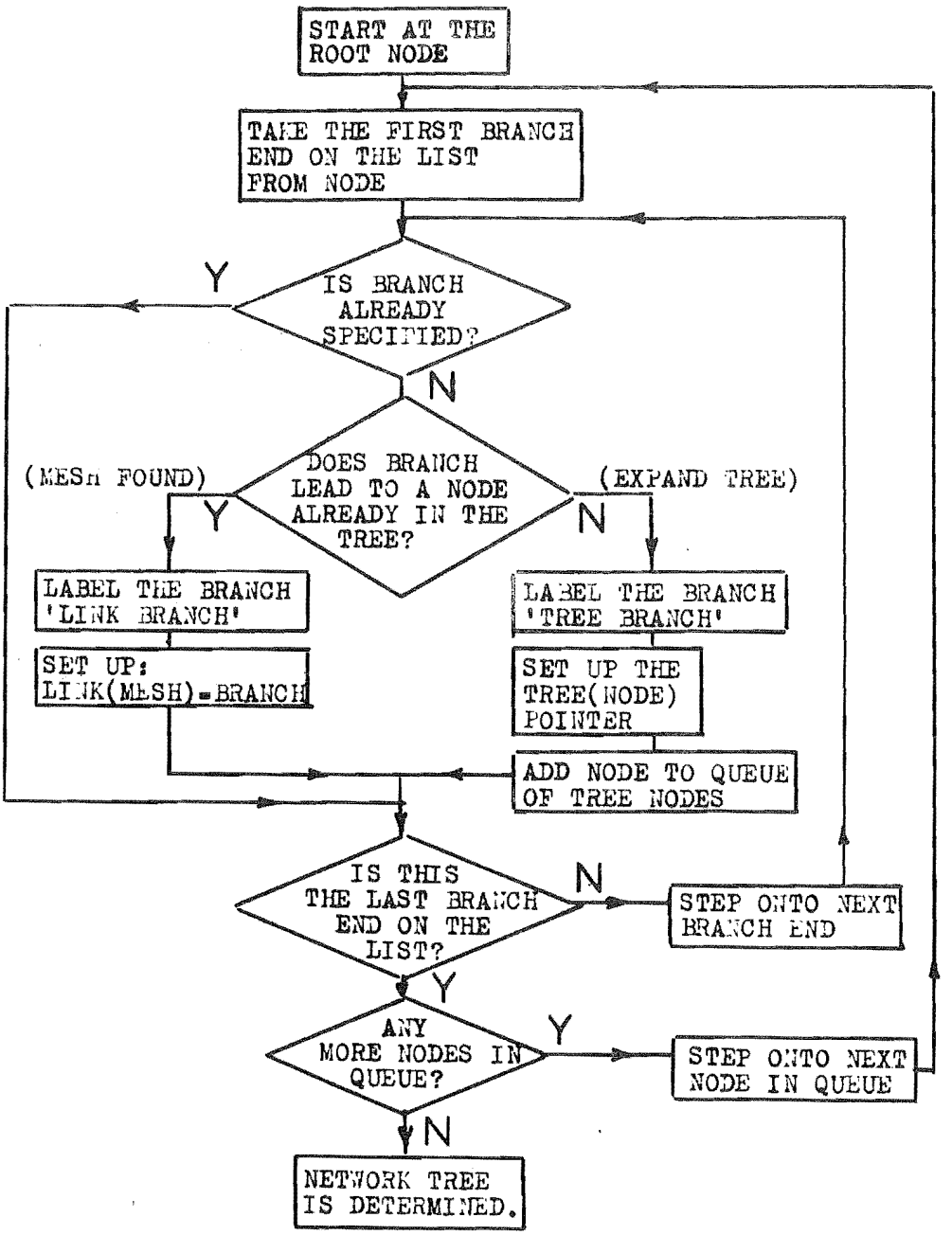

Figure 2.4: Flow Diagram of Program to Set up Network Tree

fact convenient to have the TREE(NODE) pointer indicating the branch end connecting the new tree node rather than the branch itself.

Figure 2.5 shows the resulting network tree and TREE(NODE) pointers when the algorithm is applied to a simple network. It should now be clear from this figure that the TREE(NODE) pointers allow the mesh associated with any link branch to be traced by starting with the nodes at each end of the link branch in turn and performing a series of:

```
   END = TREE(NODE)
BRANCH = h(END)
  NODE = FAR(END)
```

operations until the root node or a node common to the two paths is reached.

Now that the procedure for tracing the network meshes has been described we are in a position to describe how the mesh impedances and mesh voltages can be formed readily by inspection of the meshes.

We shall consider two meshes p and q, and describe the procedure for finding the mutual impedance between these meshes, Z_{pq}.

i) Trace through mesh p and label all the branches in this mesh.

ii) Trace through mesh q and search for labelled branches. For each labelled branch encountered: add the branch impedance to the mesh impedance if the directions of mesh p and mesh q through the branch coincide; subtract the branch impedance from the mesh impedance if the directions of mesh p and mesh q through the branch are opposite. The final value of the mesh impedance is the mutual impedance between meshes p

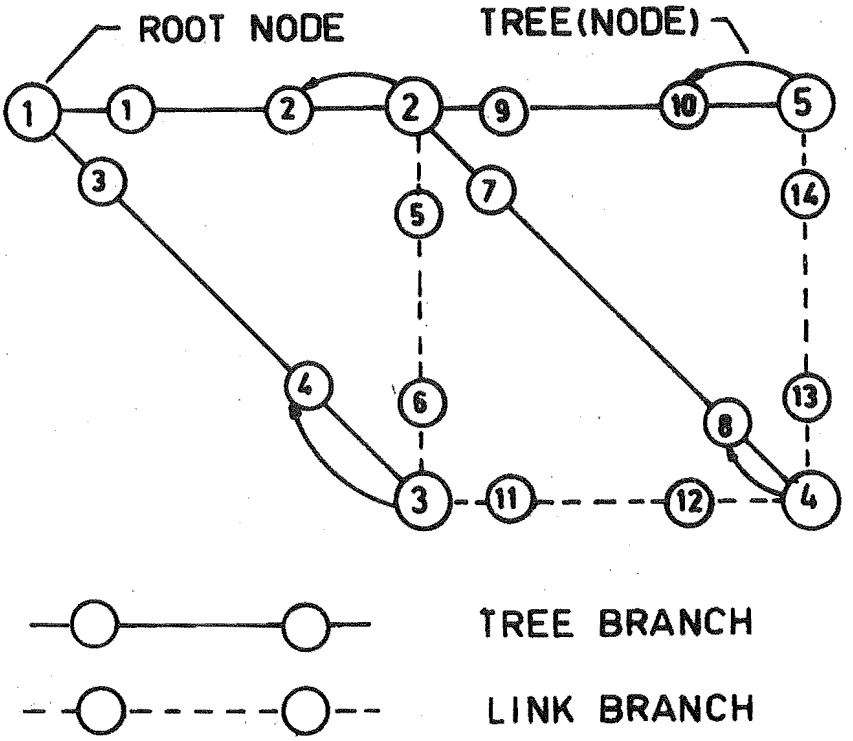

NODE	TREE(NODE
1	0
2	2
3	4
4	8
5	10

Figure 2.5: Network Tree and TREE(NODE) Pointers

and q. The voltage of mesh p is formed simply by tracing through mesh p and algebraically summing the branch voltage sources according to their direction with respect to mesh p. To enable a concise and uncomplicated description we have not considered the possibility of inductive mutual coupling between branches. This feature can be handled within the procedures which have been outlined and has been included in a test program.

2.4 CONCLUSIONS

This chapter has described LINKNET, a general purpose structure for the computer representation of networks. The application of the structure has been illustrated by forming the mesh equations of a network. The LINKNET structure has been a valuable tool in the development of the network programs which have been required for studies in this thesis. The programs which have been written using LINKNET include; a program for triangularising network matrices (section 3.4), an unbalanced short circuit program (section 4.3), a program for building bus impedance matrices (section 4.4), a nodal iterative loadflow (section 5.3), a loss coefficient program (section 7.3) and a linearized loadflow (section 7.4).

REFERENCES

1. R.T. Byerly, R.W. Long, C.W. King, "Logic for Applying Topological Methods to Electric Networks", AIEE Trans., vol. 77, pt. I, 1958, pp. 657-667.
2. H.E. Brown, "A New Y Matrix Algorithm for Transient Stability", Presented at IEEE Summer Power Meeting, Portland, Ore., 1967.
3. N. Sato, W.F. Tinney, "Techniques for Exploiting the Sparsity of the Network Admittance Matrix", IEEE Trans., Vol. 82, Pt. III, 1963, pp. 944-950.
4. D.E. Knuth, The Art of Computer Programming. Vol. 1, Fundamental Algorithms , Addison-Wesley, 1968.
5. P.M. Cashin, M.R. Mayson, R. Podmore, "LINKNET - A Structure for Computer Representation and Solution of Network Problems", Australian Computer Journal, Vol. 3, No. 3, 1971, pp. 106-113.
6. W.F. Tinney, C.M. McIntyre, "A Digital Method for Obtaining a Loop Connection Matrix", AIEE Trans., vol. 79, Pt. III, 1960, pp. 740-746.
7. H. Edelmann, "Numerical and Algebraic Generation of Mesh Impedance Matrices by Set-theoretical Intersection on a Digital Computer", IEEE, PAS 83, 1964, pp. 397-402.
* 8. G. Kron, Tensor Analysis of Networks , Wiley, New York, 1939. Reprinted Macdonald, London, 1965.

C H A P T E R 3

AN EFFICIENT PROGRAM FOR SOLVING NETWORK EQUATIONS

3.1 INTRODUCTION

The solution of simultaneous linear equations forms an intrinsic part of many problems in the analysis of power system networks. Very frequently the efficiency of an overall approach to a problem is ultimately dependent upon the method which is used for solving a large but usually sparse set of linear equations. Thus, the solution of linear network equations has received considerable attention in power system literature[1-7]. Among the methods there is one which is outstanding for its computational efficiency. It has been largely developed by Tinney and his co-workers at Bonneville Power Adminstration and is known as optimally ordered triangular factorization (OOTF)[5-7].

In this chapter the development of a program for the efficient solution of network equations is described. The program has been used as a basic tool for the network studies in this thesis. In the program the equations are solved by triangularization and the operations are ordered so that the sparsity is preserved[5-7]. A novel aspect of the program is the use of the LINKNET structure (Chapter 2) as the means of processing and storing only the non-zero terms during the matrix triangularization. For the solution of the nodal admittance equation, I = YE, the triangularization is shown to be analogous to a series of nodal eliminations. This network interpretation allows the LINKNET structure to be applied very naturally and a simple algorithm is developed. The method can,

however, be effectively applied to any sparse and symmetric set of linear equations.

3.2 TRIANGULAR DECOMPOSITION OF THE NODAL ADMITTANCE EQUATIONS

We consider the solution of the nodal admittance equations $I = Y.E$ by the well known method of triangular decomposition[8]. The equations can be expanded,

$$(1) \qquad \begin{bmatrix} I_1^{1} \\ \cdot \\ \cdot \\ \cdot \\ I_n^{1} \end{bmatrix} = \begin{bmatrix} Y_{11}^{1} & \cdot & \cdot & \cdot & Y_{1n}^{1} \\ \cdot & \cdot & \cdot & \cdot & \cdot \\ \cdot & \cdot & \cdot & \cdot & \cdot \\ \cdot & \cdot & \cdot & \cdot & \cdot \\ Y_{n1}^{1} & \cdot & \cdot & \cdot & Y_{nn}^{1} \end{bmatrix} \begin{bmatrix} E_1 \\ \cdot \\ \cdot \\ \cdot \\ E_n \end{bmatrix}$$

The superscripts indicate the order in which quantities are derived. Eliminating E_1 from all rows except the first we obtain,

$$(2) \qquad \begin{bmatrix} I_1^{1} \\ I_2^{2} \\ \cdot \\ \cdot \\ I_n^{2} \end{bmatrix} = \begin{bmatrix} Y_{11}^{1} & \cdot & \cdot & \cdot & Y_{1n}^{1} \\ 0 & Y_{22}^{2} & \cdot & \cdot & Y_{2n}^{2} \\ \cdot & \cdot & \cdot & \cdot & \cdot \\ \cdot & \cdot & \cdot & \cdot & \cdot \\ 0 & Y_{n2}^{2} & \cdot & \cdot & Y_{nn}^{2} \end{bmatrix} \begin{bmatrix} E_1 \\ \cdot \\ \cdot \\ \cdot \\ E_n \end{bmatrix}$$

where,

$$(3) \qquad I_j^{2} = I_j^{1} - Y_{j1}^{1}/Y_{11}^{1} \times I_1^{1} \qquad \text{for} \quad 1 < j \leqslant n$$

and

$$(4) \qquad Y_{jk}^{2} = Y_{jk}^{1} - Y_{j1}^{1} \times Y_{1k}^{1}/Y_{11}^{1} \qquad \text{for } 1 < j \leqslant n, \quad 1 < k \leqslant n.$$

Similarly, eliminating E_2 from all rows except the first and second we obtain,

$$(5)\qquad \begin{bmatrix} I_1^{\,1} \\ I_2^{\,2} \\ I_3^{\,3} \\ \vdots \\ I_n^{\,n} \end{bmatrix} = \begin{bmatrix} Y_{11}^{\,1} & Y_{12}^{\,1} & \cdots & Y_{1n}^{\,1} \\ 0 & Y_{22}^{\,2} & \cdots & \\ 0 & 0 & Y_{33}^{\,3} \cdots & Y_{3n}^{\,3} \\ & & \cdots & \\ 0 & 0 & Y_{n3}^{\,3} \cdots & Y_{nn}^{\,3} \end{bmatrix} \begin{bmatrix} E_1 \\ \cdot \\ \cdot \\ \cdot \\ \cdot \\ \cdot \\ E_n \end{bmatrix}$$

where,

$$(6)\qquad I_j^{\,3} = I_j^{\,2} - Y_{j2}^{\,2}/Y_{22}^{\,2} \times I_2^{\,2} \qquad \text{for } 2 < j \leqslant n$$

and

$$(7)\qquad Y_{jk}^{\,3} = Y_{jk}^{\,2} - Y_{j2}^{\,2} \times Y_{2k}^{\,2}/Y_{22}^{\,2} \qquad \text{for } 2 < j \leqslant n,\ 2 < k \leqslant n.$$

Proceeding in this manner, after n-1 eliminations we finally obtain,

$$(8)\qquad \begin{bmatrix} I_1^{\,1} \\ I_2^{\,2} \\ \cdot \\ \cdot \\ \cdot \\ I_n^{\,n} \end{bmatrix} = \begin{bmatrix} Y_{11}^{\,1} & \cdots & Y_n^{\,1} \\ & Y_{22}^{\,2} \cdots & Y_{2n}^{\,2} \\ & \cdots & \cdots \\ & \cdots & \cdots \\ & & Y_{nn}^{\,n} \end{bmatrix} \begin{bmatrix} E_1 \\ E_2 \\ \cdot \\ \cdot \\ \cdot \\ E_n \end{bmatrix}$$

The node voltages can now be calculated by back-substitution. The voltage on node n is calculated from,

$$(9)\qquad E_n = Y_{nn}^{\,n}/I_n^{\,n}$$

and the voltages on successive nodes, i = n-1,n-2,...,1, are calculated from,

$$(10)\qquad E_i = [I_i^{\,i} - \sum_{j=i+1}^{n} Y_{ij}E_j]/Y_{ii}^{\,i}$$

The situation often arises in which voltage solutions are to be obtained for different node currents but the same

admittance matrix. Upon the elimination of E_i the node currents are reduced by,

$$(11) \qquad I_j^{i+1} = I_j^i - Y_{ji}^i / Y_{ii}^i \times I_i^i \qquad \text{for } i < j \leqslant n$$

Y_{ji}^i are the elements in the lower triangle which are eliminated. However, because the Y matrix is symmetric,

$$(12) \qquad Y_{ij}^i = Y_{ji}^i$$

and

$$(13) \qquad I_j^{i+1} = I_j^i - Y_{ij}^i / Y_{ii}^i \times I_i^i \qquad \text{for } i < j \leqslant n.$$

In (13) the forward reduction of the node currents is performed using the elements which are retained in the upper triangle. Thus, repeat solutions for different sets of node currents can be easily obtained.

In developing the solution algorithm it is convenient to consider the triangularization as a series of network reductions. To illustrate this, assume that part way through the triangularization columns 1,2,...,i-1 have been processed. The equations are therefore,

$$(14) \qquad \begin{bmatrix} I_1^1 \\ \cdot \\ I_i^i \\ \cdot \\ I_n^n \end{bmatrix} = \begin{bmatrix} Y_{11}^1 & \cdot & \cdot & \cdot & \cdot \\ & \cdot & \cdot & \cdot & \cdot \\ & & Y_{ii}^i & \cdot & Y_{in}^i \\ & & \cdot & \cdot & \cdot \\ & & Y_{ni}^i & \cdot & Y_{nn}^i \end{bmatrix} \begin{bmatrix} E_1 \\ \cdot \\ E_i \\ \cdot \\ E_n \end{bmatrix}$$

Extracting the rows i,i+1,...,n we obtain,

$$(15) \qquad \begin{bmatrix} I_i^i \\ \cdot \\ I_n^i \end{bmatrix} = \begin{bmatrix} Y_{ii}^i & \cdot & Y_{in}^i \\ \cdot & \cdot & \cdot \\ Y_{ni}^i & \cdot & Y_{nn}^i \end{bmatrix} \begin{bmatrix} E_i \\ \cdot \\ E_n \end{bmatrix}$$

We can consider equation (15) to represent an admittance equivalent of the original network as viewed from nodes i,i+1,..., n. The branches in this network correspond to the non-zero admittances in the matrix. The next triangularization operation which processes column i in (14) corresponds to eliminating node i from this network as shown in figure 3.1. The subnetwork of the branches which are connected to node i is replaced by an equivalent network as viewed from the adjacent nodes. This requires the following changes to be made:

i) The injected current on each node j adjacent to node i is modified by, $-Y_{ji}^{i}/Y_{ii}^{i} \times I_{i}^{i}$.

ii) The self admittance of each node j adjacent to node i is modified by, $-Y_{ji}^{i} \times Y_{ij}^{i}/Y_{ii}^{i}$.

iii) The mutual admittance between each pair of nodes j and k which are adjacent to node i is modified by, $-Y_{ji}Y_{ik}/Y_{ii}$.

If the mutual admittance was previously zero then a new branch is introduced into the equivalent network.

3.3 ORDERING ELIMINATIONS TO PRESERVE SPARSITY

The nodal admittance matrices for power system networks are usually very sparse. Typically, the ratio of lines to buses in a power system is about 1.5. On this basis, the Y matrix of a system with 100 buses has only 4% non-zero elements and the Y matrix of a system with 1000 buses has only 0.4% non-zero elements. In reducing the Y matrix to triangular form large savings in computer time and storage can be achieved by taking advantage of the sparsity as follows[5-7].

i) The eliminations are ordered to minimize the number of non-zero elements in the final triangularized matrix.

ii) The computer program is designed to process and store only the non-zero admittances during the reduction.

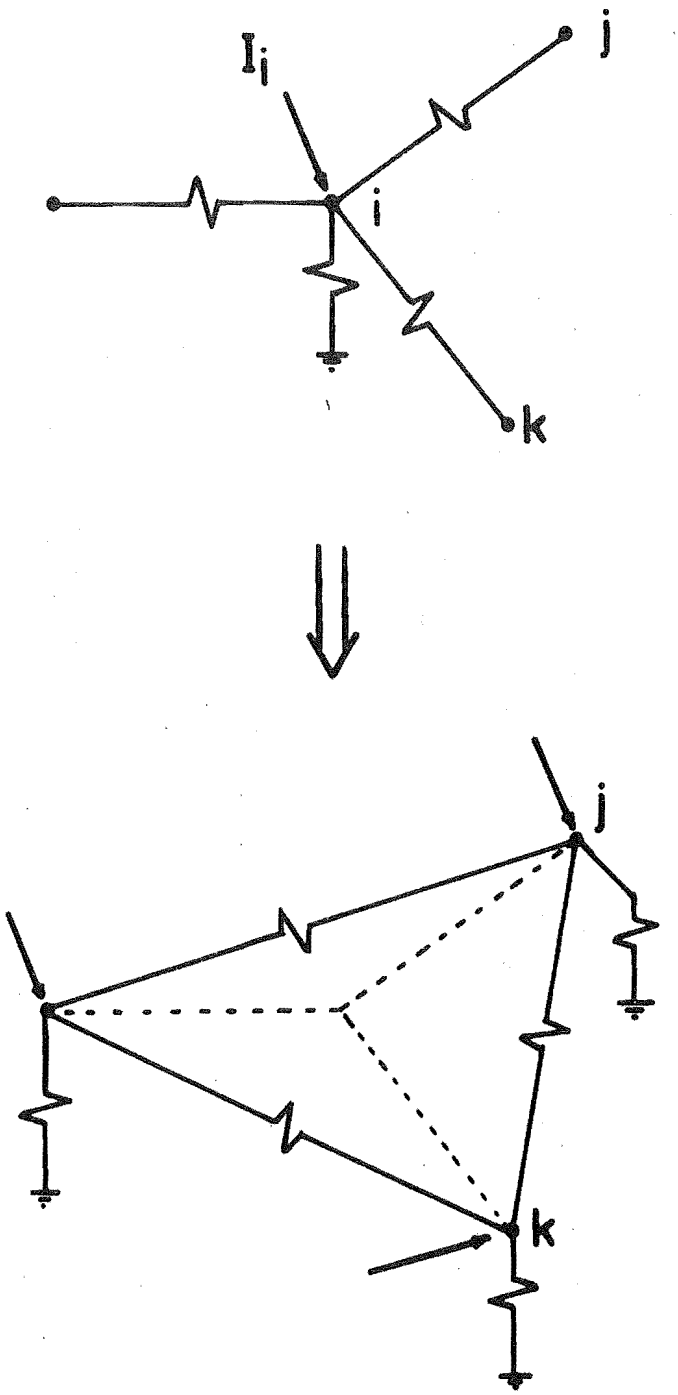

Figure 3.1: Elimination of Node i from the Equivalent Admittance Network

Although true optimal ordering of the eliminations is impractical several schemes do exist for near optimal ordering. The most common schemes are generally known as schemes I, II and III[6].

Scheme I: The nodes are eliminated according to the branches in the original network. Nodes with the least branches are eliminated first and nodes with the most branches are eliminated last.

Scheme II: The nodes are eliminated according to the branches in the equivalent network. At each step the node with the least number of equivalent branches is eliminated.

Scheme III: The nodes are eliminated according to the branches in the equivalent network. However, in this case the node which introduces the least number of new branches into the equivalent network is always eliminated.

Scheme I is the simplest and least optimal whereas scheme III is the most complex and nearest to optimal. For the solution of power system networks scheme II has been found preferable[6]. It provides the most satisfactory trade off between the time required to compute the ordering and the savings achieved in the reduction and solution of the equations. Scheme II is therefore used in the method developed.

3.4 RECORDING THE TRIANGULARIZATION OF THE Y MATRIX WITH LINKNET

The LINKNET structure can be very naturally applied to store only the non-zero terms during the reduction of the admittance matrix to triangular form. Figure 3.2 shows the partially triangularized or reduced Y matrix, the corresponding equivalent network and the corresponding LINKNET structure at

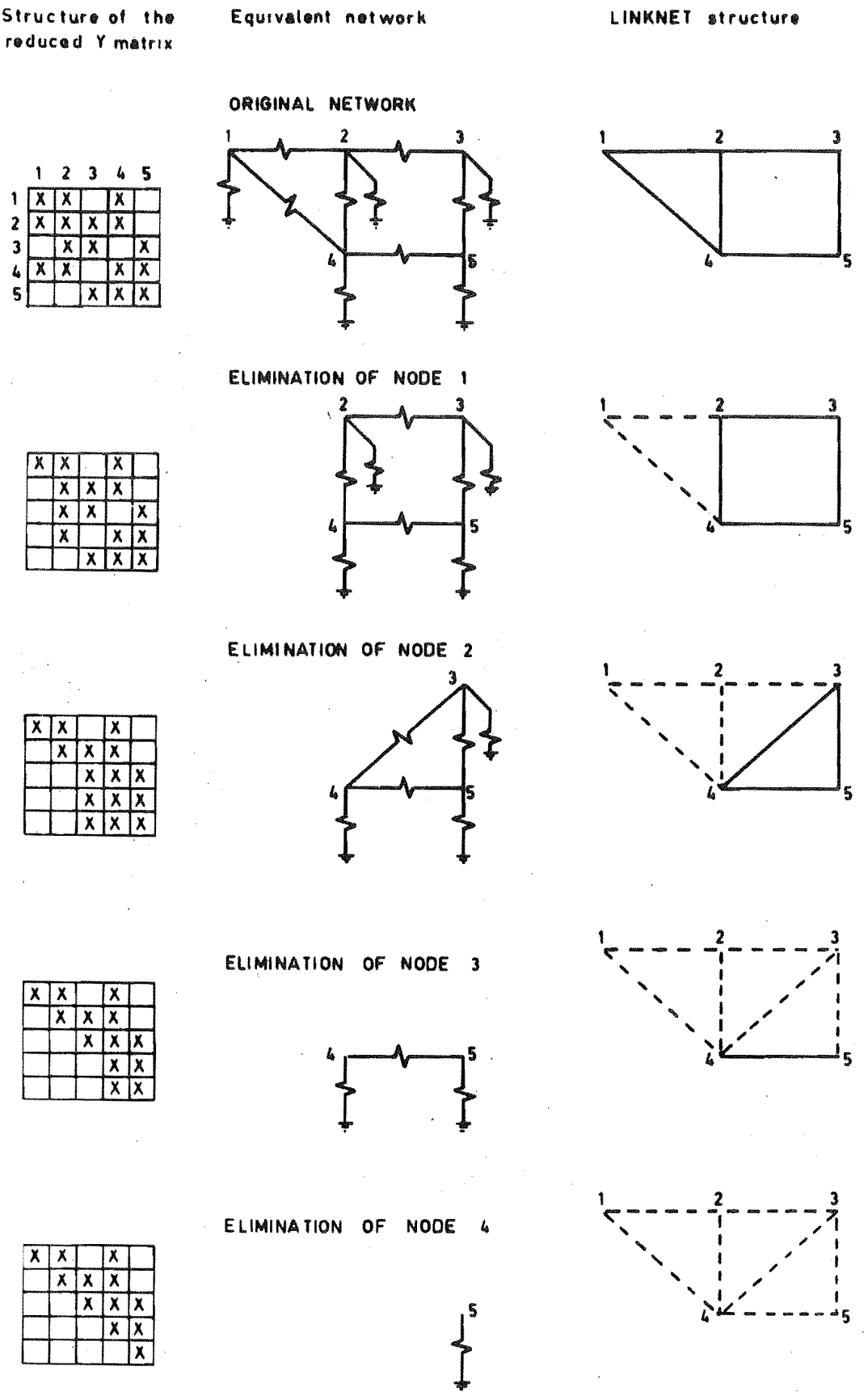

Figure 3.2: Recording the Reduction of the Y Matrix to Triangular Form with LINKNET

each step of the reduction. Only the series elements in the network are explicitly represented by the LINKNET structure. The Y matrix self admittances are stored as node data and the mutual admittances are stored as branch data. When a node and its connected branches are eliminated from the equivalent network they are retained in the LINKNET structure and simply marked as eliminated. In figure 3.2 these branches are represented by the dashed arcs in the LINKNET structure. It is implicit that the admittances which are stored for these branches occur only in the upper triangle of the reduced matrix. The solid arcs in figure 3.2 represent the branches which remain in the equivalent network; it is implicit that the admittances stored for these branches occur in both the lower and upper triangles of the reduced admittance matrix.

3.5 ALGORITHM

The algorithm for the triangularization of the nodal admittance matrix is described as follows.

i) Read the branch data and form the LINKNET structure (section 2.2). Store self admittances as node data and mutual admittances as branch data.

ii) Initialize the elimination count, m=1.

iii) Initialize elements of vector C equal to the number of branches connected to each node.

iv) Find the node i for which C_i is a minimum among the uneliminated nodes.

v) If $C_i = 0$, all nodes except i have been eliminated; therefore exit.

vi) Eliminate node i from the equivalent network as follows,

(a) Modify the self admittance of each node j adjacent to

node i:

$$Y_{jj}^{m+1} = Y_{jj}^{m} - Y_{ji}^{m} Y_{ij}^{m} / Y_{ii}^{m}$$

(b) Modify the mutual admittance between each pair of nodes j and k which are adjacent to node i. If there is an existing branch between nodes j and k set:

$$Y_{kj}^{m+1} = Y_{jk}^{m+1} = Y_{jk}^{m} - Y_{ji}^{m} Y_{ik}^{m} / Y_{ii}^{m}$$

If no branch exists between nodes j and k add a new branch to the LINKNET structure and for this branch store;

$$Y_{kj}^{m+1} = Y_{jk}^{m+1} = - Y_{ji}^{m} Y_{ik}^{m} / Y_{ii}^{m}$$

Then, update C for the addition of this branch to nodes j and k:

$$C_j = C_j + 1$$

$$C_k = C_k + 1$$

(c) Update C for the elimination of the branches connected to node i. For each node j which was adjacent to node i set:

$$C_j = C_j - 1$$

(d) Mark the elimination of node i by setting $C_i = 1000$.

vii) Record the order in which the nodes are eliminated by setting $R_m = i$.

viii) Increment the elimination count, m = m+1, and return to step iv.

When the procedure terminates the nodal admittance matrix is fully triangularized. In situations where the equivalent

admittance matrix of a number of nodes is to be obtained[9,10] the procedure can be modified simply so that these nodes are not eliminated.

3.6 PROGRAM DESCRIPTION

The program for the solution of linear symmetric sets of equations has been written in Fortran IV for the IBM 360/44 machine. The program is written as three subroutines, triangularization, forward reduction and back-substitution. In all, the subroutines require less than 200 Fortran statements.

3.6.1 Storage Requirements

The main storage requirements for the program data can be detailed as follows. (n is the number of nodes, b is the number of off-diagonal admittances in the triangularized matrix.)

Current vector I	: n floating point words
Voltage vector E	: n floating point words
Diagonal admittances Y_{ii}	: n floating point words
Off-diagonal admittances Y_{ij}	: b floating point words
LINKNET indexes	: n+4b integer words
Node connection vector C	: n integer words
Elimination record R	: n integer words

Thus, there is a total storage requirement of 3n+b floating point words (these may be complex) and 3n+4b integer words.

3.6.2 Operation Counts

The operation counts for a complete solution of the nodal admittance equations can be detailed as follows. (Assume C_i is the number of branches connected to node i when it is eliminated.)

Triangularization of Y matrix : n divisions and $b+\sum_{i=1}^{n}(C_i^2+C_i)/2$. multiplications.

Forward reduction of currents : n divisions and b multiplications.

Back-substitution of voltages : n divisions and b multiplications.

The operation counts are the same as for the OOTF method[6] except that an extra n divisions are required for each back-substitution. These can be eliminated by normalizing the diagonal elements of the triangularized matrix but this requires some sacrifice in the simplicity of the algorithm.

3.6.3 Timing Example

The following results were obtained from a timing study on the IEEE 118 Bus system. This system has 179 branches and the final triangularized admittance matrix had 263 off-diagonal terms. The DC loadflow was used as the example application, thus a real set of equations was solved.

Triangularization time : 1.74s.

Forward reduction time : 0.12s.

Back-substitution time : 0.12s.

3.7 CONCLUSION

This chapter has described the development of a program for the efficient solution of large sets of network equations. The program has been developed primarily as a tool for the network studies in this thesis. It has been used for unbalanced fault analysis (section 4.3.3), linearized loadflow (section 7.4.3), calculation of loss coefficients (section 7.3) and calculation of line security constraints for power dispatch (section 8.3.1).

REFERENCES

1. A.F. Glimn, R. Habermann,Jr., J.M. Henderson, L.K. Kirchmayer, "Digital Calculation of Network Impedances", AIEE Trans., Vol. 74, pt.III, 1955, pp. 1285-1297.
2. R.B. Shipley, D. Coleman, "A New Direct Matrix Inversion Method", AIEE Trans., Vol.78, Pt.I, 1959, pp.568-572.
3. H.E. Brown, C.E. Person, L.K. Kirchmayer, G.W. Stagg, "Digital Calculation of Three-Phase Short Circuits by Matrix Method", AIEE Trans., Vol. 79, pt. III, 1960, pp.1277-1282.
4. R. Baumann, "Some New Aspects on Loadflow Calculation: I - Impedance Matrix Generation Controlled by Network Topology", IEEE, PAS-85, 1966, pp.1164-1176.

*5. N. Sato, W.F. Tinney, "Techniques for Exploiting the Sparsity of the Network Admittance Matrix", IEEE Trans., vol. 82, pt.III, 1963, pp.944-950.

*6. W.F. Tinney, J.W. Walker, "Direct Solutions of Sparse Network Equations by Optimally Ordered Triangular Factorization", IEEE Proc., Vol.55, 1967, pp.1801-1809.

7. W.F. Tinney, "Some Examples of Sparse Matrix Methods for Power Network Problems", Proc. Third Power System Computation Conf., Rome, 1969.
8. A. Ralston, A First Course in Numerical Analysis, McGraw-Hill, 1965.

*9. H.E. Brown, "A New Y Matrix Algorithm for Transient Stability", Presented at IEEE Summer Power Meeting, Portland, Ore., 1967.

10. H.E. Brown, R.B. Shipley, D. Coleman, R. Nied,Jr., "A Study of Stability Equivalents", IEEE, PAS 88, 1969, pp.200-207.

C H A P T E R 4

GENERAL METHOD FOR UNBALANCED FAULT ANALYSIS

4.1 INTRODUCTION

The analysis of power system networks under fault conditions plays an important role in the design and operation of protection systems. Methods which use sequence components for the analysis of common types of fault, such as three phase and single phase short circuits, have been highly developed and used successfully for some years[1,2]. There are, however, a number of more general unbalanced fault situations which are still quite difficult to analyze. Practical examples include the analysis of simultaneous faults and unbalanced circuit breaker or fuse operation. The majority of the methods which have been developed for unbalanced fault analysis can be divided into those which use sequence components[1-5] and those which use phase coordinates[6-10]. Figure 4.1 illustrates the respective representations of a three phase network element. Generally, the methods which use sequence components are characterized by:

i) The ability to obtain savings in computer time and storage because the sequence equations for all the balanced network elements are uncoupled.

ii) The network unbalances are commonly represented as constraint equations which produce a mutual coupling between the otherwise independent sets of sequence equations. Because the form of the constraint equations is variable it is difficult to treat faults generally, and this limits the range of fault conditions which can be handled using sequence components.

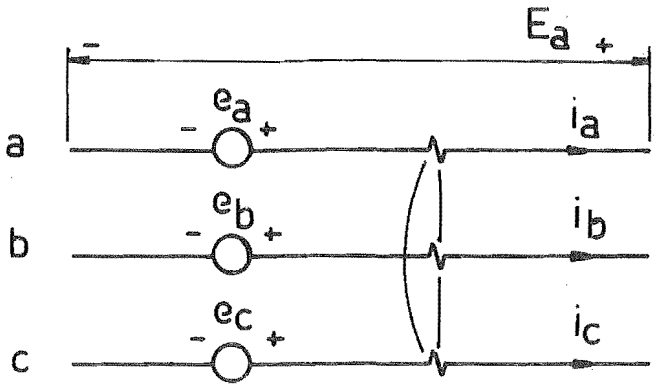

$$\begin{bmatrix} E_a \\ E_b \\ E_c \end{bmatrix} = \begin{bmatrix} e_a \\ e_b \\ e_c \end{bmatrix} - \begin{bmatrix} z_{aa} & z_{ab} & z_{ac} \\ z_{ba} & z_{bb} & z_{bc} \\ z_{ca} & z_{cb} & z_{cc} \end{bmatrix} \begin{bmatrix} i_a \\ i_b \\ i_c \end{bmatrix}$$

PHASE CO-ORDINATE REPRESENTATION OF THREE PHASE ELEMENT

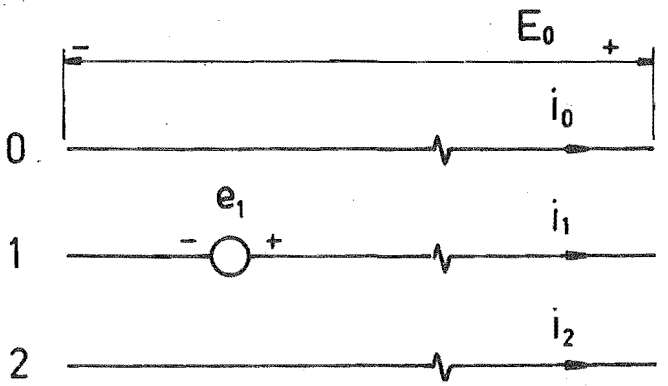

$$\begin{bmatrix} E_0 \\ E_1 \\ E_2 \end{bmatrix} = \begin{bmatrix} 0 \\ e_1 \\ 0 \end{bmatrix} - \begin{bmatrix} z_{00} & & \\ & z_{11} & \\ & & z_{22} \end{bmatrix} \begin{bmatrix} i_0 \\ i_1 \\ i_2 \end{bmatrix}$$

SEQUENCE COMPONENT REPRESENTATION OF A BALANCED THREE PHASE ELEMENT

Figure 4.1

On the other hand, the methods which use phase coordinates are characterized by:

i) Extra computer time and storage demands due to the 3 x 3 matrix representation of the network elements.

ii) A much greater flexibility in the types of unbalance which can be treated. It is quite possible to develop a single program which can handle all types of unbalanced fault.

The method developed here is a piecewise method in which the network is partitioned into a balanced subnetwork and a number of unbalanced subnetworks. The concept of the method is similar to Kron's method of tearing[11-13] but the formulation is simplified by the special form of partitioning. The solution of the balanced subnetwork is initially obtained in terms of sequence components and is then transformed to phase coordinates. The solutions of the unbalanced subnetworks are directly obtained in terms of phase coordinates. The phase coordinate solutions of all the subnetworks are then combined to form the solution of the original unpartitioned network. For practical fault studies the unbalanced subnetworks are typically very small even though the complete network may be large. Consequently, the respective advantages of using phase and sequence coordinates are obtained simultaneously. The computational savings through the sequence component representation of the balanced subnetwork are obtained and also the method deals with very general types of unbalance.

4.2 THEORETICAL DEVELOPMENT

The steps in the theoretical development of the method are illustrated for an example network in figures 4.2 to 4.6. In figures 4.3 to 4.6 the balanced and unbalanced subnetworks are represented by generalized Thévenin mesh equivalents[11]. In each figure the subnetworks are viewed from a different set of node pairs; these are marked by the double ended arrows. The node pairs which include the reference node are described as node-reference pairs and the node pairs which do not include the reference node are described as node-node pairs. Where a single equivalent mesh is labelled by voltage and current vectors it is to be understood that the elements of the vector apply to each equivalent mesh. Superscripts U and B denote that variables apply to the unbalanced or balanced subnetworks respectively. Subscripts P and S denote that the variables are in terms of phase or sequence components respectively. The superscript ' is used to indicate the variables which are defined on a general node-node basis rather than the more usual node-reference basis.

A brief outline of the development can be followed with reference to figures 4.2 to 4.6.

Step 1: The network is partitioned into a balanced subnetwork and a number of unbalanced subnetworks.

Step 2: The phase equivalents for the unbalanced subnetworks are calculated on a node-node basis.

Step 3: The 0,1,2 sequence equivalents for the balanced subnetwork are independently calculated on a node-reference basis.

Step 4: The sequence equivalents from step 3 are transformed to a three phase equivalent; also on a node-reference basis.

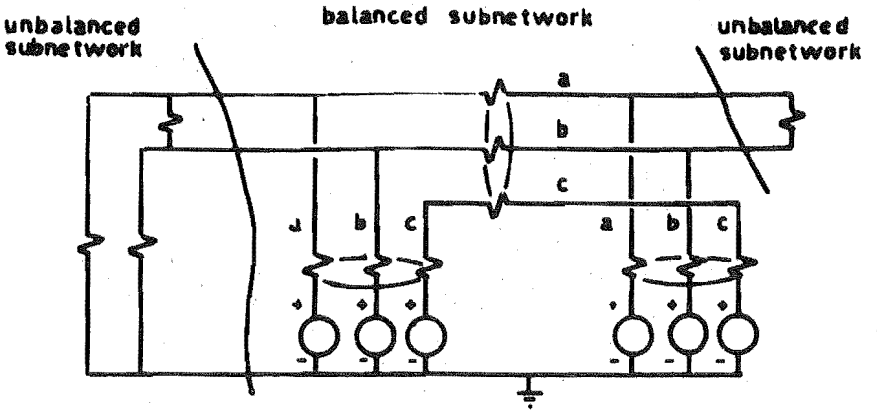

PARTITIONING OF UNBALANCED NETWORK

Figure 4.2

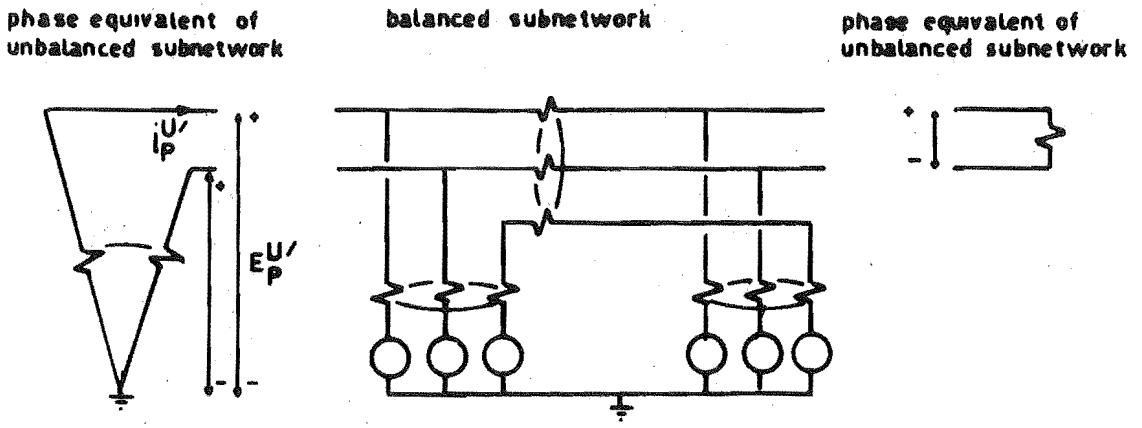

NETWORK REPRESENTATION IN STEP 2

Figure 4.3

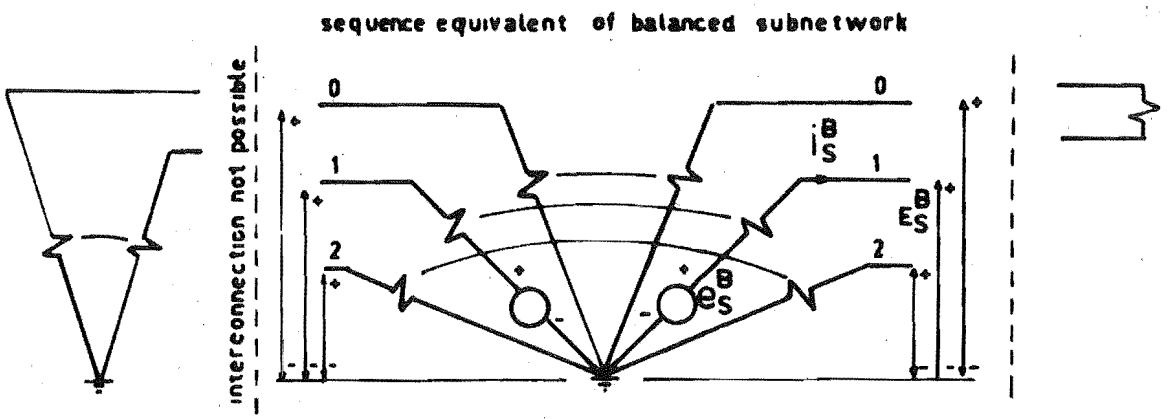

NETWORK REPRESENTATION IN STEP 3

Figure 4.4

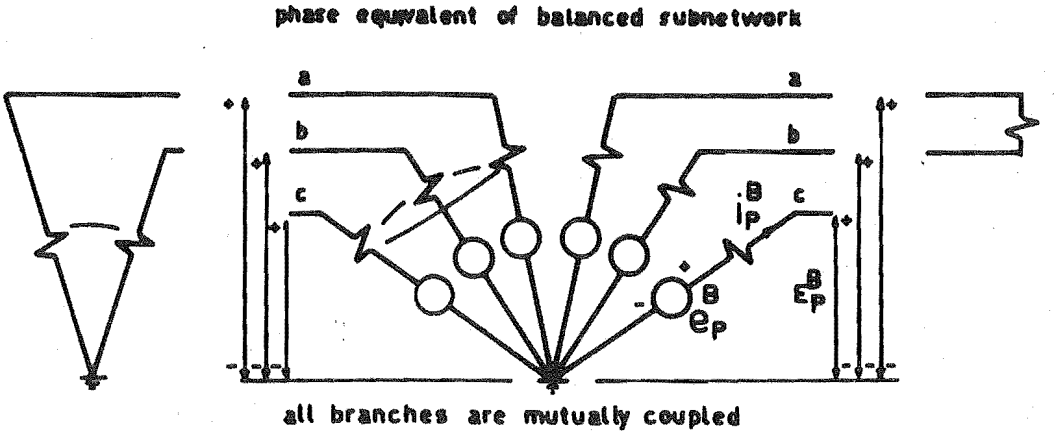

NETWORK REPRESENTATION IN STEP 4

Figure 4.5

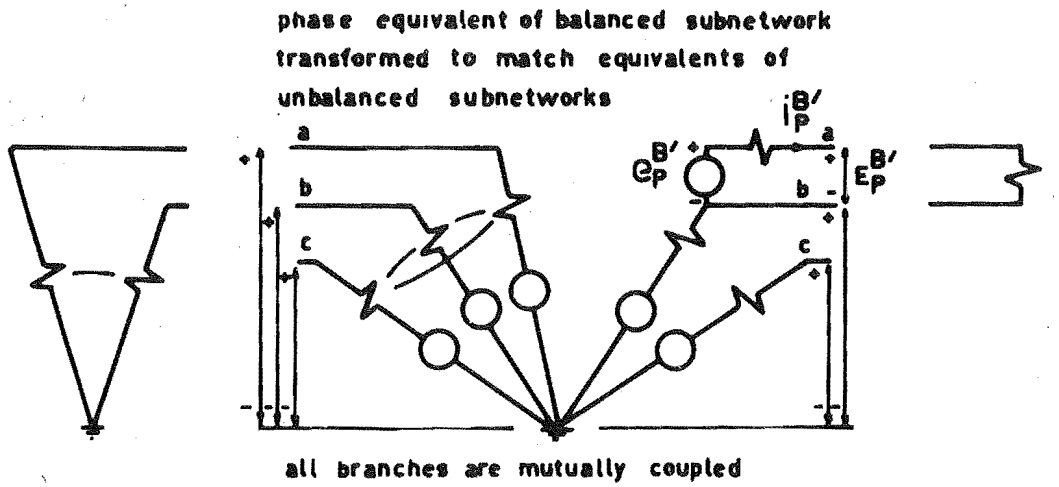

NETWORK REPRESENTATION IN STEP 5

Figure 4.6

Step 5: The node-reference basis of the equivalent in step 4 is transformed to match the node-node basis of the unbalanced subnetwork equivalents.

Step 6: The phase equivalents for the balanced and unbalanced subnetworks are combined and the solution is obtained for the interconnecting phase voltages and currents.

Step 7: The sequence voltages and currents are calculated from the phase voltages and currents.

The theoretical development of the above steps is now described more fully.

Step 1: The network is partitioned through its nodes into an axial balanced network and a number of radial unbalanced networks as shown in figure 4.2.

Step 2: The open circuit phase impedances $Z_{PP}^{U'}$ are calculated for the partitioned nodes in the unbalanced subnetworks. The unbalanced subnetworks will not generally contain sources and their open circuit voltages will be zero. Thus, the equivalent mesh equation of the unbalanced subnetworks is,

$$E_P^{U'} = - Z_{PP}^{U'} \, i_P^{U'} \tag{1}$$

As shown in figure 4.3 the voltages $E_P^{U'}$ and the currents $i_P^{U'}$ must be defined on a general node-node basis unless all the partitioned subnetworks contain the reference node.

Step 3: For the balanced subnetwork the open circuit sequence impedances Z_{SS}^{B} and voltages e_S^B are calculated for each three phase bus in which any single phase node is partitioned. For computational ease we assume the impedances and voltages are all calculated on a node-reference basis. In terms of sequence components the equivalent mesh equation of the balanced subnetwork is,

$$E_S^B = e_S^B - Z_{SS}^B \, i_S^B \tag{2}$$

Since the subnetwork is balanced there are no mutual sequence impedances. Usually, the network excitation is balanced and the 0 and 2 sequence open circuit voltages are zero. Thus, (2) can be expanded as,

$$\begin{bmatrix} E_0^B \\ E_1^B \\ E_2^B \end{bmatrix} = \begin{bmatrix} 0 \\ e_1^B \\ 0 \end{bmatrix} - \begin{bmatrix} Z_{00}^B & & \\ & Z_{11}^B & \\ & & Z_{22}^B \end{bmatrix} \begin{bmatrix} i_0^B \\ i_1^B \\ i_2^B \end{bmatrix} \tag{3}$$

The equivalent mesh network which corresponds to (3) is shown in figure 4.4. At this stage the balanced and unbalanced network equivalents cannot be connected since they are based on different coordinates.

Step 4: The open circuit sequence impedances and voltages for the balanced subnetwork are transformed to open circuit phase impedances and voltages. Let T be the phase-sequence transformation matrix[6,11], i.e.,

$$T = \frac{1}{\sqrt{3}} \begin{bmatrix} 1 & 1 & 1 \\ 1 & a^2 & a \\ 1 & a & a^2 \end{bmatrix} \tag{4}$$

The open circuit phase impedances are given by[6,11],

$$Z_{PP}^B = T \, Z_{SS}^B \, T^* \tag{5}$$

and the open circuit phase voltages are given by[6,11],

$$e_P^B = T \, e_S^B \tag{6}$$

Thus, in terms of phase coordinates the equivalent mesh equation of the balanced subnetwork is,

$$E_P^B = e_P^B - Z_{PP}^B \, i_P^B \tag{7}$$

Figure 4.5 shows the equivalent balanced subnetwork which corresponds to (7).

Step 5: We define for the balanced subnetwork a new set of node pairs which includes the node pairs in the unbalanced subnetworks. Let A be the transformation matrix which relates the new node-node voltages to the old node-reference voltages, i.e.,

$$e_P^{B'} = A \, e_P^B \tag{8}$$

and

$$E_P^{B'} = A \, E_P^B \tag{9}$$

From the invariance of power[11],

$$i_P^B = A^t \, i_P^{B'} \tag{10}$$

and the new equivalent mesh equation is,

$$E_P^{B'} = e_P^{B'} - Z_{PP}^{B'} \, i_P^{B'} \tag{11}$$

where the new set of open circuit impedances is defined by,

$$Z_{PP}^{B'} = A \, Z_{PP}^B \, A^t \tag{12}$$

Figure 4.6 shows the equivalent network which corresponds to equation (11). The voltages and currents in the unbalanced networks are now matched with a subset of the voltages and currents in the balanced subnetworks.

Step 6: In this step the balanced and unbalanced subnetworks are interconnected and the currents which flow between them are solved. Let $E_{P1}^{B'}$ and $i_{P1}^{B'}$ be the voltages and currents across the node pairs which are common to both the balanced and unbalanced subnetworks. The equivalent mesh equation (1)

of the unbalanced subnetworks must be satisfied; therefore,

$$(13) \qquad E_{P1}^{B'} = Z_{PP}^{U'}\, i_{P1}^{B'}$$

Let $E_{P2}^{B'}$ and $i_{P2}^{B'}$ be the voltages and currents across the node pairs which are not common to the unbalanced subnetworks. These node pairs remain open circuited when the subnetworks are interconnected and therefore,

$$(14) \qquad i_{P2}^{B'} = 0.$$

Equations (13) and (14) represent the constraints imposed on voltages $E_{P}^{B'}$ and currents $i_{P}^{B'}$ by the conditions external to the balanced subnetwork. Now, expanding equation (11) for the balanced subnetwork,

$$(15) \qquad \begin{bmatrix} E_{P1}^{B'} \\ E_{P2}^{B'} \end{bmatrix} = \begin{bmatrix} e_{P1}^{B'} \\ e_{P2}^{B'} \end{bmatrix} - \begin{bmatrix} Z_{PP11}^{B'} & Z_{PP12}^{B'} \\ Z_{PP21}^{B'} & Z_{PP22}^{B'} \end{bmatrix} \cdot \begin{bmatrix} i_{P1}^{B'} \\ i_{P2}^{B'} \end{bmatrix}$$

Substitution of (13) and (14) into (15) gives,

$$(16) \qquad e_{P1}^{B'} = (Z_{PP}^{U'} + Z_{PP11}^{B'}) . i_{P1}^{B'}$$

The solution for the phase currents which flow from the balanced subnetwork is thus,

$$(17) \qquad i_{P1}^{B'} = (Z_{PP}^{U'} + Z_{PP11}^{B'})^{-1}\, e_{P1}^{B'}$$

and,

$$(18) \qquad i_{P2}^{B'} = 0.$$

Step 7: The node-reference phase currents are calculated by transforming the node-node phase currents,

$$(19) \qquad i_{P}^{B} = A^{t}\, i_{P}^{B'}.$$

The sequence currents are then obtained from,

$$(20) \qquad i_S^B = T^* \; i_P^B$$

and the sequence voltages are obtained from,

$$(21) \qquad E_S^B = e_S^B - Z_{SS}^B \; i_S^B$$

The voltages and currents on the partitioned nodes are now completely determined.

4.3 IMPLEMENTATION

4.3.1 Network Partitioning

For practical situations the network partitioning is a simple manual task but requires a great deal more program complexity if performed automatically. The manner in which the network is partitioned is flexible; however it is better if the number of partitioned nodes and the size of the unbalanced subnetworks are kept as low as possible. For fault studies the network can be appropriately partitioned simply by removing the unbalanced components or the unbalanced faults from the main balanced part of the network. In figure 4.7 a number of common unbalanced faults are considered to illustrate.

4.3.2 Calculation of the Mesh Equivalents of the Unbalanced Subnetworks

Generally, the unbalanced subnetworks are of a very simple form and it will be possible to define an independent set of node pairs and to determine the corresponding impedances by direct inspection. These steps are also shown for the examples in figure 4.7. Notice that it is quite satisfactory if the matrix $Z_{PP}^{U'}$ is singular due to the equivalent impedance of a short circuit being zero. The matrix $Z_{PP}^{U'}$ and the list

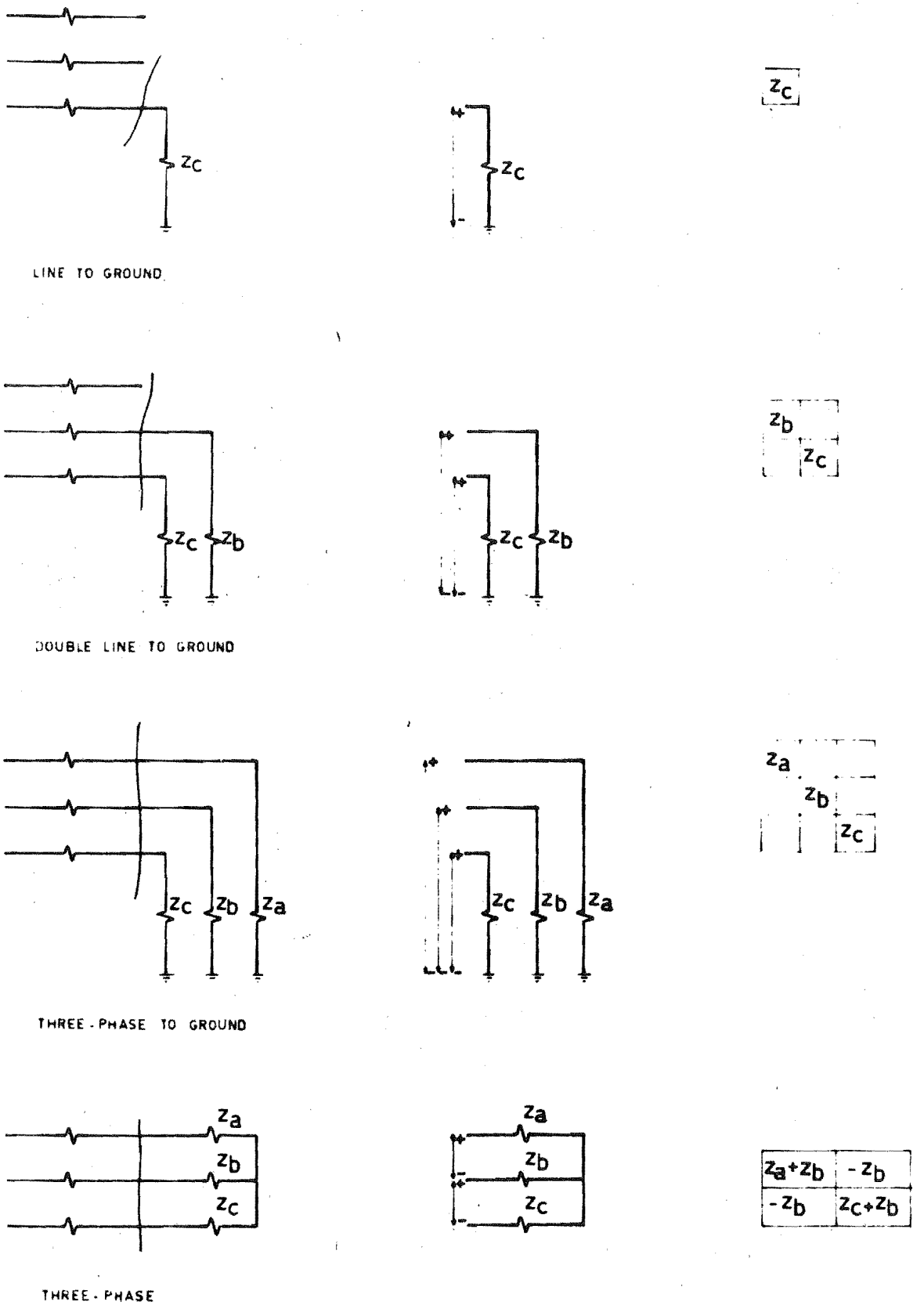

Figure 4.7a: Formation of Mesh Equivalents for Common Faults

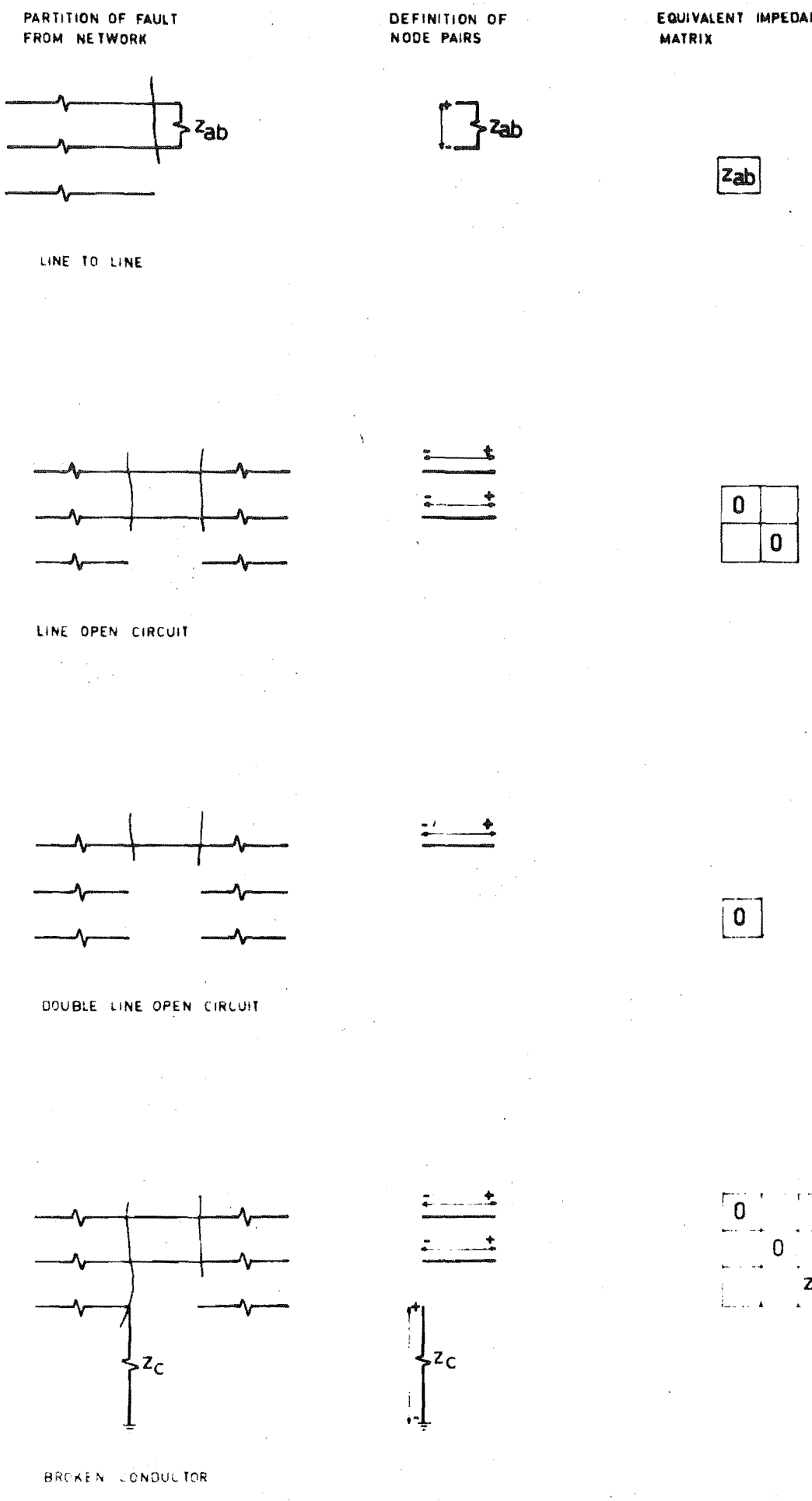

Figure 4.7b: Formation of Mesh Equivalents for Common Faults

of the node pairs which are specified in its calculation are all the information that is used to represent the unbalanced subnetworks in the fault program.

4.3.3 Solution of the Balanced Subnetwork

In the analysis of power system faults a number of assumptions are commonly made[6];

i) Each generator is represented by the same constant and balanced voltage source behind its subtransient reactance.

ii) The generator positive and negative sequence reactances are equal.

iii) Shunt elements in the network are neglected, e.g. loads, line charging, etc.

iv) All transformers have unity tap setting.

v) All impedances are completely reactive.

The computation for calculating the mesh equivalent of the balanced subnetwork is considerably reduced by these assumptions. However, the method is not inherently dependent upon the assumptions and any of them may be relaxed if desired.

As a result of assumptions i), iii) and iv), when the balanced subnetwork is partitioned there is no current flow and the bus voltages are all equal. Consequently, the calculation of the open circuit voltages is trivial. We simply set,

$$(22) \qquad e_S^B = \begin{bmatrix} e_0^B \\ e_1^B \\ e_2^B \end{bmatrix} = \begin{bmatrix} 0 \\ e_r \\ 0 \end{bmatrix}$$

where e_r is the positive sequence voltage source of each generator.

Because the 0 and 2 sequence impedances are equal, equivalent impedances are only calculated for the 0 and 1 sequence networks. The 0 and 1 sequence admittance matrices are triangularized for all the network buses except those which are partitioned. A very efficient procedure for this operation has been described in Chapter 3. The submatrices which result for the partitioned buses Y^B_{00} and Y^B_{11} are extracted; these represent admittance equivalents of the 0 and 1 sequence networks. The equivalent impedance matrices Z^B_{00} and Z^B_{11} are then obtained as the inverses of Y^B_{00} and Y^B_{11} respectively. The inversion requires little computation since the order of these matrices equals the number of partitioned buses which is typically small.

In practical studies the solution for the current at the fault location is of prime interest and the complete solution of the bus voltages is not so important. In the proposed method the complete solution for the bus voltages is optional. If required, they are obtained by back-substituting the sequence voltages on the partitioned buses into the triangularized 0 and 1 sequence admittance matrices.

4.3.4 Sequence - Phase Transformations

In step 4 the sequence voltages and impedances in the equivalent of the balanced subnetwork are transformed to phase voltages and impedances. The simplified form of e^B_S and Z^B_{SS} enables simplified formulas to be used for calculating e^B_P and Z^B_{PP}. Substitution for T and e^B_S into (5) shows that,

$$(23) \qquad e^B_P = \frac{1}{\sqrt{3}} \begin{bmatrix} e_r \\ a^2 e_r \\ a\ e_r \end{bmatrix}$$

and substitution for T and Z^B_{SS} into (4) shows that,

$$(24) \qquad Z^B_{PP} = \frac{1}{3}\begin{bmatrix} Z^B_{00}+2Z^B_{11} & Z^B_{00}-Z^B_{11} & Z^B_{00}-Z^B_{11} \\ Z^B_{00}-Z^B_{11} & Z^B_{00}+2Z^B_{11} & Z^B_{00}-Z^B_{11} \\ Z^B_{00}-Z^B_{11} & Z^B_{00}-Z^B_{11} & Z^B_{00}+2Z^B_{11} \end{bmatrix}$$

4.3.5 Node-Reference to Node-Node Transformation

In step 5 it is necessary to define for the balanced subnetwork a new set of node pairs which includes as a subset the node pairs defined earlier for the unbalanced subnetworks. The convention which is adopted for defining the new set of node pairs is illustrated in figure 4.8. We assume that the polarities are assigned to the node pairs in the subnetworks so that no node is defined as the 'plus' node for more than one node pair. A node-node pair is included in the new set by replacing the node-reference pair which contains the 'plus' node of the node-node pair. The A matrix which is obtained by expressing the new voltages in terms of the old voltages is shown for each of the examples in figure 4.8. With the convention adopted the A matrix has unity diagonal elements and minus unity off-diagonal elements which correspond to the replacement of a node-reference pair by a node-node pair. The special form of the A matrix enables the transformation,

$$(25) \qquad Z^{B'}_{PP} = A\ Z^B_{PP}\ A^t$$

to be performed very easily. The new matrix $Z^{B'}_{PP}$ is calculated by adding the rows and columns of the old matrix Z^B_{PP} according to the node pairs in the unbalanced subnetworks.

LINE TO LINE FAULT

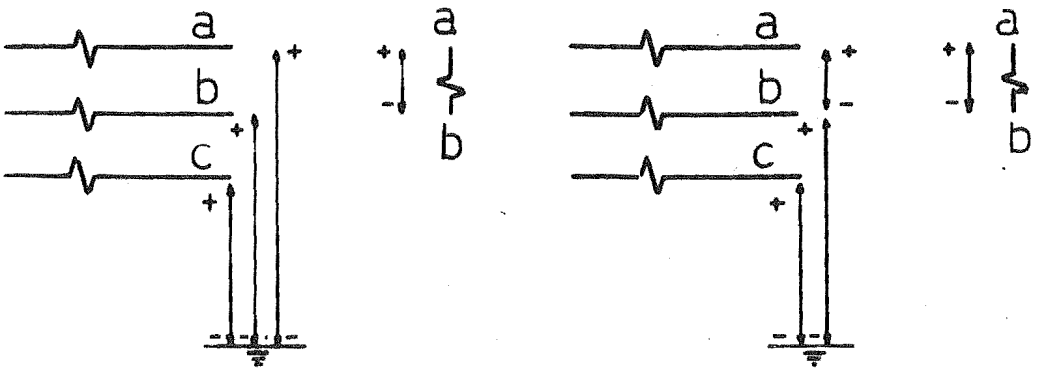

OLD NODE-REFERENCE PAIRS NEW NODE-NODE PAIRS

$$\begin{bmatrix} E_{ab} \\ E_b \\ E_c \end{bmatrix} = \begin{bmatrix} 1 & -1 & \\ & 1 & \\ & & 1 \end{bmatrix} \begin{bmatrix} E_a \\ E_b \\ E_c \end{bmatrix}$$

THREE PHASE FAULT

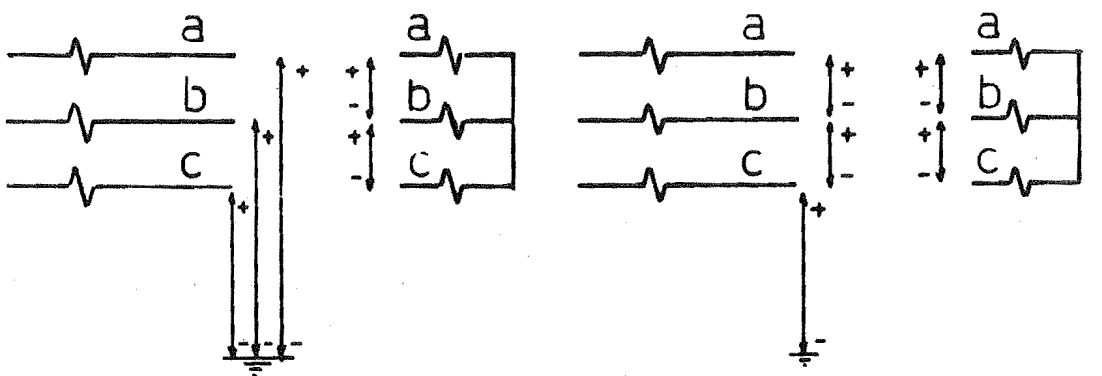

OLD NODE-REFERENCE PAIRS NEW NODE-NODE PAIRS

$$\begin{bmatrix} E_{ab} \\ E_{bc} \\ E_c \end{bmatrix} = \begin{bmatrix} 1 & -1 & \\ & 1 & -1 \\ & & 1 \end{bmatrix} \begin{bmatrix} E_a \\ E_b \\ E_c \end{bmatrix}$$

Figure 4.8: Node-reference to Node-node Transformations for Line to Line and Three Phase Fault

4.3.6 Summary of Procedure

The procedure of the program which has been developed for the analysis of general unbalanced faults is as follows:

i) Read the 0 and 1 sequence reactances and form the 0 and 1 sequence admittance matrices for the balanced subnetwork.

ii) Read the unbalanced fault data, consisting of the equivalent impedance matrix $Z_{PP}^{U'}$ and the list of node pairs defined in its calculation.

iii) Triangularize the 0 and 1 sequence admittance matrix for all buses except the partitioned buses, and invert Y_{00}^{B} and Y_{11}^{B} to obtain Z_{00}^{B} and Z_{11}^{B}.

iv) Calculate e_P^B from (23) and Z_{PP}^{B} from (24).

v) Calculate, $e_P^{B'} = A\, e_P^B$

and $Z_{PP}^{B'} = A\, Z_{PP}^{B}\, A^t$

vi) Solve $e_P^{B'} = (Z_{PP11}^{B'} + Z_{PP}^{U'})\, i_P^{B'}$ for $i_P^{B'}$.

vii) Calculate, $i_P^B = A^t\, i_P^{B'}$

and $i_S^B = T^*\, i_P^B$

and $E_S^B = e_S^B - Z_{SS}^B\, i_S^B$

viii) If required, calculate the sequence voltages on the unpartitioned buses by backsubstituting E_0^B into the triangularized 0 sequence admittance matrix and alternately backsubstituting E_1^B and E_2^B into the triangularized 1 sequence admittance matrix.

4.4 COMPUTATIONAL RESULTS

A comparison of the computational requirements of several methods for solving general three phase network unbalances has been made. Test programs have been written in Fortran IV and executed on an IBM 360/44 with 128k bytes of core storage for the following methods:

i) The piecewise method.

ii) A variation of the piecewise method with building of the complete 0 and 1 sequence bus impedance matrices[1] in place of triangularization of the 0 and 1 sequence admittance matrices.

iii) A method recently proposed by D.R. Smith[4]. In this method the complete network including unbalances is represented by sequence components.

The results of timing studies with a number of test systems of different sizes including the IEEE 118 Bus Test System and a NZED 185 bus system are shown in figure 4.9. Also shown in figure 4.9 is the maximum system size which could be handled within the available storage of about 100k bytes. In each case a double unbalance consisting of a single phase series open circuit and a two phase to ground short circuit was solved. However, the computer requirements of the methods were essentially independent of the type of unbalance which was solved. The results clearly show the superior efficiency of the piecewise method which uses the triangularized Y Bus matrix. For the piecewise methods almost all the time and storage is used in the solution of the 0 and 1 sequence networks; this step is also required for the solution of standard single phase unbalances. Consequently, the piecewise method actually enables very general types of network

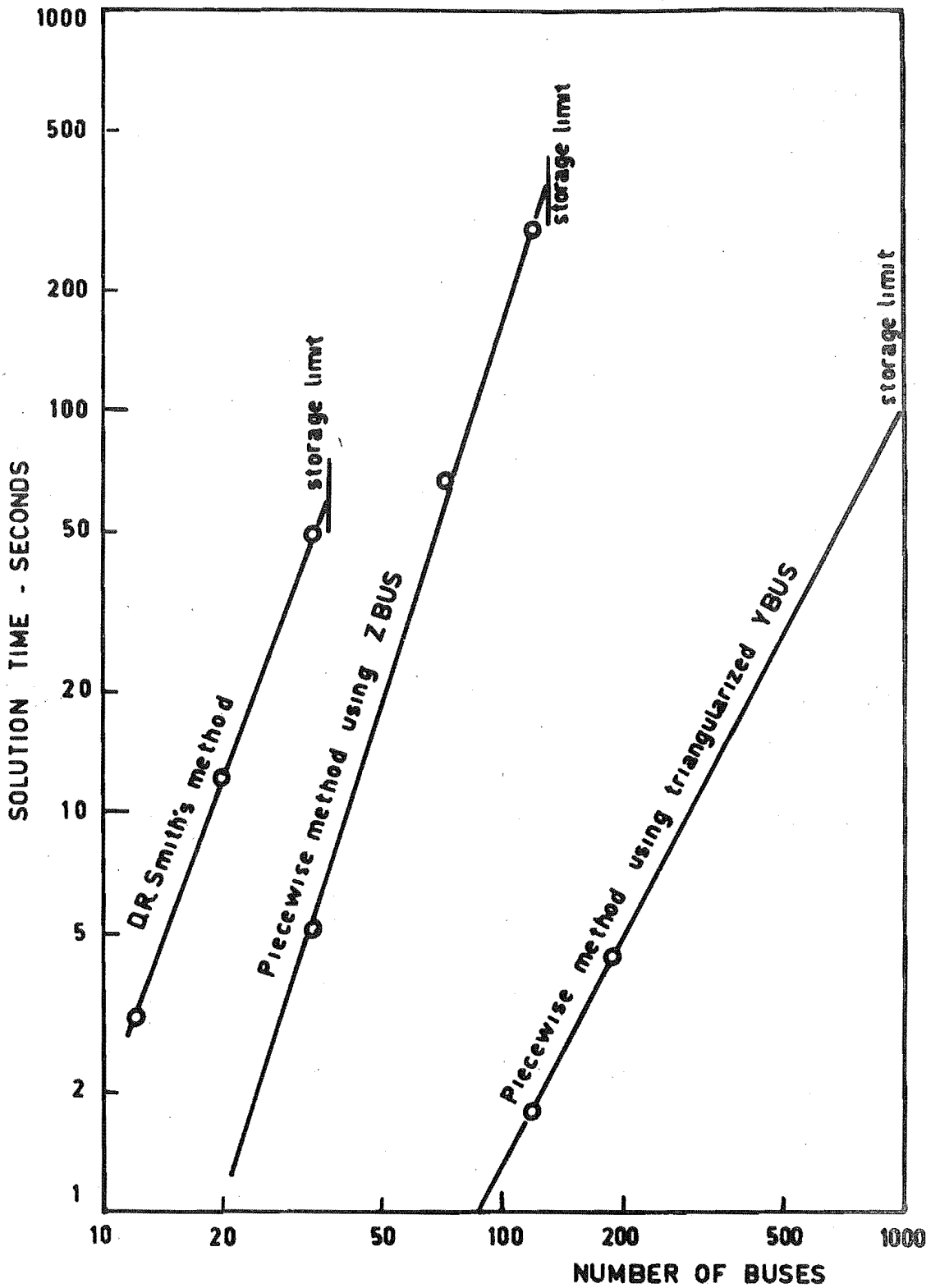

Figure 4.9: Computational Requirements of Unbalanced Fault Programs

unbalance to be solved with the same computational ease as standard single phase faults.

4.5 CONCLUSION

A piecewise method for the analysis of unbalanced faults has been developed and evaluated. The method enables general types of network unbalance to be analyzed with greatly reduced time and storage requirements. Computationally, general types of unbalanced fault are now no more difficult to analyze than the standard single phase short circuit. In practice, the method will be useful for the analysis of simultaneous faults, and unbalanced circuit breaker or fuse operation.

REFERENCES

*1. H.E. Brown, C.E. Person, L.K. Kirchmayer, G.W. Stagg, "Digital Calculation of 3-Phase Short Circuits by Matrix Method", AIEE Trans., vol. 79, Pt. III, 1960, pp. 1277-1282.

2. A.H. El-Abiad, "Digital Calculation of Line-to-ground Short Circuits by Matrix Method", AIEE Trans., vol. 79, pt. III, 1960, pp. 323-332.

3. E. Clarke, "Simultaneous Faults on Three Phase Systems", AIEE Trans., vol. 50, 1931, pp. 919-941.

4. D.R. Smith, "Digital Simulation of Simultaneous Unbalances Involving Open and Faulted Conductors", IEEE, PAS 89, 1970, pp. 1826-1835.

5. P.M. Anderson, "Analysis of Simultaneous Faults by Two-Port Network Theory", IEEE, PAS 90, 1971, pp. 2199-2205.

6. G.W. Stagg, A.H. El-Abiad, Computer Methods in Power System Analysis, McGraw Hill, New York, 1968.

7. M.A. Laughton, "Analysis of Unbalanced Polyphase Networks by the Method of Phase Coordinates - Part 1. System Representation in Phase Frame of Reference", Proc. IEE, vol. 115, 1968, pp. 1163-1172.

8. M.A. Laughton, "Analysis of Unbalanced Polyphase Networks by the Method of Phase Coordinates - Part 2. Fault Analysis", Proc. IEE, vol. 116, 1969, pp. 857-865.

9. P.K. Dash, "Analysis of Power System Faults by Phase Impedance Matrix Method: I - General Fault Analysis", IEEE, PAS 91, 1972, pp. 592-600.

10. P.K. Dash, "Analysis of Power System Faults by Phase Impedance Matrix Method: II - Simultaneous Unbalances and Transient Analysis", IEEE, PAS 91, 1972, pp. 601-610.

*11. G. Kron, Tensor Analysis of Networks, Wiley, New York, 1939. Reprinted MacDonald, London, 1965.

12. G. Kron, Diakoptics - The Piecewise Solution of Large Scale Systems, Macdonald, London, 1963.

13. H.H. Happ, "Z Diakoptics - Torn Subdivisions Radially Attached", IEEE, PAS 86, 1967, pp. 751-769.

C H A P T E R 5

MODIFIED NODAL ITERATIVE LOADFLOW ALGORITHM - IMPROVEMENT IN SPEED OF CONVERGENCE

5.1 INTRODUCTION

The Gauss-Seidel Nodal Iterative Loadflow[1] has been well established as a method of power system loadflow analysis. Even with the development of more sophisticated methods using direct solution of the network equations[2,3] the nodal iterative method continues to be used in both routine and specialized loadflow studies[4]. The main advantages of the nodal iterative method are its low storage requirement and basic simplicity; on the other hand its main disadvantage has been its comparatively slow convergence. In this chapter a modification for increasing the speed of convergence of the nodal iterative loadflow is proposed and its performance is evaluated.

5.2 THE PROPOSED MODIFICATION

5.2.1 Qualitative Description

It is well known that the nodal iterative loadflow requires a comparatively large number of iterations for convergence and that this is due to the slow rate at which the effects of bus voltage adjustments are propagated through the network. The proposed modification is based upon the philosophy that the convergence should be improved by increasing this rate of propagation. As each bus undergoes a normal or "primary" voltage adjustment supplementary "secondary" adjustments are simultaneously applied to adjacent buses. Thus, the effects of the normal bus adjustment reach the adjacent buses much earlier than in the conventional method.

5.2.2 Conventional Adjustment Formula

The conventional adjustment formula of the nodal iterative method is[1],

$$(1) \qquad E_p^{NEW} = (S_p^*/E_p^{*OLD} - \Sigma_q Y_{pq} E_q^{OLD})/Y_{pp}$$

and is applied at load buses for which,

$$(2) \qquad S_p = E_p I_p^* = \text{constant}.$$

The application of (1) may be conveniently analyzed into several steps. In the first step the current mismatch, or difference between the required and actual current, is calculated as,

$$(3) \qquad \Delta I_p = S_p^*/E_p^{*OLD} - (Y_{pp} E_p^{OLD} + \sum_q Y_{pq} E_q^{OLD})$$

The required current S_p^*/E_p^* is considered constant during the adjustment since changes in E_p are small. By assuming that the voltages on adjacent buses remain constant the voltage on bus p is then adjusted to equal the actual current with the required current:

$$(4) \qquad \Delta E_p = \Delta I_p/Y_{pp}$$

and

$$(5) \qquad E_p^{NEW} = E_p^{OLD} + \Delta E_p$$

Substitution of (3) and (4) into (5) will show that they are in fact equivalent to the direct application of (1).

5.2.3 Primary and Secondary Adjustment Formulas

As with the conventional method the current mismatch on bus p is first calculated using,

$$(6) \qquad \Delta I_p = S_p^*/E_p^{*OLD} - (Y_{pp} E_p^{OLD} + \sum_q Y_{pq} E_q^{OLD})$$

In this instance, however, the voltages on buses adjacent to bus p are also adjusted to eliminate the current mismatch. The situation is illustrated in figure 5.1. For bus p we require that,

$$(7) \qquad \Delta I_p = Y_{pp}\Delta E_p + \Sigma_q Y_{pq}\Delta E_q$$

For the buses adjacent to bus p we assume that the injected current, S_q^*/E_q^* is constant and therefore,

$$(8) \qquad \Delta I_q = 0 = Y_{qq}\Delta E_q + Y_{qp}\Delta E_p$$

Equation (8) will be an approximation if any node connected to node q is also connected to node p as it will also receive a voltage change. Subsitution of (8) into (7) gives the primary adjustment formula for bus p,

$$(9) \qquad \Delta E_p = \Delta I_p/(Y_{pp} - \Sigma_q \frac{Y_{pq}Y_{qp}}{Y_{qq}})$$

Rearranging (8) gives the secondary adjustment formula for the adjacent buses,

$$(10) \qquad \Delta E_q = -Y_{qp}/Y_{qq}\ \Delta E_p.$$

For each bus we may define an effective admittance,

$$(11) \qquad Y_{pp}^{eff} = Y_{pp} - \Sigma_q \frac{Y_{pq}Y_{qp}}{Y_{qq}}$$

Physically, Y_{pp}^{eff} represents the effective admittance seen from node p when nodes two removed from node p are grounded. The primary adjustment formula can thus be rewritten as,

$$(12) \qquad \Delta E_p = \Delta I_p/Y_{pp}^{eff}.$$

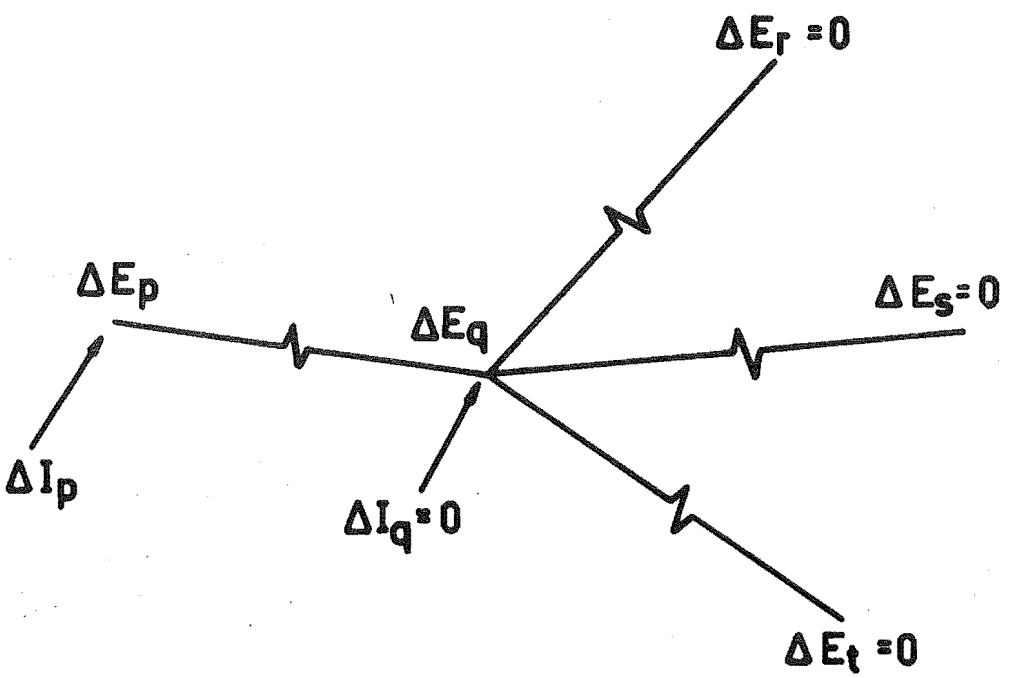

Figure 5.1: Secondary Adjustment at Bus q when Primary Adjustment is at Bus p

5.2.4 Voltage Controlled Buses

The development of the bus adjustment formulas has so far been limited to the consideration of load buses. We now consider the adjustment of voltage controlled buses. Before a voltage controlled bus receives primary adjustment the reactive power is adjusted to meet the specified voltage magnitude[1]. The primary adjustment to satisfy the bus boundary condition and the corresponding secondary adjustments on the adjacent buses can then be applied in the same manner for a load bus. The voltage controlled buses do not however receive secondary adjustments. Consequently, in this instance the summation in the expression for the effective admittance,

$$(13) \qquad Y_{pp}^{eff} = Y_{pp} - \Sigma_q \frac{Y_{pq} Y_{qp}}{Y_{qq}}$$

does not include any adjacent buses which are voltage controlled.

5.2.5 Acceleration Factors

As with the conventional method the rate of convergence can be increased by accelerating the voltage adjustments. Several schemes have been tested and the most rapid convergence has been obtained by increasing the total bus voltage difference between successive iterations by a constant acceleration factor.

5.3 DESCRIPTION OF THE ALGORITHM

This section describes the procedure of the modified nodal iterative loadflow. The following procedure can, if desired, be implemented with simple changes to a conventional nodal iterative loadflow program.

i) Initialize all bus voltages to 1.0+j0.0.

ii) Calculate the effective admittance for each bus,

$$Y_{pp}^{eff} = Y_{pp} - \sum_{q} Y_{pq}Y_{qp}/Y_{qq}$$

iii) Commence a new iteration, initialize p=1.

iv) Calculate the current mismatch on bus p,

$$\Delta I_p = S_p^*/E_p^{*OLD} - (Y_{pp}E_p^{OLD} + \Sigma_q Y_{pq}E_q^{OLD})$$

v) Calculate the primary adjustment,

$$\Delta E_p = \Delta I_p/Y_{pp}^{eff}.$$

vi) Calculate the new bus voltage including acceleration,

$$E_p^{NEW} = E_p^{SAVE} + \alpha(E_p^{OLD} - E_p^{SAVE} + \Delta E_p).$$

vii) Apply secondary adjustments to adjacent buses,

$$E_q^{NEW} = E_q^{OLD} - \frac{Y_{qp}}{Y_{qq}} (E_p^{NEW} - E_p^{OLD})$$

viii) Save the new voltage on bus p,

$$E_p^{SAVE} = E_p^{NEW}.$$

ix) Step onto the next bus and return to step iv) if all buses have not been adjusted. Otherwise, check for convergence and return to step iii) if further iterations are required.

In the modified procedure additional storage is required only for the variables Y_{pp}^{eff} and E_p^{SAVE}.

5.4 EVALUATION OF PROPOSED ALGORITHM

5.4.1 Test Systems

The performance of the proposed algorithm has been compared with that of the conventional and bootstrap[5] algorithms with several practical test systems:

i) A 39 bus system

ii) The NZED South Island system

iii) The IEEE 118 bus test system

iv) A modified version of the IEEE system with synchronous condenser buses converted to load buses.

Principal characteristics of these systems are given in Table 5.1. In each loadflow study a voltage tolerance of .0001 was used as the test for convergence.

	39 Bus	NZED South Island	IEEE 118 Bus	Modified IEEE
Buses	39	185	118	118
Lines	35	123	170	170
Transformers	11	133	9	9
Loads	19	51	91	91
Shunts	0	8	14	14
Voltage Controlled buses	10	26	54	18

Table 5.1: Principal System Characteristics.

5.4.2 Convergence Characteristics

The convergence characteristics of the various algorithms are compared in figures 5.2 to 5.5 for each test system. Each point on the curves represents a loadflow solution. Care has been taken to accurately determine the minimum point on each curve. If we compare the minimum points the proposed

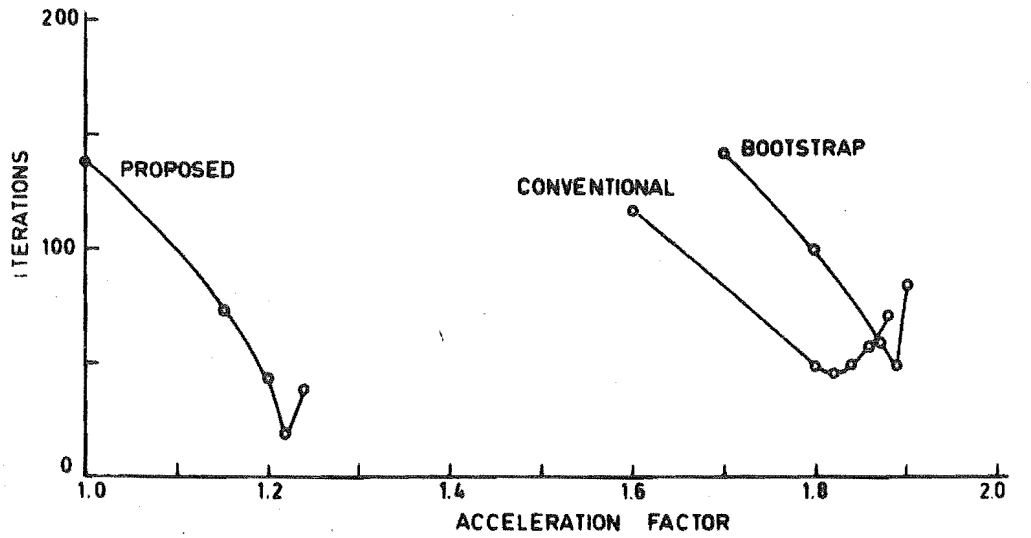

Figure 5.2: Convergence Characteristic for 39 Bus System

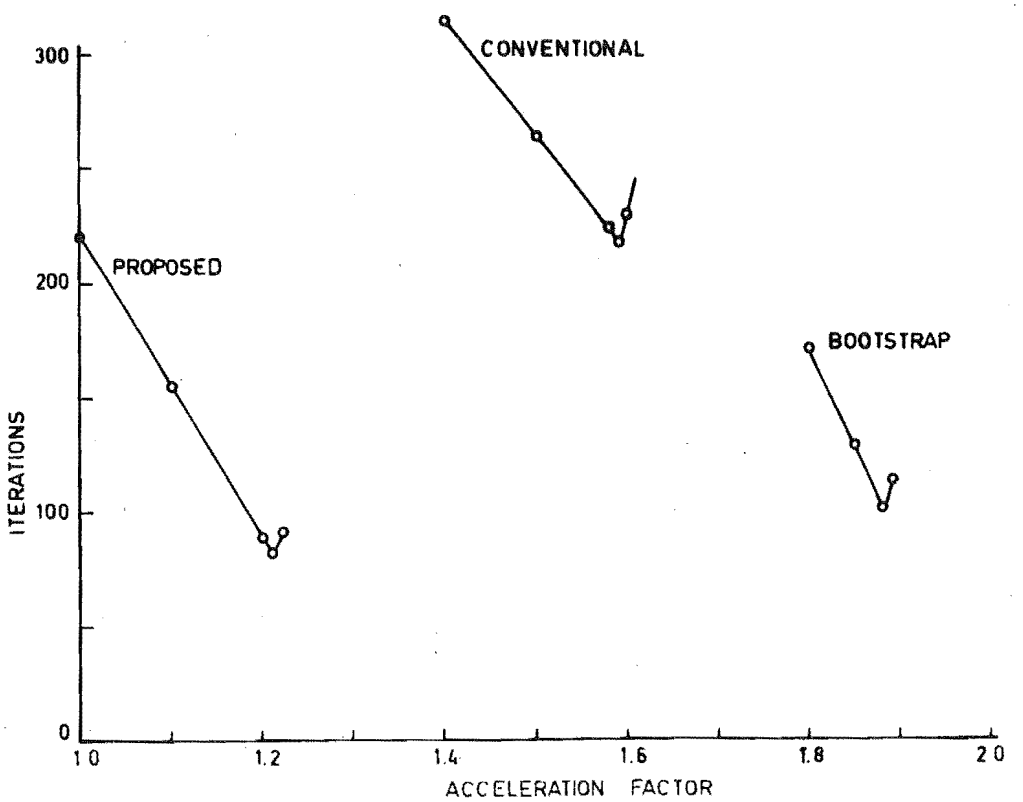

Figure 5.3: Convergence Characteristic for NZED South Island System

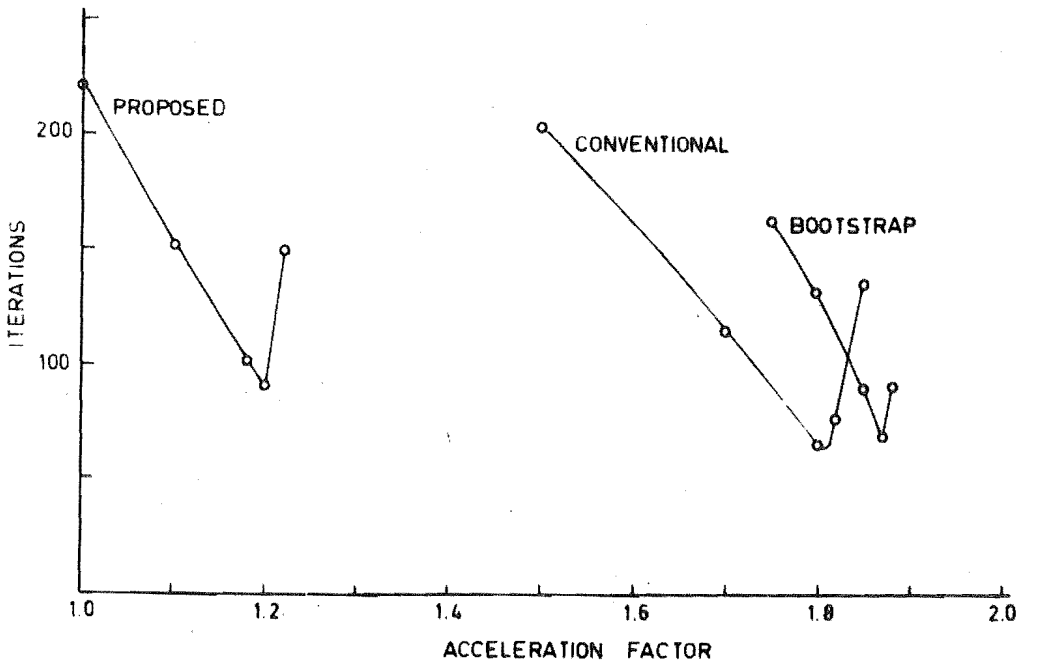

Figure 5.4: Convergence Characteristic for IEEE 118 Bus Test System

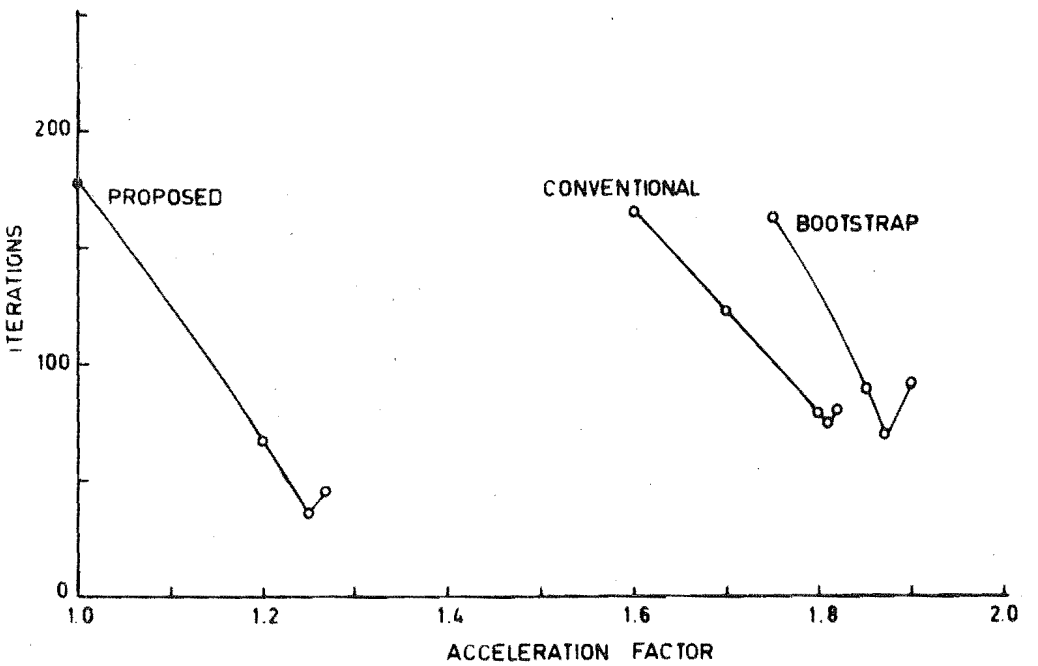

Figure 5.5: Convergence Characteristic for Modified IEEE System

algorithm requires significantly less iterations than the conventional or bootstrap algorithms for the 39 bus and NZED systems, but somewhat more iterations for the IEEE system. The slower convergence in the IEEE system was found to be associated with an unusually high proportion of non-radial voltage-controlled buses. Since secondary adjustments are not applied to voltage controlled buses the full benefits of the proposed modification are not obtained. When the IEEE 118 bus system was altered by converting a fairly large number of synchronous condenser buses to load buses the proposed method again required less iterations than the others (see figure 5.5).

The proposed method is not nearly so dependent upon the use of acceleration factors to obtain fast convergence. Even when no acceleration is applied ($\alpha = 1.0$) the proposed algorithm converges in a comparatively low number of iterations. In loadflow studies where there is little prior information on convergence behaviour an acceleration factor of 1.2 will generally be a suitable choice. It is a fairly safe value and usually gives near optimum convergence.

5.4.3 Comparison of Solution Times

From figures 5.2 to 5.5 the studies with optimum acceleration factors have been taken and the solution times with an IBM 360/44 are given in Table 5.2. These times are naturally dependent to some extent upon programming but they will serve to give a representative comparison of the methods. The times per iteration, which are independent of the acceleration factor, have also been included in Table 5.2 to show the relative amount of computation required by each algorithm. Both the bootstrap algorithm and the proposed algorithm require approximately 50% more time per iteration than the conventional

	Optimum acceleration	Iterations	Time per iteration, sec.	Solution time sec.	Solution time % of conventional	Largest mismatch MVA
39 Bus system						
Conventional	1.82	44	.130	5.7	100	.75
Bootstrap	1.89	48	.202	9.7	170	3.7
Proposed	1.22	18	.194	3.5	61	.45
NZED system						
Conventional	1.59	218	.447	97.7	100	1.73
Bootstrap	1.88	101	.731	73.9	76	.10
Proposed	1.21	80	.746	59.6	61	.52
IEEE system						
Conventional	1.8	65	.412	26.8	100	.68
Bootstrap	1.87	69	.586	40.4	152	.23
Proposed	1.20	90	.580	52.1	194	.69
Modified IEEE system						
Conventional	1.81	74	.316	23.4	100	.63
Bootstrap	1.87	69	.500	34.5	147	.12
Proposed	1.25	36	.508	18.3	78	.14

Table 5.2: Performance of Proposed Algorithm in Comparison with Conventional and Bootstrap Algorithms.

algorithm. Table 5.2 shows that for all systems except the original IEEE system the proposed algorithm requires significantly less solution time than either the conventional or bootstrap algorithms.

5.4.4 Comparison of Mismatches

Although the criterion for solution convergence was that the magnitude of the largest voltage change during an iteration should not exceed .0001, a more practical and meaningful assessment of the solution accuracy is given by using the converged solution to calculate the mismatch in power at each bus. Table 5.2 includes the magnitudes of the greatest power mismatches for the studies with optimum acceleration. The mismatches for the proposed and bootstrap algorithms are usually several times less than those for the conventional algorithm.

5.5 CONCLUSIONS

This chapter has described a modified nodal iterative loadflow algorithm. Test studies with practical systems have demonstrated that the proposed algorithm may give significant savings in solution time. The modification can be incorporated into existing nodal iterative programs with little increase in program complexity or storage requirement.

This chapter has concentrated on the improvement in the speed of convergence with the proposed algorithm. In the following chapter the proposed algorithm is further studied and it is shown that it also gives improved reliability in convergence with series capacitors.

REFERENCES

*1. A.F. Glimn, G.W. Stagg, "Automatic Calculation of Load Flows", AIEE Trans., vol.76, pt.III, 1957, pp.817-828.

2. H.E. Brown, G.K. Carter, H.H. Happ, C.E. Person, "Power Flow Solution by Impedance Matrix Iterative Method", IEEE, PAS-82, 1963, pp.1-9.

3. W.F. Tinney, C.E. Hart, "Power Flow Solution by Newton's Method", IEEE, PAS-86, 1967, pp.1449-1460 .

*4. J.M. Undrill, O.J. Denison, D. Hayward, "Dispatchers Load Flow for the REMVEC Dispatch Centre", Presented at IEEE Summer Power Meeting, Dallas, Texas, 1969.

5. J.A. Treece, "Bootstrap Gauss-Seidel Load Flow", Proc. IEE, Vol.116, 1969, pp.866-870.

CHAPTER 6

MODIFIED NODAL ITERATIVE LOADFLOW ALGORITHM - IMPROVEMENT IN RELIABILITY WITH SERIES CAPACITORS

6.1 INTRODUCTION

A well known characteristic of the conventional nodal iterative method is its failure to converge in the presence of series capacitors. In loadflow studies these elements may occur due to the series compensation of transmission lines[1,2] and they may also occur in the equivalent circuits of three winding transformers[3]. In this chapter the problem of obtaining convergence with series capacitors is studied. It is shown that for practical situations the problem can be largely overcome by the use of the modified nodal iterative method which has been proposed in Chapter 5.

6.2 NETWORK EQUATIONS

For the purpose of describing the convergence of the nodal iterative method with series capacitors we consider the solution of the bus admittance equations:

$$I = Y E \tag{1}$$

It is convenient to consider this set of equations because the developments can be easily adapted to either the linearized D.C. loadflow or the normal A.C. loadflow. The majority of the computer studies have in fact been made with a D.C. loadflow program. Both D.C. and A.C. nodal iterative loadflows have similar convergence difficulties with series capacitors and the conclusions drawn from the D.C. loadflow studies are equally applicable to the A.C. loadflow problem. However, the D.C.

loadflow is easier to analyze and requires less computation than the A.C. loadflow.

6.3 AN APPROXIMATE CONVERGENCE CRITERION

A criterion is developed for evaluating the convergence behaviour of the methods which are studied. We define the current mismatch as the difference between the required current and the current with the assumed voltages on a given iteration:

$$\Delta I^K = I - YE^K \tag{2}$$

The condition for convergence is that the current mismatch on each bus must tend to zero as the iteration procedure progresses; i.e. $\Delta I^K \to 0$ as K, the number of iterations, increases. On successive iterations the vectors of bus current mismatch can be related by a transition matrix:

$$\Delta I^{K+1} = A\Delta I^K \tag{3}$$

An exact criterion for convergence is that the eigenvalues of the matrix A must all have less than unit magnitude[4]. However, there are several limitations in using the eigenvalues to evaluate convergence behaviour:

i) The eigenvalues cannot be easily related to the network admittances. They can be calculated only for specific networks and this gives little insight into general convergence behaviour.

ii) If the convergence of a specific network is to be studied then it is much easier to simply attempt a solution rather than calculate the eigenvalues of the transition matrix.

These limitations are overcome by considering an approximate convergence criterion which requires the diagonal transition elements to have less than unit magnitude. That is, we require:

$$(4) \qquad |A_{pp}| < 1.$$

This approximate criterion has a number of advantages:

i) The elements of the transition matrix can be expressed in terms of network admittances.

ii) For power system networks the transition matrix is diagonally dominant and the approximate criterion gives a remarkably good assessment of the convergence.

iii) One of the main convergence problems with series capacitors actually arises from singularities in the diagonal transition elements.

Expressions for the diagonal transition elements in terms of admittances are derived in an appendix (section 6.7).

6.4 D.C. LOADFLOW STUDIES

The convergence of the nodal iterative method has been studied by including several different series capacitor configurations into the 39 bus system which was also used in chapter 5. The modified sections of the 39 bus system are shown in figure 6.1. A study of the convergence of three nodal iterative methods has been made while the value of capacitor reactance, X_c, is varied. The methods are:

i) The conventional nodal iterative method.

ii) The modified nodal iterative method with primary and secondary adjustments (see chapter 5). This method is referred to as modified method-I.

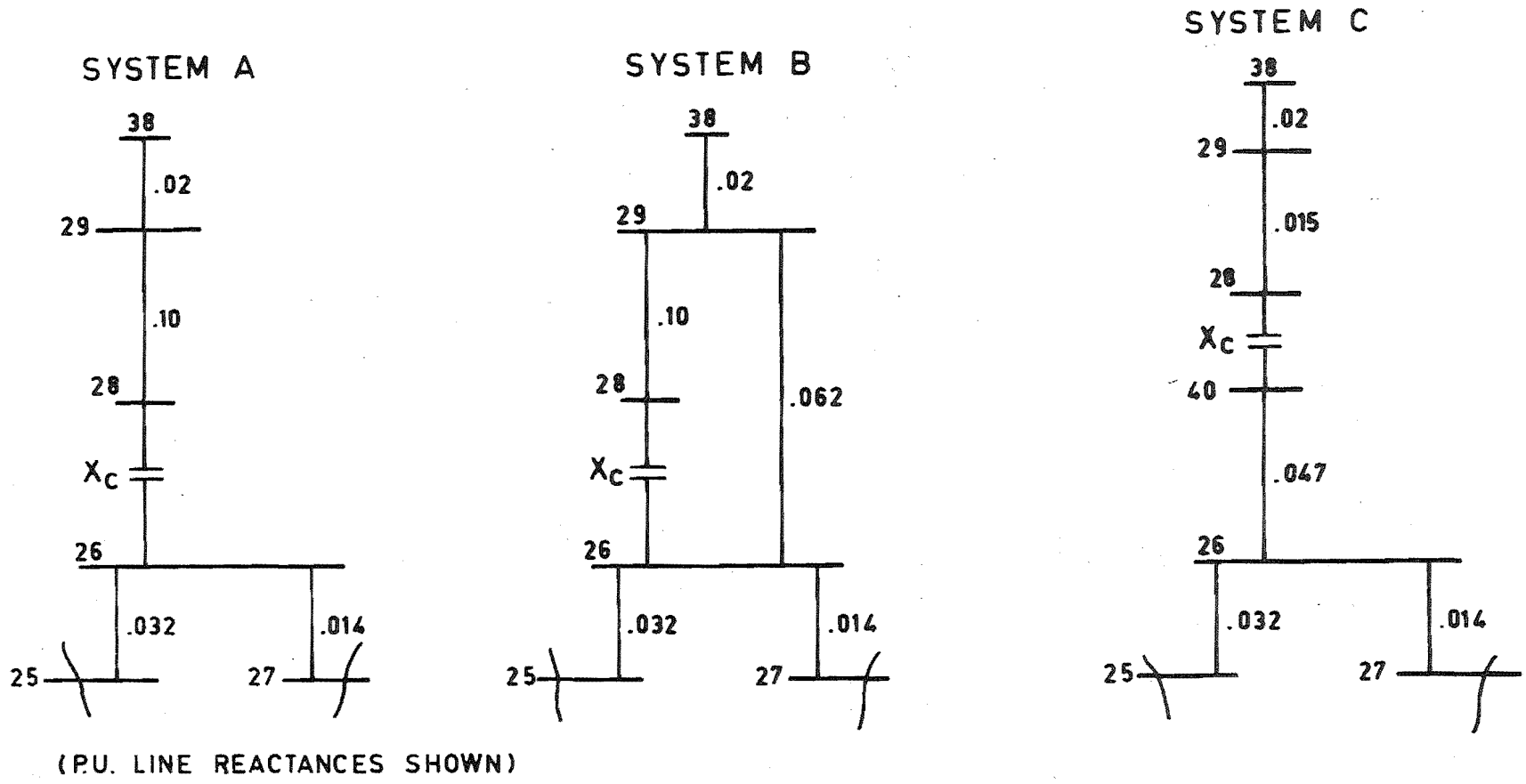

Figure 6.1: Test Configurations with Series Capacitors

iii) A variation of the modified nodal iterative method in which secondary adjustments are applied at capacitor buses only when the bus at the other end of the capacitor receives primary adjustment. This method is referred to as modified method-II.

The results of applying the three methods to the series capacitor configurations in figure 6.1 are shown in figures 6.2, 6.3 and 6.4. The regions in these figures where no graph is plotted indicate that the method in concern would not converge. The figures show that the conventional method diverged for a very large range of X_c values and thus confirm the poor performance of the conventional method with series capacitors. On the other hand a considerable improvement in convergence is obtained with modified method-I and an even greater improvement is obtained with modified method-II. In each system, modified method-II converges over a range of X_c which extends from the lower limit almost right up to the 100% compensation level. This is in fact the complete range which is of practical interest. The convergence behaviour of each method is now explained in turn. To illustrate, the results for system B are analyzed in figures 6.5 to 6.10.

i) Conventional method

Figure 6.5 shows graphs of the self admittances of the buses connected to the series capacitor in system B. In section 6.7 the diagonal transition elements for the conventional method are derived as:

$$A_{pp} = \sum_{q} \frac{Y_{pq} Y_{qp}}{Y_{pp} Y_{qq}} \qquad (5)$$

Graphs of the transition elements for the capacitor buses are shown in figure 6.6. The divergence of the conventional

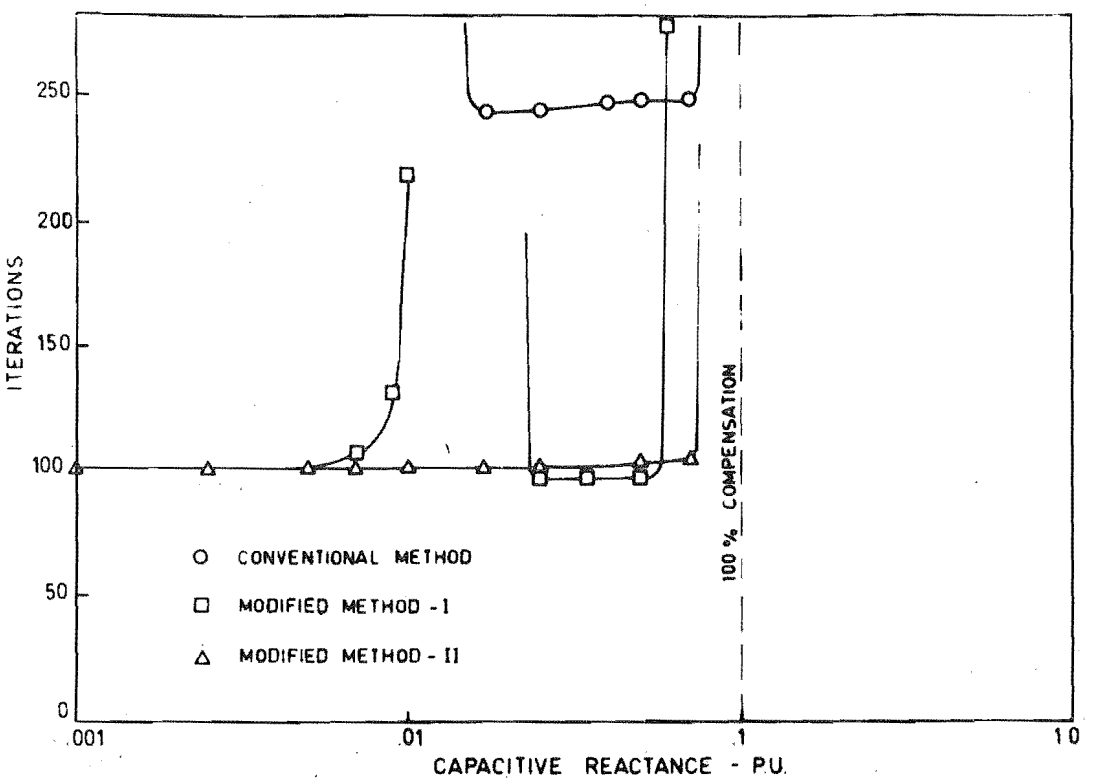

Figure 6.2: D.C. Loadflow Convergence for System A

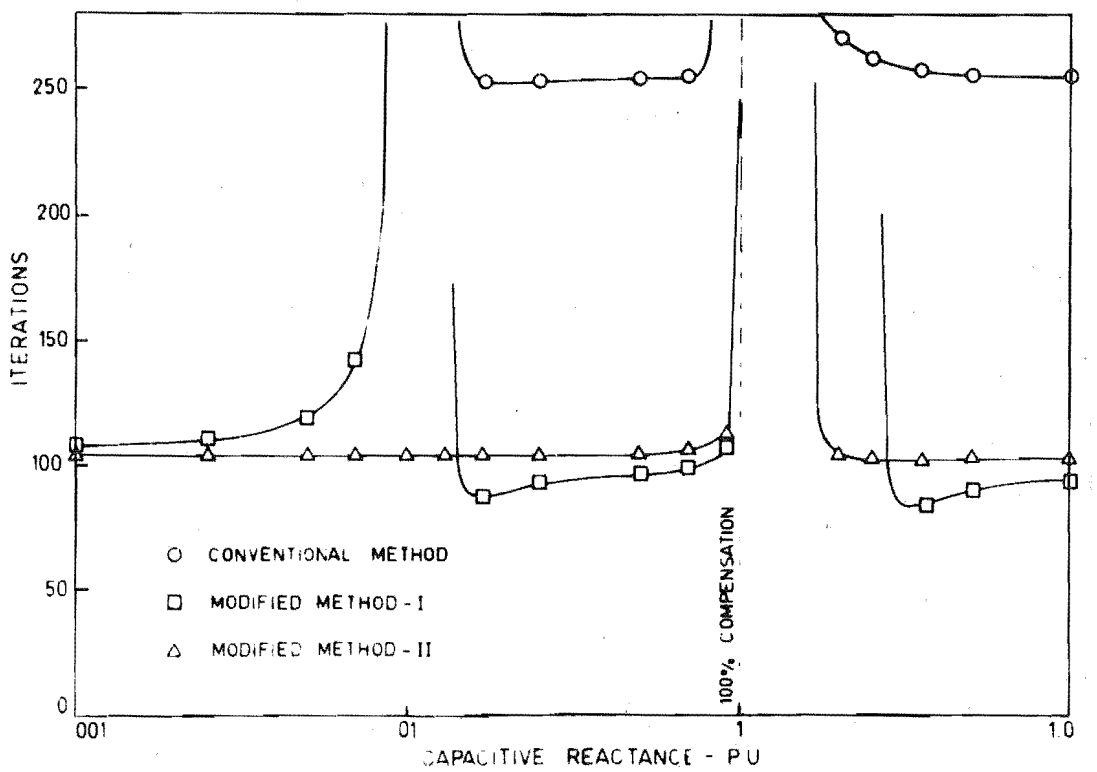

Figure 6.3: D.C. Loadflow Convergence for System B

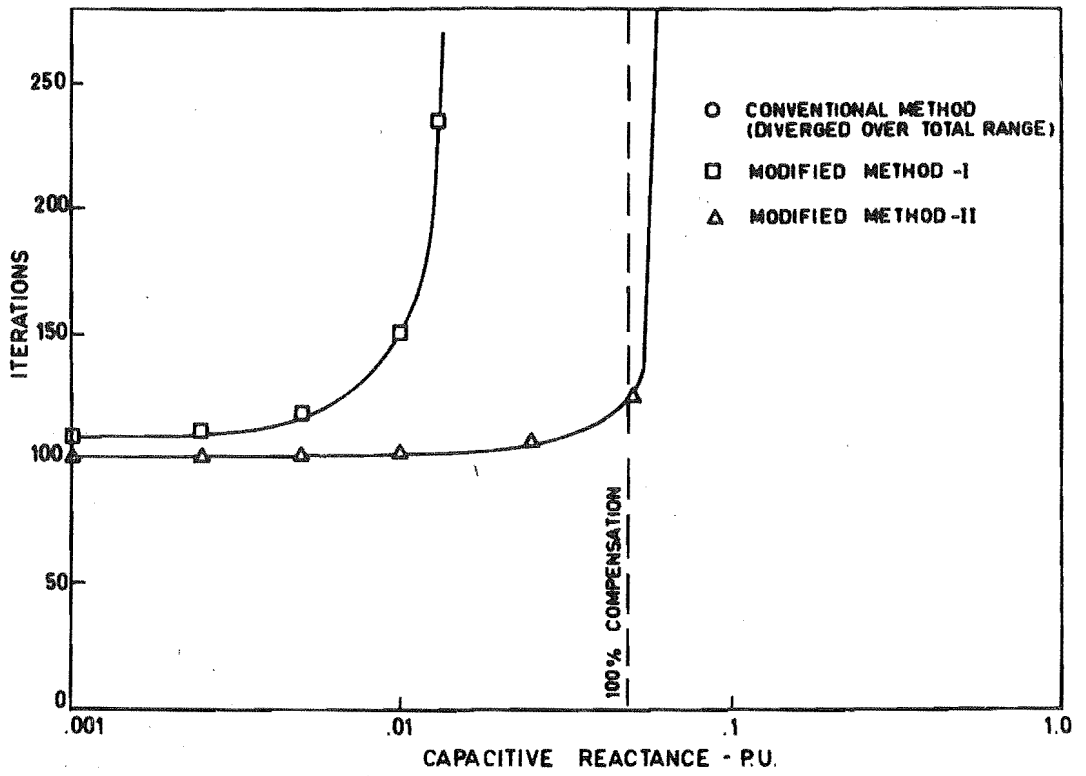

Figure 6.4: D.C. Loadflow Convergence for System C

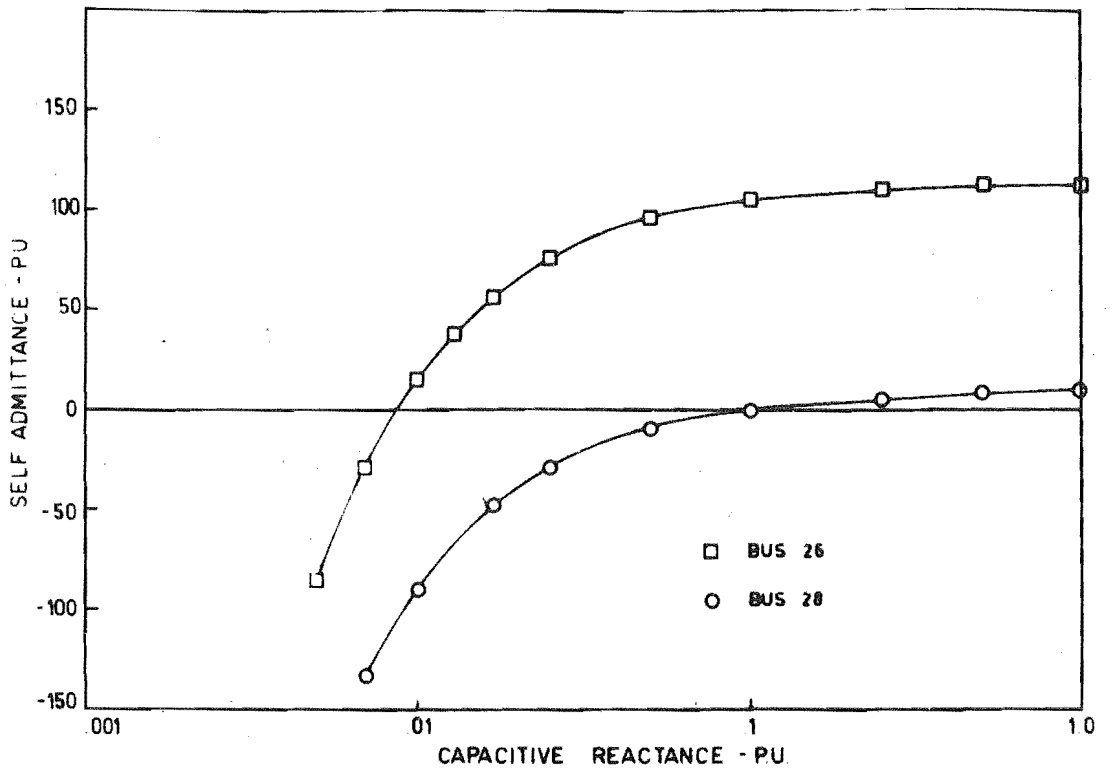

Figure 6.5: Self Admittances of Capacitor Buses

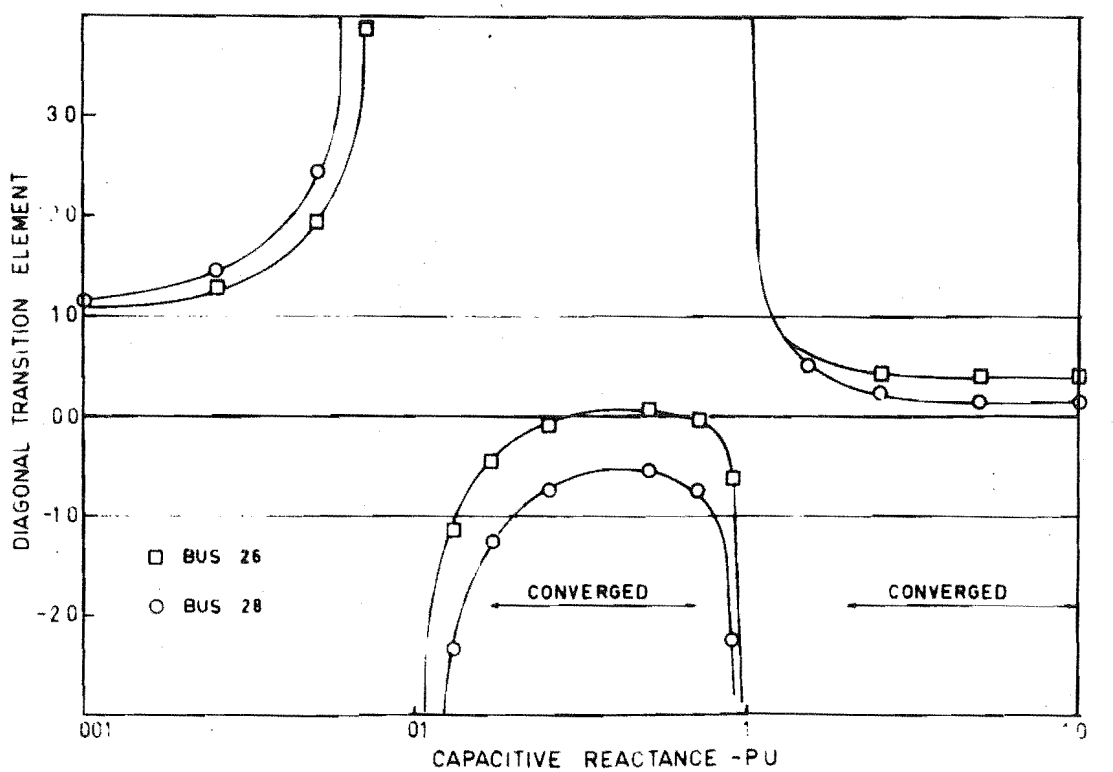

Figure 6.6: Transition Elements of Capacitor Buses with Conventional Method

method is associated with two factors:

i) The low values of X_c give values of $\left|\frac{Y_{pq}}{Y_{pp}}\right|$ and hence $|A_{pp}|$ which are slightly greater than unity.

ii) A zero in the self admittance of a capacitor bus introduces a singularity into the transition element of the capacitor bus and adjacent buses. A zero in Y_{pp} can also be interpreted as a resonant condition which is induced by grounding buses adjacent to bus p.

ii) Modified method-I

In modified method-I the effective bus admittance:

$$(6) \qquad Y_{pp}^{eff} = Y_{pp} - \Sigma_q \frac{Y_{pq}Y_{qp}}{Y_{qq}}$$

is used in performing the primary bus adjustments (see Chapter 5). The divergence of the modified method is associated with the zeros in the effective admittances which occur on capacitor buses and buses adjacent to capacitor buses (see figures 6.7 and 6.8). The zeros in the effective admittances introduce singularities into the diagonal transition elements (section 6.7):

$$(7) \qquad A_{pp} = \frac{1}{Y_{pp}^{eff}} \Sigma_q \frac{Y_{pq}Y_{qp}}{Y_{qq}Y_{pp}} \Sigma_r \frac{Y_{qr}Y_{rq}}{Y_{rr}^{eff}} .$$

Figure 6.9 shows graphs of A_{pp} for the capacitor buses. A zero in Y_{pp}^{eff} can be interpreted as a resonant condition which is induced by grounding buses two removed from bus p.

Modified method-I gives good convergence for low values of X_c since the effective admittances are insensitive to values in this range. This will not apply, however, if there is a chain of two or more capacitors.

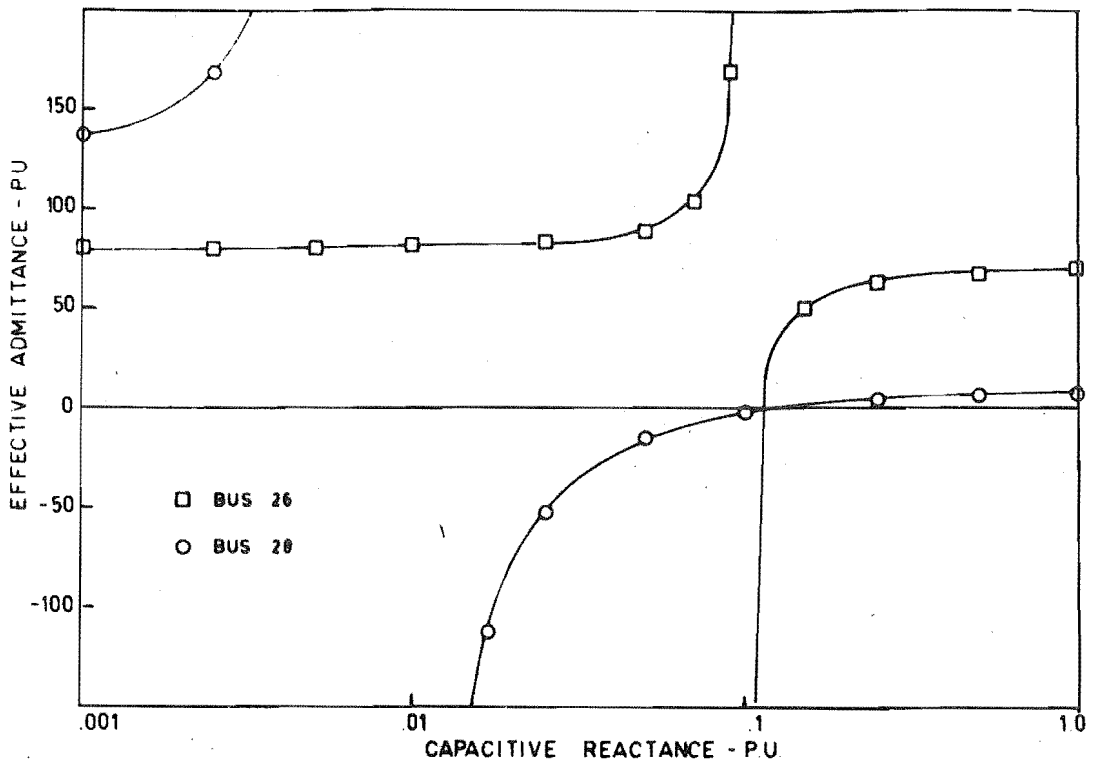

Figure 6.7: Effective Admittances of Capacitor Buses for Modified Methods

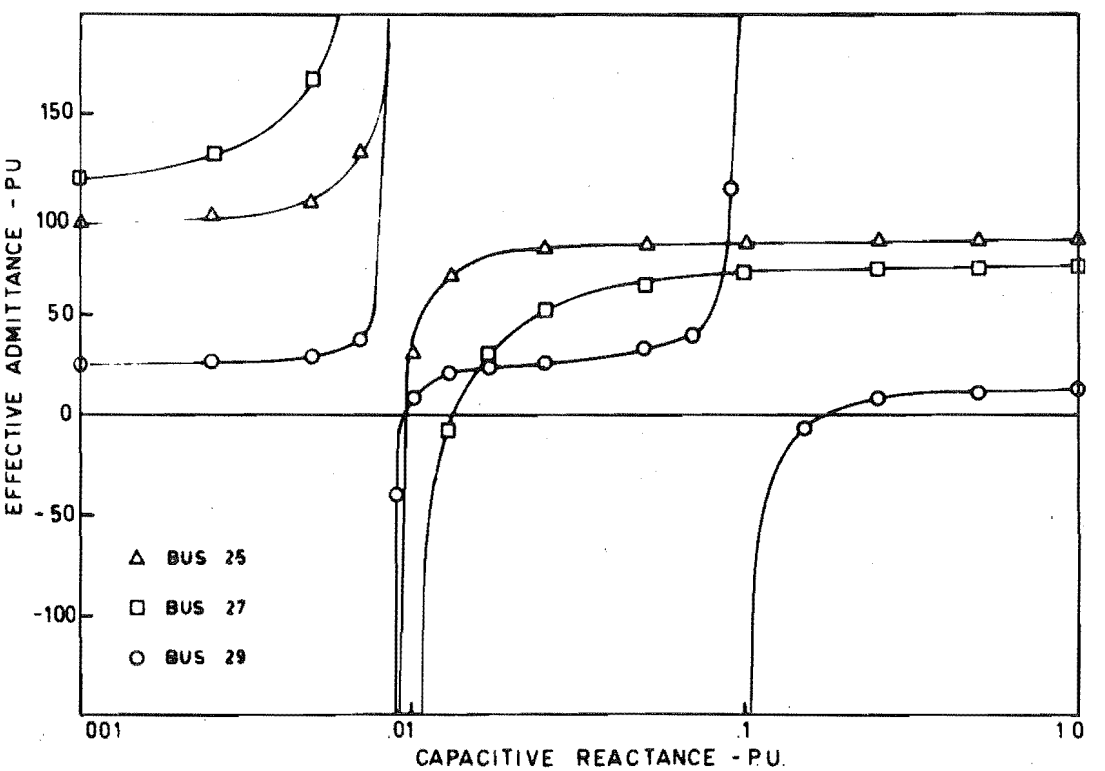

Figure 6.8: Effective Admittances of Buses Adjacent to Capacitor Buses for Modified Method-I

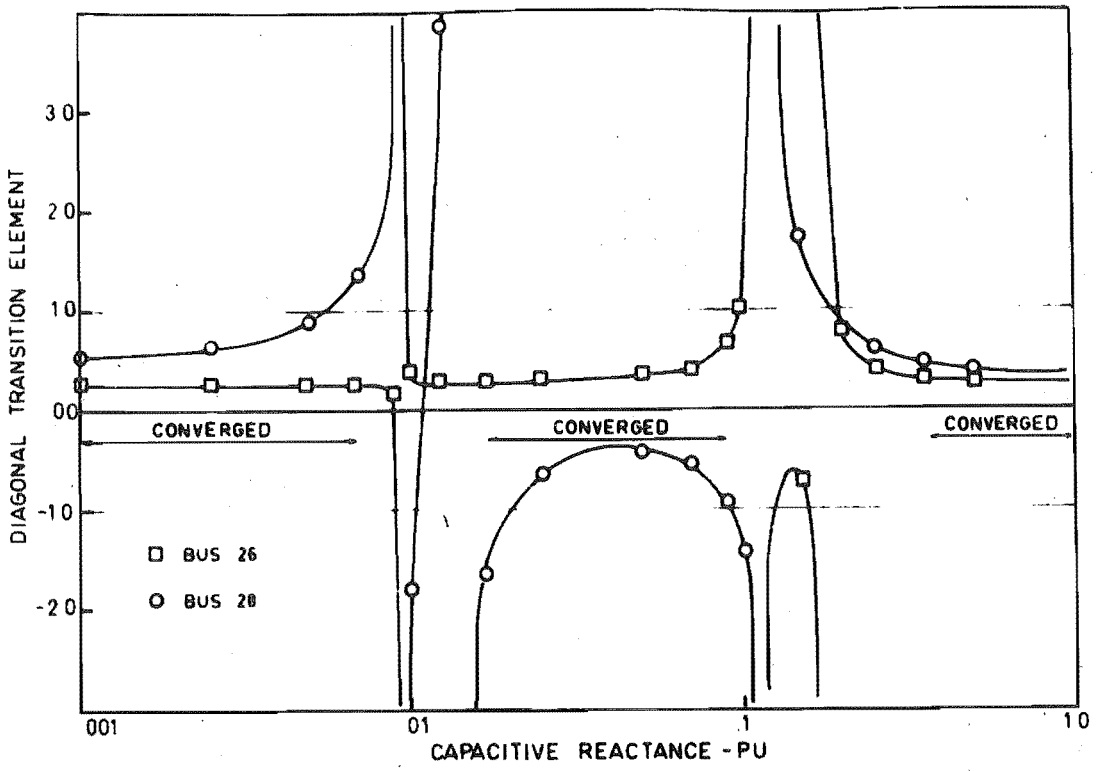

Figure 6.9: Transition Elements of Capacitor Buses for Modified Method-I

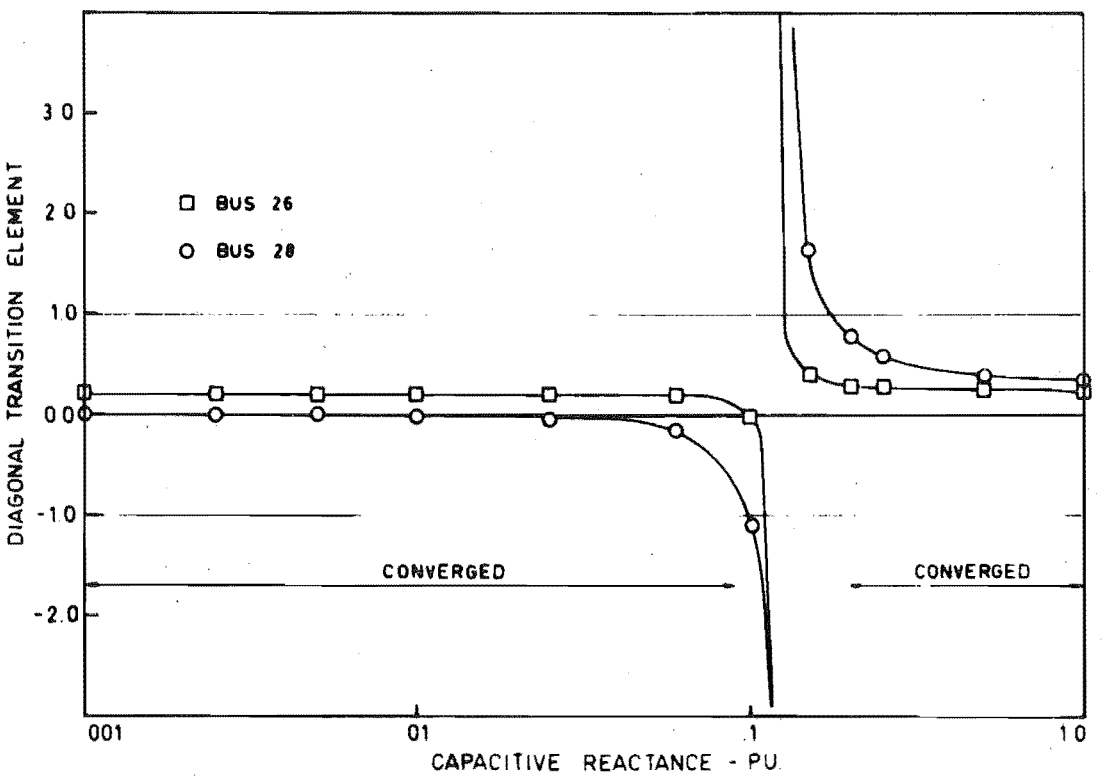

Figure 6.10: Transition Elements of Capacitor Buses for Modified Method-II

iii) Modified Method-II

In this method secondary adjustments are applied to capacitor buses only when the bus at the other end of the capacitor receives primary adjustment. Thus, in the expression for the effective admittance:

$$(8) \qquad Y_{pp}^{eff} = Y_{pp} - \Sigma_q \frac{Y_{pq} Y_{qp}}{Y_{qq}}$$

the index q does not include adjacent capacitor buses unless bus p is at the other end of the capacitor. The effective admittances of buses adjacent to capacitor buses are therefore independent of X_c. Consequently, in modified method-II zeros occur in the effective admittances of only the capacitor buses. This is the reason for the improved convergence. The graphs in figure 6.7 represent the effective admittances of the capacitor buses for modified method-II as well as method-I. For method-II all the zeros in the effective admittances occur for overcompensated values of X_c, that is outside the practical range. Figure 6.10 shows the transition elements of the capacitor buses and explains the improved convergence. The graphs in figure 6.10 were obtained using (37) as derived in section 6.7.

6.5 A.C. LOADFLOW STUDIES

The results of A.C. loadflow studies on system A are shown in figure 6.11. The results confirm that the convergence behaviour of the three methods is similar for both the D.C. and A.C. loadflow situations (compare figures 6.2 and 6.11). Thus, the conclusions which were drawn from the D.C. loadflow studies can be equally applied to the A.C. loadflow situation.

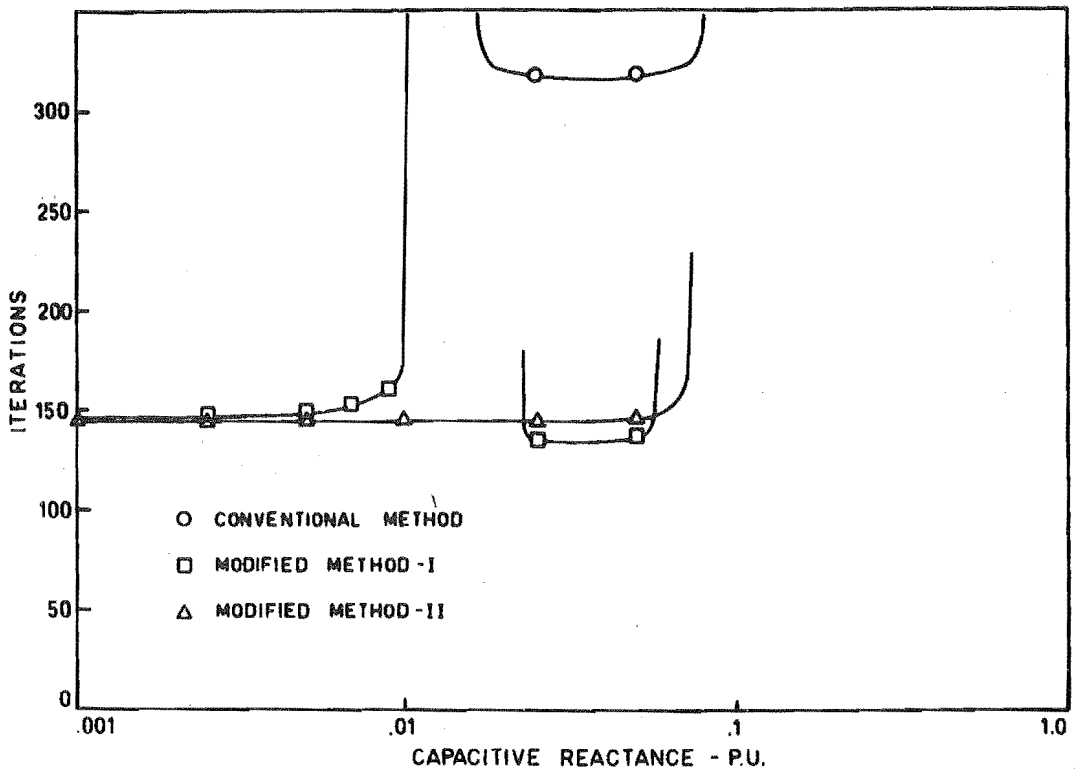

Figure 6.11: A.C. Loadflow Convergence for System A

A.C. loadflow studies have been made of the NZED South Island system which contains series capacitor elements in the star equivalents of nine three winding transformers. The conventional method would not converge in the presence of any of the low capacitive reactances which existed in the star equivalents. To obtain convergence it was necessary to transform the star equivalents to delta equivalents so that the low capacitive reactances were replaced by comparatively large capacitive reactances. When all three winding transformers were represented as delta equivalents the conventional method converged in 230 iterations with an acceleration of 1.6.

In modified method-I the three winding star equivalents caused divergence in only two situations. These are shown in figures 6.12 and 6.13. In figure 6.12 divergence is caused by two capacitive elements being connected to the common 33 kV bus. In figure 6.13 divergence is caused by a very low effective admittance on the 11 kV generator bus. The modified method-I converged when one of the Halfway Bush transformers and the Roxburgh transformer were represented by delta equivalents. With no acceleration convergence was obtained in 239 iterations.

For the modified method-II only the capacitor configuration in figure 6.12 caused divergence. When one of the Halfway Bush transformers was represented by a delta equivalent the method converged in 320 iterations with no acceleration.

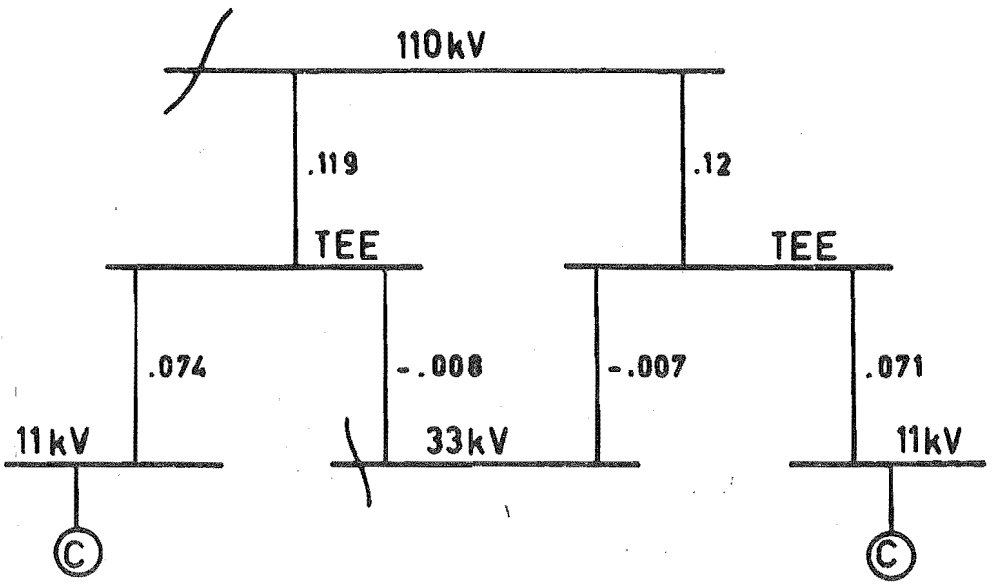

Figure 6.12: Reactances of Halfway Bush Three Winding Transformer Star Equivalents

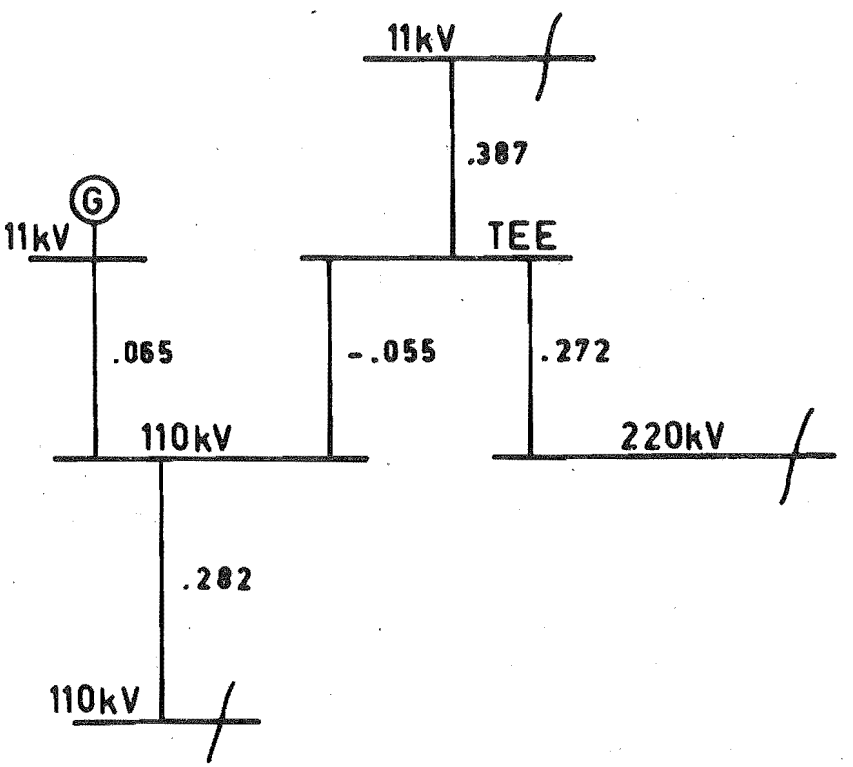

Figure 6.13: Reactances in Vicinity of Roxburgh Three Winding Transformer Star Equivalent

6.6 CONCLUSIONS

This chapter has evaluated the ability of the conventional nodal iterative and the modified nodal iterative method developed in chapter 5 to converge in the presence of series capacitors. The results have confirmed that the reliability of the conventional method is very poor in these circumstances. The modified nodal iterative method has given greatly improved convergence. By applying the secondary adjustments selectively convergence has been obtained in almost all the practical situations considered.

The advantages of the modification which has been proposed are thus twofold; it significantly improves the nodal iterative method in both speed and reliability.

6.7 APPENDIX - DERIVATION OF TRANSITION ELEMENTS

We consider an initial condition in which the mismatch vector ΔI^o has only one non-zero element, ΔI_p^o. After one iteration a new mismatch vector is given by,

$$\Delta I^1 = A\Delta I^o \tag{9}$$

Thus,

$$\Delta I_p^1 = A_{pp}\Delta I_p^o. \tag{10}$$

For the given initial condition the transition element A_{pp} is simply the ratio of mismatches $\Delta I_p^1/\Delta I_p^o$. This fact is conveniently used for deriving the diagonal transition elements of the nodal iterative methods described in section 6.4.

i) Conventional method

The mismatch ΔI_p^o is removed from bus p by adjusting the voltage by, (section 5.2.2)

$$\Delta E_p = \Delta I_p^{o}/Y_{pp}. \quad (11)$$

However, new mismatches are subsequently introduced onto the adjacent buses,

$$\Delta I_q = -Y_{qp}\Delta E_p \quad (12)$$

$$= -Y_{qp}/Y_{pp}\ \Delta I_p^{o} \quad (13)$$

For simplicity connections between the adjacent q buses are neglected. The voltage adjustments on the adjacent buses are then,

$$\Delta E_q = -\frac{Y_{qp}}{Y_{qq}Y_{pp}}\ \Delta I_p^{o} \quad (14)$$

These in turn create a new mismatch on bus p,

$$\Delta I_p^{1} = -\Sigma_q\ Y_{pq}\ \Delta E_q \quad (15)$$

$$= \Sigma_q \frac{Y_{pq}Y_{qp}}{Y_{qq}Y_{pp}}\ \Delta I_p^{o} \quad (16)$$

Therefore for the conventional nodal iterative method,

$$A_{pp} = \Sigma_q \frac{Y_{pq}Y_{qp}}{Y_{qq}Y_{pp}} \quad (17)$$

ii) Modified method-I

The transition element A_{pp} is derived with reference to figure 6.14. For simplicity the effects of connections between buses adjacent to bus p and between buses two removed from bus p are neglected. The mismatch ΔI_p^{o} is removed from bus p by the primary adjustment, (section 5.2.3)

$$\Delta E_p = \Delta I_p^{o}/Y_{pp}^{eff}. \quad (18)$$

Corresponding secondary adjustments are also applied to prevent mismatches on the adjacent buses,

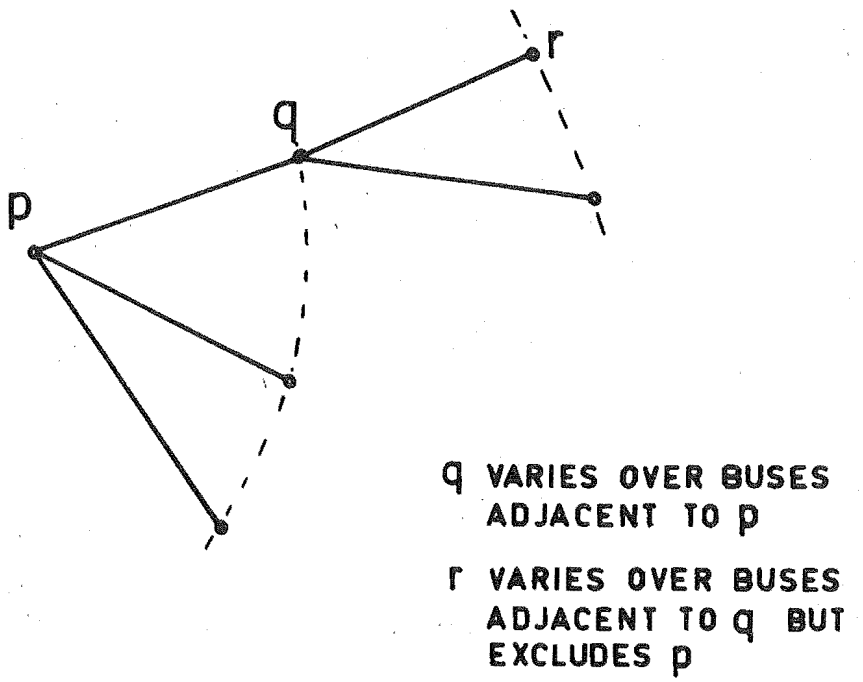

Figure 6.14: Definition of Bus Indexes for Derivation of Transition Elements

$$(19) \qquad \Delta E_q^{\,p} = - \frac{Y_{qp}}{Y_{qq} Y_{pp}^{eff}} \Delta I_p^{\,o}$$

(Superscript p indicates that the secondary adjustment corresponds to the primary adjustment of bus p). As there is no mismatch on the adjacent buses q, their primary adjustment is given by,

$$(20) \qquad \Delta E_q = 0$$

and the corresponding secondary adjustments are,

$$(21) \qquad \Delta E_p^{\,q} = 0$$

and

$$(22) \qquad \Delta E_r^{\,q} = 0$$

A current mismatch is, however, created on the r buses by the earlier secondary adjustments on the q buses,

$$(23) \qquad \Delta I_r = -Y_{rq} \Delta E_q^{\,p}$$

Substituting (19),

$$(24) \qquad \Delta I_r = \frac{Y_{rq} Y_{qp}}{Y_{qq} Y_{pp}^{eff}} \Delta I_p^{\,o}$$

The primary adjustments on the r buses are therefore,

$$(25) \qquad \Delta E_r = \frac{Y_{rq} Y_{qp}}{Y_{qq} Y_{pp}^{eff}} \frac{\Delta I_p^{\,o}}{Y_{rr}^{eff}}$$

The combined secondary adjustments on the q buses are,

$$(26) \qquad \Sigma_r \Delta E_q^{\,r} = -\Sigma_r \frac{Y_{qr} Y_{rq} Y_{qp}}{Y_{qq} Y_{qq} Y_{pp}^{eff} Y_{rr}^{eff}} \Delta I_p^{\,o}$$

The q bus adjustments create a new mismatch on bus p,

$$\Delta I_p^1 = - \Sigma_q Y_{pq} \Sigma_r \Delta E_q^r \quad (27)$$

Substituting (26),

$$\Delta I_p^1 = \frac{1}{Y_{pp}^{eff}} \Sigma_q \frac{Y_{pq}Y_{qp}}{Y_{qq}Y_{qq}} \Sigma_r \frac{Y_{qr}Y_{rq}}{Y_{rr}^{eff}} \Delta I_p^o \quad (28)$$

Thus, for modified method-I the diagonal transition elements are given by,

$$A_{pp} = \frac{1}{Y_{pp}^{eff}} \Sigma_q \frac{Y_{pq}Y_{qp}}{Y_{qq}Y_{qq}} \Sigma_r \frac{Y_{qr}Y_{rq}}{Y_{rr}^{eff}} \quad (29)$$

iii) Modified method-II

In this method secondary adjustments are applied at capacitor buses only when the bus at the other end of the capacitor receives primary adjustment. The expression for the transition element is again derived with reference to figure 6.14. In this case, however, we consider that a capacitor is connected between bus p and an adjacent bus q_c. Assuming an initial mismatch on bus p, the procedure of method-II is the same as for method-I until the primary adjustment of the r buses. At this stage the mismatch on the r buses is given by (24). That is,

$$\Delta I_r = \frac{Y_{rq}Y_{qp}}{Y_{qq}Y_{pp}^{eff}} \Delta I_p^o \quad (30)$$

The primary adjustment of the r buses is,

$$\Delta E_r = \frac{Y_{rq}Y_{qp}}{Y_{qq}Y_{pp}^{eff}} \frac{\Delta I_p^o}{Y_{rr}^{eff}} \quad (31)$$

In this case the effective admittances of the r buses connected to capacitor bus q_c are defined:

$$(32) \qquad Y_{rr}^{eff} = Y_{rr} - \sum_{s \neq q_c} \frac{Y_{rs} Y_{sr}}{Y_{ss}}$$

The secondary adjustments on the q buses are given by,

$$(33) \qquad \Sigma_r \Delta E_q^r = - \sum_r \frac{Y_{qr} Y_{rq} Y_{qp}}{Y_{qq} Y_{qq} Y_{pp}^{eff} Y_{rr}^{eff}} \Delta I_p^o$$

for $q \neq q_c$, and

$$(34) \qquad \Sigma_r \Delta E_q^r = 0 \qquad \text{for } q = q_c.$$

The mismatch created on bus p by the q bus adjustments is,

$$(35) \qquad \Delta I_p^1 = - \sum_{q \neq q_c} Y_{pq} \sum_r \Delta E_q^r$$

$$(36) \qquad = \frac{1}{Y_{pp}^{eff}} \sum_{q \neq q_c} \frac{Y_{pq} Y_{qp}}{Y_{qq} Y_{qq}} \sum_r \frac{Y_{qr} Y_{rq}}{Y_{rr}^{eff}} \Delta I_p^o$$

Thus, for modified method-II the diagonal transition element for a capacitor bus is given by,

$$(37) \qquad A_{pp} = \frac{1}{Y_{pp}^{eff}} \sum_{q \neq q_c} \frac{Y_{pq} Y_{qp}}{Y_{qq} Y_{qq}} \sum_r \frac{Y_{qr} Y_{rq}}{Y_{rr}^{eff}} .$$

REFERENCES

1. E.C. Starr, R.D. Evans, "Series Capacitors for Transmission Circuits", AIEE Trans., vol. 61, 1942, pp.963-973.
2. G.D. Breuer, H.M. Rustebakke, R.A. Gibley, H.O. Simmons, Jr., "The Use of Series Capacitors to Obtain Maximum EHV Transmission Capability", IEEE PAS-83, 1964, pp.1090-1102.
3. E.W. Kimbark, Power System Stability, vol.I, Chapter 3, Wiley, New York, 1948.
4. National Physical Laboratory, Modern Computing Methods, Her Majesty's Stationery Office, London, 1961.

C H A P T E R 7

A SIMPLIFIED AND IMPROVED METHOD FOR CALCULATING TRANSMISSION LOSS FORMULAS

7.1 INTRODUCTION

The economic dispatch of power systems is based upon scheduling generation so that the cost of supplying the system load is minimized. This involves the coordination of generator production costs with system transmission losses. In practice, this is classically achieved by the solution of the coordination equations[1,2],

$$(1) \qquad \frac{dF_i}{dP_{Gi}} \frac{1}{1 - \frac{\partial P_L}{\partial P_{Gi}}} = \lambda$$

The solution of the coordination equations is based upon a loss formula which approximates the system losses in terms of the generator outputs. The most commonly accepted loss formula is based on Kron's B coefficients[5],

$$(2) \qquad P_L = P_G{}^t B_{GG} P_G + P_G{}^t B_{G0} + B_{00}$$

The incremental losses are therefore;

$$(3) \qquad \frac{\partial P_L}{\partial P_G} = 2B_{GG}P_G + B_{G0}$$

The loss formula provides a fast means for calculating incremental losses without the need for direct network solutions. Thus, transmission losses can be coordinated into economic schedules without large overheads in computer time and storage. However, the calculation of the loss formula itself does involve a considerable computation effort. Further, the

simplified form of the loss formula necessarily involves assumptions on the network behaviour and significant errors may occur if these assumptions are violated. Consequently, even though loss formulas have been in use for many years[3-9], there is a continuing interest in methods for improving both their accuracy and speed of calculation[10-15].

In this chapter the development and evaluation of an improved and simplified method for calculating transmission loss formulas is described. The method which is proposed offers the following advantages:

i) The method has a simple theoretical basis. The physical network is retained throughout the derivation.

ii) The method does not require the assumption of generator P/Q relationships.

iii) The loss coefficients can be determined directly from branch admittance and load power data. Supplementary data from A.C. loadflows is not necessary.

iv) Computation requirements are reduced to the extent that loss coefficients can be easily updated on-line to represent actual network status and load conditions.

v) The proposed method gives highly accurate incremental losses, particularly for modern systems with high transmission X/R ratios.

7.2 LOSS FORMULA DEVELOPMENT

The basic problem is to express the system losses as a function of the generator power outputs. A preliminary outline of the development follows.

i) The system losses are separated into voltage magnitude and angle dependent components. They are expressed in the form

$$P_L = \delta^t G_{NN} \delta + P_E \quad (4)$$

ii) The bus voltage magnitudes are assumed to be constant under variations in active power and only variations in the angle dependent loss are considered. The assumption is exact for an all voltage controlled system and is a close approximation for a system with load buses.

iii) The D.C. loadflow is applied to express the bus angles linearly in terms of the bus powers,

$$\delta = Z_{NN} P_N \quad (5)$$

Thus,

$$P_L = P_N^t Z_{NN} G_{NN} Z_{NN} P_N + P_E \quad (6)$$

iv) By separating the load and generator powers and substituting for the loads we obtain an expression of the form,

$$P_L = P_G^t E_{GG} P_G + P_G^t E_{GO} + E_{OO} + P_E \quad (7)$$

which is the desired expression of the losses in terms of the generator powers.

7.2.1 Angle and Magnitude Dependent Losses

The real power loss in the branch pq in figure 7.1 is,

$$P_L = E_{pq}^2 \, g_{pq} \tag{8}$$

Using the cosine rule to expand E_{pq},

$$P_L = (E_p^2 + E_q^2 - 2E_pE_q \cos(\delta_p-\delta_q)) \, g_{pq} \tag{9}$$

In power system operation $\delta_p-\delta_q$ is small and we can approximate,

$$\cos(\delta_p-\delta_q) = 1 - (\delta_p-\delta_q)^2/2 \tag{10}$$

Therefore,

$$P_L = (E_p-E_q)^2 g_{pq} + E_pE_q(\delta_p-\delta_q)^2 g_{pq} \tag{11}$$

In (11) the branch loss is separated into a component which is dependent only on voltage magnitudes and a component which is predominantly dependent on voltage angles. By considering the summation of the components over all the system branches the system loss may be expressed as,

$$P_L = P_\delta + P_E \tag{12}$$

where the magnitude dependent system loss is defined by,

$$P_E = \Sigma_p\Sigma_q \, (E_p-E_q)^2 g_{pq} \tag{13}$$

and the angle dependent system loss is defined by,

$$P_\delta = \Sigma_p\Sigma_q \, E_pE_q(\delta_p-\delta_q)^2 g_{pq} \tag{14}$$

Now, we define the elements of G_{NN} by,

$$G_{NN}(p,p) = \Sigma_q \, E_pE_q \, g_{pq} \tag{15}$$

$$G_{NN}(p,q) = - E_pE_q \, g_{pq}. \tag{16}$$

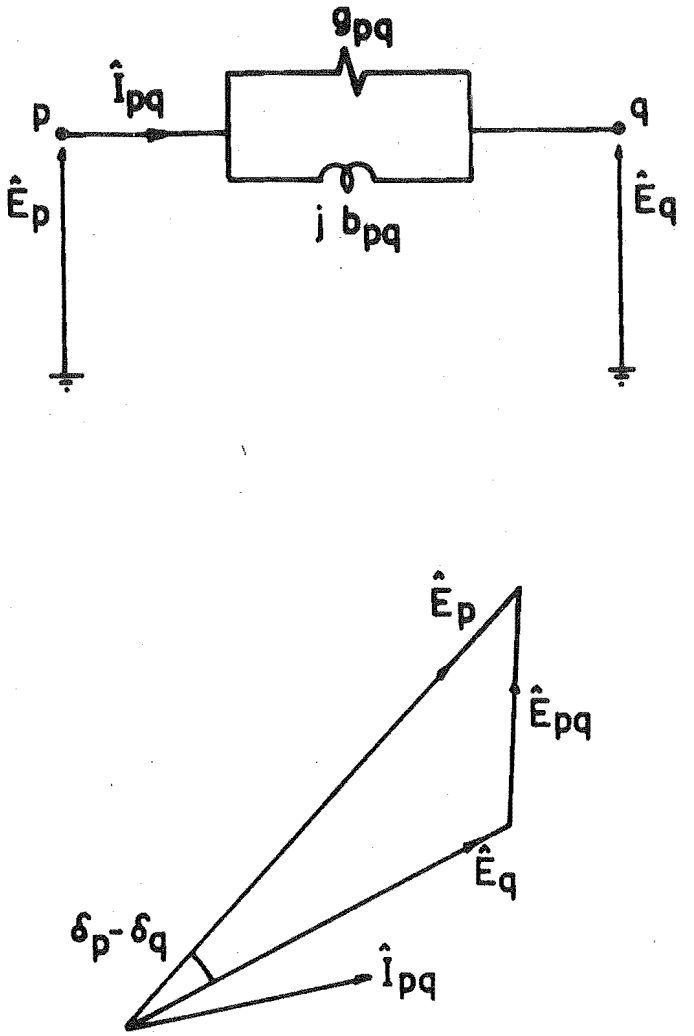

Figure 7.1: Branch Voltage and Current Relationships

The total system loss is therefore,

$$(17) \qquad P_L = \delta^t G_{NN} \delta + P_E.$$

The first step in the loss formula development is achieved. The system losses have been expressed as a quadratic function of the bus voltage angles.

7.2.2 The Linearized D.C. Loadflow

The power flow in branch pq of figure 7.1 can be exactly expressed as,

$$(18) \qquad P_{pq} = E_p . R(\hat{I}_{pq})$$

where $R(\hat{I}_{pq})$ is defined as the component of $\hat{I}_{pq}$ in phase with $\hat{E}_p$. From the vector diagram in figure 7.1, we derive

$$(19) \qquad R(\hat{I}_{pq}) = (E_p - E_q \cos(\delta_p - \delta_q)) g_{pq} - E_q \sin(\delta_p - \delta_q) b_{pq}$$

Thus substituting (19) into (18),

$$(20) \qquad P_{pq} = E_p (E_p - E_q \cos(\delta_p - \delta_q)) g_{pq} - E_p E_q \sin(\delta_p - \delta_q) b_{pq}$$

The terms in (20) are the components of power flow through the branch conductance and the branch susceptance respectively. For the susceptance term we approximate,

$$(21) \qquad \sin(\delta_p - \delta_q) = \delta_p - \delta_q$$

and for the conductance term we approximate,

$$(22) \qquad \cos(\delta_p - \delta_q) = 1.$$

The effect of the error in the latter approximation is reduced by the high X/R ratios of modern transmission systems. (The approximation is studied further in section 7.2.4). Substituting (21) and (22) into (20), we obtain a linearized relation between the branch power and the bus angles,

$$P_{pq} = E_p(E_p - E_q)g_{pq} - E_pE_qb_{pq}(\delta_p - \delta_q) \quad (23)$$

If the equation describing the power balance at each bus is considered we obtain,

$$P_N = M_N + B_{NN}\delta \quad (24)$$

where we define $M_N(p)$, the net conductive flow from bus p, as

$$M_N(p) = \sum_q E_p(E_p - E_q)g_{pq} \quad (25)$$

and B_{NN} by,

$$B_{NN}(p,p) = -\sum_q E_pE_q\, b_{pq} \quad (26)$$

$$B_{NN}(p,q) = E_pE_q\, b_{pq} \quad (27)$$

Equation (24) expresses the bus powers P_N linearly in terms of bus angles δ and it is commonly known as the D.C. loadflow equation. In its most common form the term M_N is neglected but improved accuracy can be obtained by its inclusion. For convenience we hereafter consider the M_N terms to be lumped with the load powers and thus equation (24) becomes,

$$P_N = B_{NN}\delta \quad (28)$$

7.2.3 The D.C. Loadflow Loss Formula

The D.C. loadflow equation (28) is solved for the bus angles,

$$\delta = Z_{NN}\, P_N \quad (29)$$

Substituting (29) into (17) we obtain the losses as a quadratic function of the bus powers,

$$P_L = P_N{}^t Z_{NN}\, G_{NN}\, Z_{NN}\, P_N + P_E. \quad (30)$$

Now, we separate the generator powers P_G from the load powers P_{NL},

$$(31) \qquad \begin{bmatrix} P_N \end{bmatrix} = \begin{bmatrix} P_G \\ 0 \end{bmatrix} + \begin{bmatrix} P_{NL} \end{bmatrix}$$

and we define Z_{NG} as a submatrix of the generator bus columns of Z_{NN}. Substitution of (31) into (30) thus gives,

$$(32) \qquad P_L = P_G{}^t Z_{NG}{}^t G_{NN} Z_{NG} P_G + 2P_G{}^t Z_{NG}{}^t G_{NN} Z_{NN} P_{NL} + P_{NL}{}^t Z_{NN} G_{NN} Z_{NN} P_{NL} + P_E$$

The D.C. loadflow loss coefficients are defined as,

$$(33) \qquad E_{GG} = Z_{NG}{}^t G_{NN} Z_{NG}$$

$$(34) \qquad E_{G0} = 2Z_{NG}{}^t G_{NN} Z_{NN} P_{NL}$$

$$(35) \qquad E_{00} = P_{NL}{}^t Z_{NN} G_{NN} Z_{NN} P_{NL}$$

Thus, the system losses are expressed in terms of the generator powers as,

$$(36) \qquad P_L = P_G{}^t E_{GG} P_G + P_G{}^t E_{G0} + E_{00} + P_E$$

Equation (36) is referred to as the D.C. loadflow loss formula. From (36) the incremental losses are therefore,

$$(37) \qquad \frac{\partial P_L}{\partial P_G} = 2E_{GG} P_G + E_{G0}$$

In the D.C. loadflow loss formula the generation on the slack bus is the dependent variable whereas in Kron's B coefficient loss formula the total system load is the dependent variable[1]. Consequently, calculation of $\frac{\partial P_L}{\partial P_{Gi}}$ from the D.C. loadflow loss coefficients gives the incremental loss when an increment of power is delivered from generator i

to the slack generator. On the other hand, calculation of $\frac{\partial P_L}{\partial P_{Gi}}$ from Kron's B coefficients gives the incremental loss when an increment of power is delivered from generator i to the total load. Nevertheless, the coordination equations (1) are valid for both definitions and they are equally acceptable in practice. Hereafter, we assume that the incremental losses are calculated from the D.C. loadflow loss coefficients in (37).

The matrix E_{GG} is independent of the load powers and only the vector E_{G0} and the scalar E_{00} are affected. It is commonly assumed that the load powers vary uniformly as a fixed proportion of the total load. In this case the E_{G0} coefficients are linear functions and the E_{00} coefficient is a quadratic function of the total load.

7.2.4 Versions of D.C. Loadflow Loss Formula

Three versions of the D.C. loadflow loss formula are proposed to suit different practical situations (Section 7.4.5). As shown in Table 7.1, each version requires a different amount of system data. As more data is used the loss formula becomes more accurate but over a more restricted range of system conditions. The voltage magnitude data required for versions II and III can be obtained from A.C. loadflows, but for on-line application telemetered measurements could be conveniently used.

The foregoing development has been specifically for version II. However, only minor modifications are required for versions I and III. For version I all bus voltage magnitudes are simply set to unity. The vector M_N in the D.C. loadflow equation (24) then becomes zero in line with the

more common form. For version III a base case set of generator outputs is used to further improve the accuracy of the D.C. loadflow equation (24). For the conductance term in the branch power equation (20), we approximate,

$$\cos(\delta_p - \delta_q) = \cos(\delta_p' - \delta_q') \tag{38}$$

where the angles δ' are determined by a preliminary D.C. loadflow using the base case generator outputs.

	Version I	Version II	Version III
Branch Admittances	Yes	Yes	Yes
Load Powers	Yes	Yes	Yes
Bus Voltage Magnitudes	No	Yes	Yes
Generator Powers	No	No	Yes

Table 7.1: Data Requirements of D.C. Loadflow Loss Formulas.

7.3 ALGORITHM

The algorithm for calculating the D.C. loadflow loss coefficients (Version II) is as follows:

1. Read the branch admittances and the load powers. Also read the bus voltage magnitudes and the generator powers if these are required.
2. Assemble the matrices G_{NN} and B_{NN} from (15), (16) and (26), (27).
3. Calculate M_N from (25).
4. Reduce B_{NN} by ordered elimination to triangular form. (See Chapter 3).

5. Calculate each column of Z_{NG} by repeated solution of,

$$P_N = B_{NN}\delta$$

Each generator bus power is respectively set to unity with all other bus powers zero. The resulting solutions for δ form the respective columns of Z_{NG}.

6. Calculate,

$$E_{GG} = Z_{NG}{}^{t}G_{NN}Z_{NG}$$

7. Calculate the term $Z_{NN}P_{NL}$ by solving,

$$P_{NL} = B_{NN}(Z_{NN}P_{NL})$$

8. Calculate,

$$E_{G0} = 2.Z_{NG}{}^{t}G_{NN}(Z_{NN}P_{NL})$$

9. Calculate,

$$E_{00} = (Z_{NN}P_{NL})^{t}G_{NN}(Z_{NN}P_{NL})$$

The complete inverse of the matrix Z_{NN} is not calculated. Only the generator columns Z_{NG} are calculated and they will be a small proportion of the total. The large amount of time and storage which would be required for calculating the complete Z_{NN} is avoided by directly calculating the product $Z_{NN}P_{NL}$ in step 7.

In practice it will be necessary for loss coefficients to be calculated for various load conditions in a certain network configuration. Only the coefficients E_{G0} and E_{00} are affected by the load condition. Thus, only steps 7 to 9 need to be re-executed.

7.4 EVALUATION

7.4.1 Test Systems

The accuracy of the D.C. loadflow loss formulas has been evaluated by comparing their losses and incremental losses with A.C. loadflow results. For the evaluation a number of practical systems with varying characteristics have been studied. The systems and the characteristics are listed in Table 7.2. The AGE system is a representation of the American Gas and Electric system which was originally studied by Kirchmayer[1,6]. Both the AGE system and the IEEE 118 Bus Test system are old systems with low X/R ratios and provide a good test of the accuracy of the D.C. loadflow approximation. The NZED system is a full representation of the New Zealand South Island System. This system gives a good test of the D.C. loadflow loss formula under a wide range of transmission X/R ratios. The NZED-220 system includes only the 220 kv network of the full NZED system. This system is a convenient size to enable a detailed study of the losses and incremental losses with swings in generation. The 39 bus system represents a modern 345 kv transmission system with a high X/R ratio and the accuracy of the D.C. loadflow loss formulas should be greatest for this system.

System	No. Buses	No. voltage controlled buses	No. Generators	Voltage levels kv	Typical X/R
AGE	28	18	8	132	3
NZED-220	27	8	7	220	5
NZED	185	26	8	220,110, 66	5,3,2
39 BUS	39	10	10	345	10
IEEE	118	54	18	132	3

Table 7.2: Test System Characteristics

7.4.2 Calculation of Angle and Magnitude Dependent Losses

For each of the test systems the exact bus voltages have been calculated with an A.C. loadflow. The magnitude and angle dependent components of system loss have been calculated from (13) and (14). The results are shown in Table 7.3.

System	P_δ	P_E	$P_\delta + P_E$	Exact Total Loss
AGE	38.54	3.11	41.65	41.59
NZED-220	40.62	2.28	42.90	42.78
NZED	71.15	12.34	83.49	83.28
39 BUS	32.15	2.20	34.35	34.32
IEEE	114.62	18.23	132.85	132.65

Table 7.3: Angle and Magnitude Dependent Losses from A.C. Loadflows.

The magnitude dependent loss comprises only a small proportion (5-15%) of the total system loss. Table 7.3 also includes the exact system losses as calculated by (8). There is only a small difference between the exact system loss and the sum of P_δ and P_E due to the approximation;

$$\text{Cos}(\delta_p - \delta_q) = 1 - (\delta_p - \delta_q)^2/2$$

The variation of the angle and magnitude dependent loss with system load level is shown in figure 7.2 for the NZED-220 system. The generator and load MW have been varied with a uniform profile while the controlled bus voltages and the load bus MVAR have been held constant. The results agree with the theoretical expectations. The magnitude dependent loss is

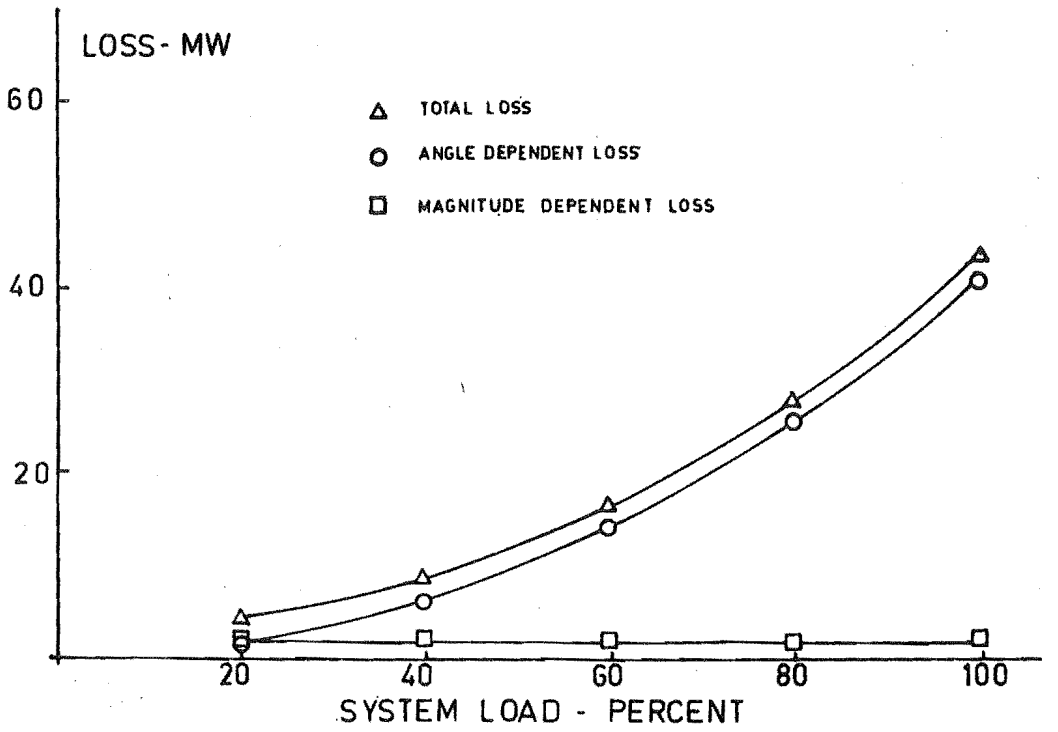

Figure 7.2: Variation of NZED-220 Losses with System Load

almost constant, and the angle dependent loss varies closely as the square of the system load level. The latter result can be deduced from (30).

7.4.3 D.C. Loadflow Loss Calculations

The approximations in the loss formula development have been examined by solving the linearized D.C. loadflow equation (24) for the bus angles and calculating the magnitude and angle dependent losses from (13) and (14). This approach gives identical values of system loss as a full development of the loss formula; however, it is easier to experiment with.

System	A.C.	D.C. Version I	D.C. Version II	D.C. Version III
AGE	38.54	40.57	35.28	38.16
NZED-220	40.62	44.63	40.26	40.24
NZED	71.15	87.71	70.57	73.44
39 BUS	32.15	34.97	32.39	32.02
IEEE	114.62	126.11	110.69	115.2

Table 7.4: Comparison of Angle Dependent Losses from A.C. and D.C. Loadflows.

In table 7.4 the angle dependent losses obtained by the versions of the D.C. loadflow method are compared with the A.C. loadflow values. Version I gives angle dependent losses which are significantly higher than the A.C. loadflow values. This is due to the complete neglect of the conductive component of branch power flow in (20). This results in high estimates of branch angles and hence high estimates of angle

dependent loss. When bus voltage magnitude data is not used the magnitude dependent loss cannot be calculated and the total system loss is approximated by just the angle dependent component. The two approximations often compensate quite well, but version I cannot be generally expected to give total losses very accurately.

In versions II and III the bus voltage magnitudes have been taken from A.C. loadflow solutions. Table 7.4 shows that these methods give more accurate estimates of the angle dependent losses. Furthermore, the bus voltage magnitudes also allow the magnitude dependent loss to be calculated and therefore more accurate estimates of the total system loss are also obtained.

For the NZED-220 system the losses have been compared as power is swung between generators. Results are shown in figures 7.3 to 7.6. The angle dependent loss of version I gives a good representation of the change in total loss with varying generation conditions and thus promises to provide good estimates of incremental losses. For versions II and III the magnitude dependent loss has been calculated for the base case condition and assumed constant. This assumption was in fact very good. In the A.C. loadflow studies the variation in the magnitude dependent loss accounted for less than 1% of the total loss variation. With version II the most significant errors occur at the extremities of the power swings. Then, the branch angles are highest and the approximation to the conductive component of power flow in (20),

$$E_p(E_p-E_q)g_{pq} \approx E_p(E_p - E_p\cos(\delta_p-\delta_q))g_{pq}$$

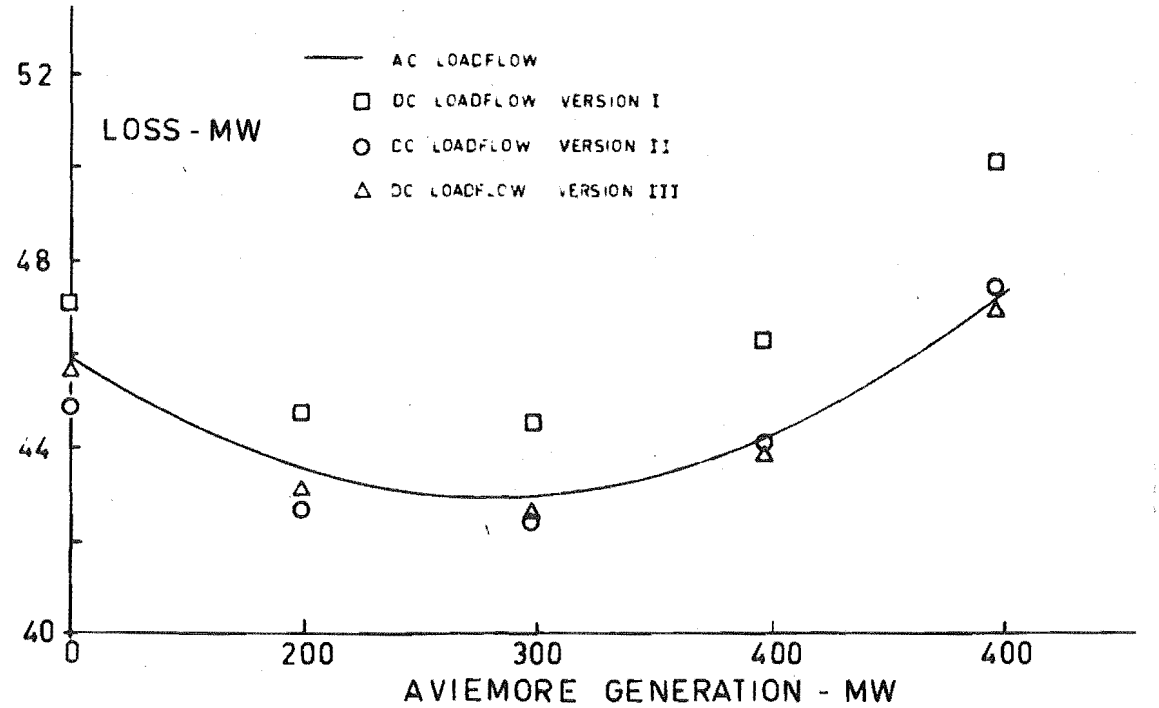

Figure 7.3: Loss Variation with Generation Swing Between Aviemore and Roxburgh

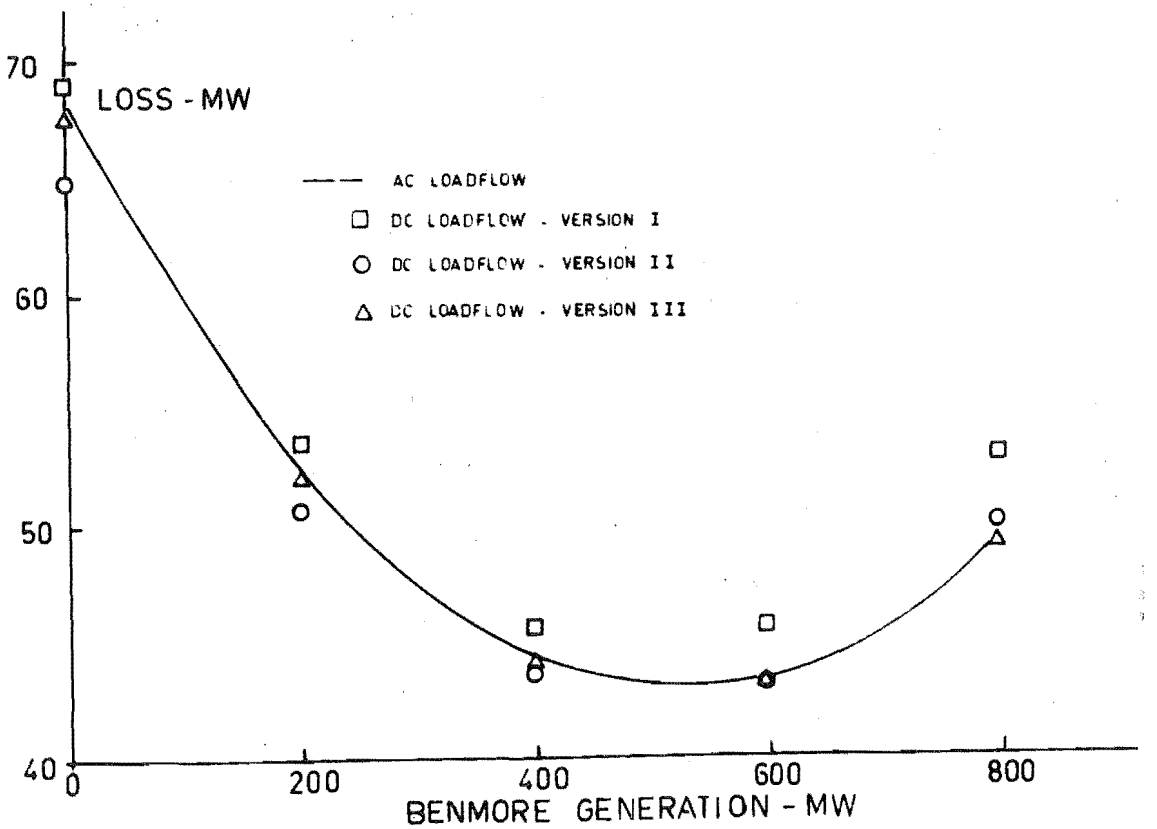

Figure 7.4: Loss Variation with Generation Swing Between Benmore and Roxburgh

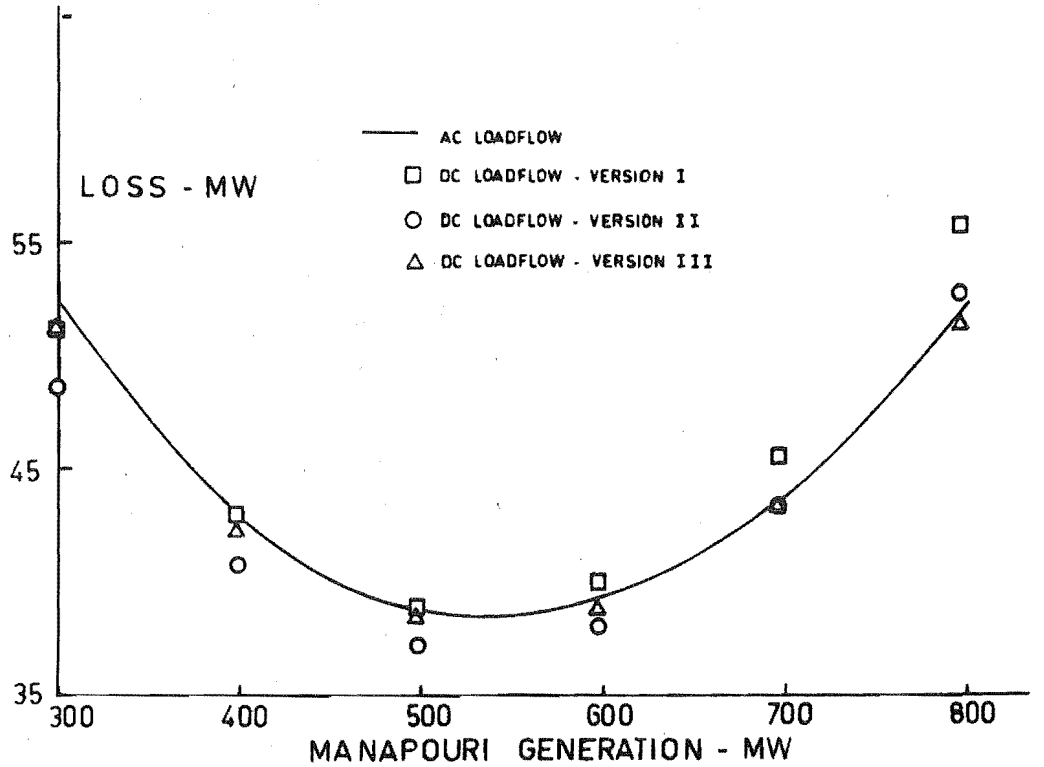

Figure 7.5: Loss Variation with Generation Swing Between Manapouri and Roxburgh

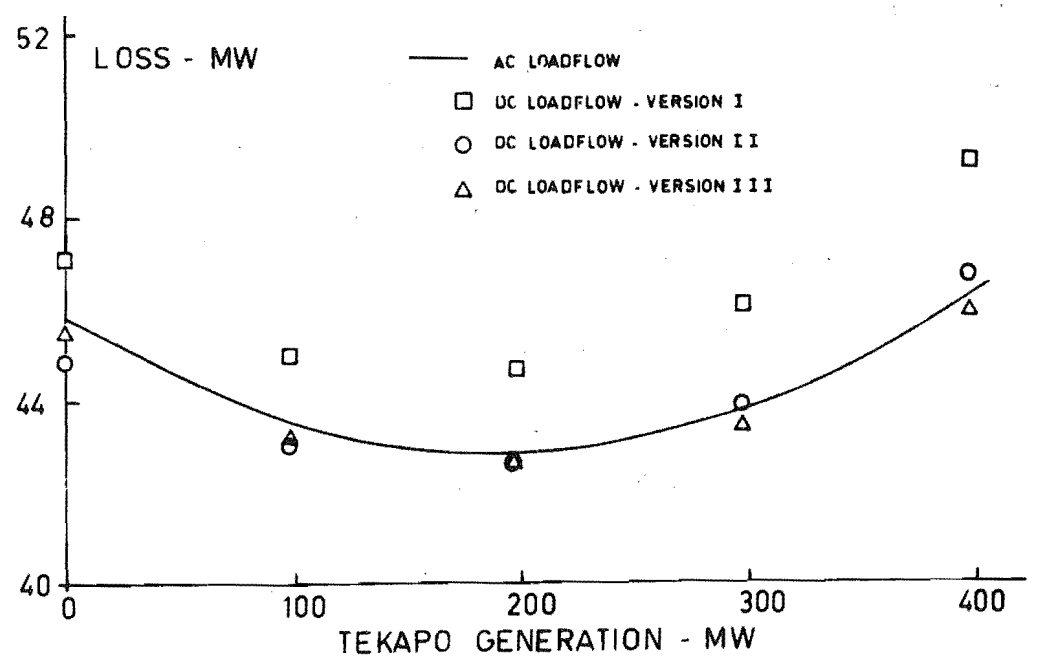

Figure 7.6: Loss Variation with Generation Swing Between Tekapo and Roxburgh

has more effect. In version III the D.C. loadflow equation is solved twice over and the angles from the first solution are used to give a more accurate estimate of,

$$E_p(E_p - E_p\cos(\delta_p-\delta_q))g_{pq}$$

for use in the second solution. This modification eliminates most of the error in the version II estimates.

7.4.4 Incremental Loss Calculations

To evaluate the accuracy of the loss formulas, incremental losses have been calculated by the modified nodal iterative A.C. loadflow. (Chapter 5. The required accuracy was obtained by using a voltage tolerance of .00001.) The change in loss divided by the change in generation is alternately calculated for a small increase and a small decrease in generation (± 10 MW). The average of the two ratios then gives a very accurate estimate of the exact incremental loss. The A.C. loadflow incremental losses are shown in figures 7.7 to 7.11 along with the incremental losses obtained by the D.C. loadflow loss formulas. The average and maximum incremental loss errors are shown for each system in Tables 7.5 and 7.6.

System	DC Loadflow Loss Formula			
	V.I	V.II	V.III	B Coeff.
AGE	.025	.031	.010	.036
NZED-220	.004	.003	.000	-
NZED	.010	.006	.002	-
39 BUS	.002	.001	.000	-
IEEE	.014	.015	.003	-

Table 7.5: Average Incremental Loss Errors.

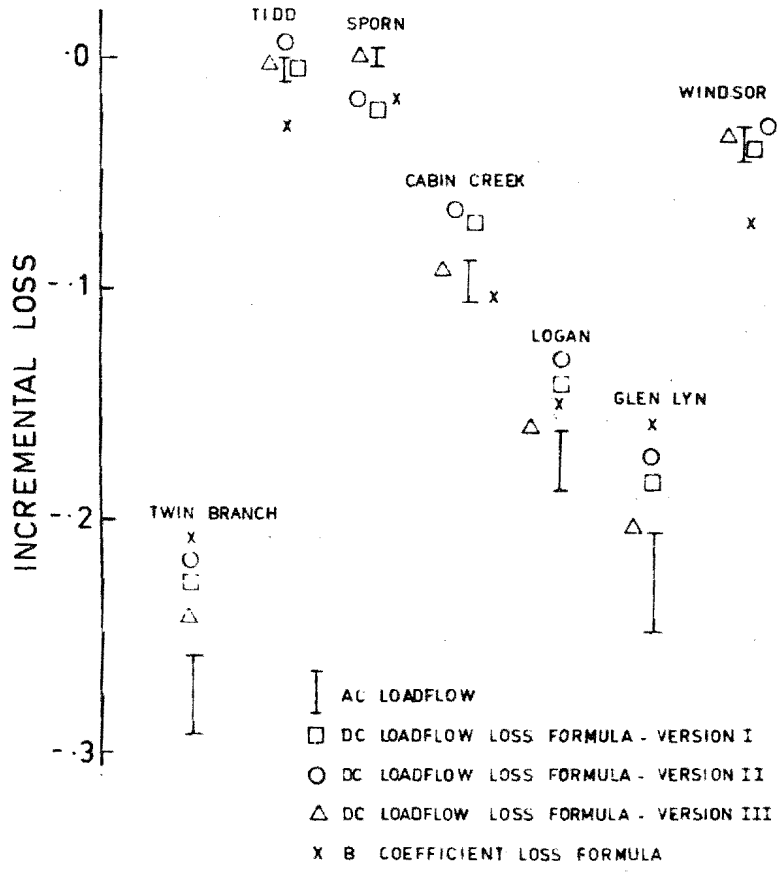

Figure 7.7: AGE System Incremental Losses

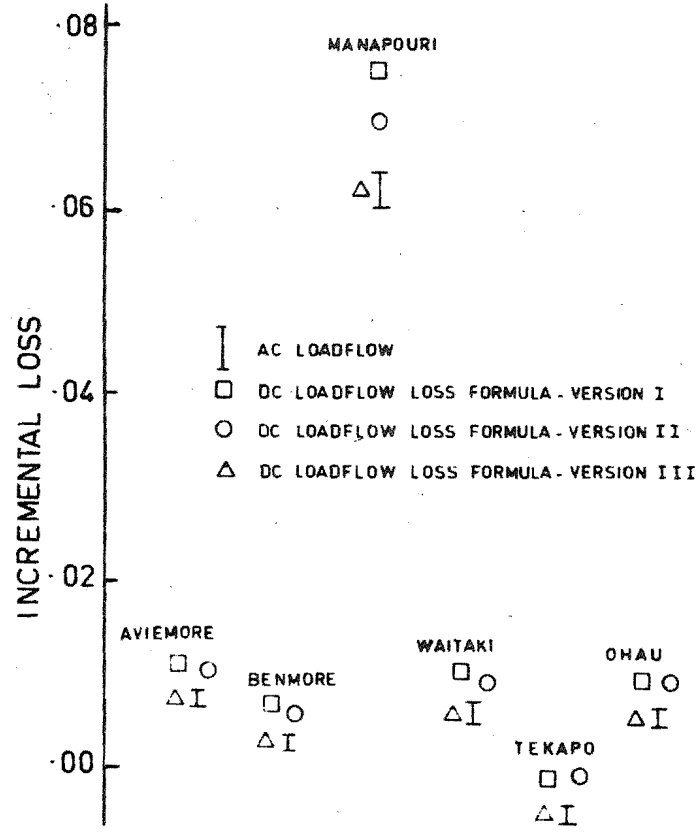

Figure 7.8: NZED-220 System Incremental Losses

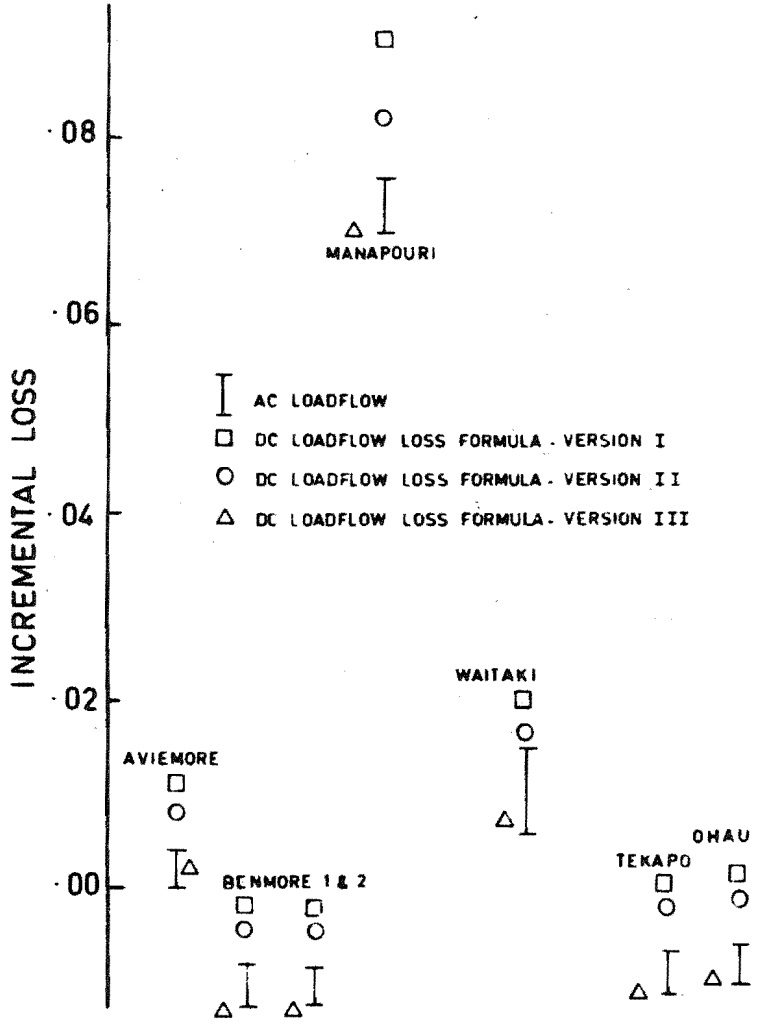

Figure 7.9: NZED System Incremental Losses

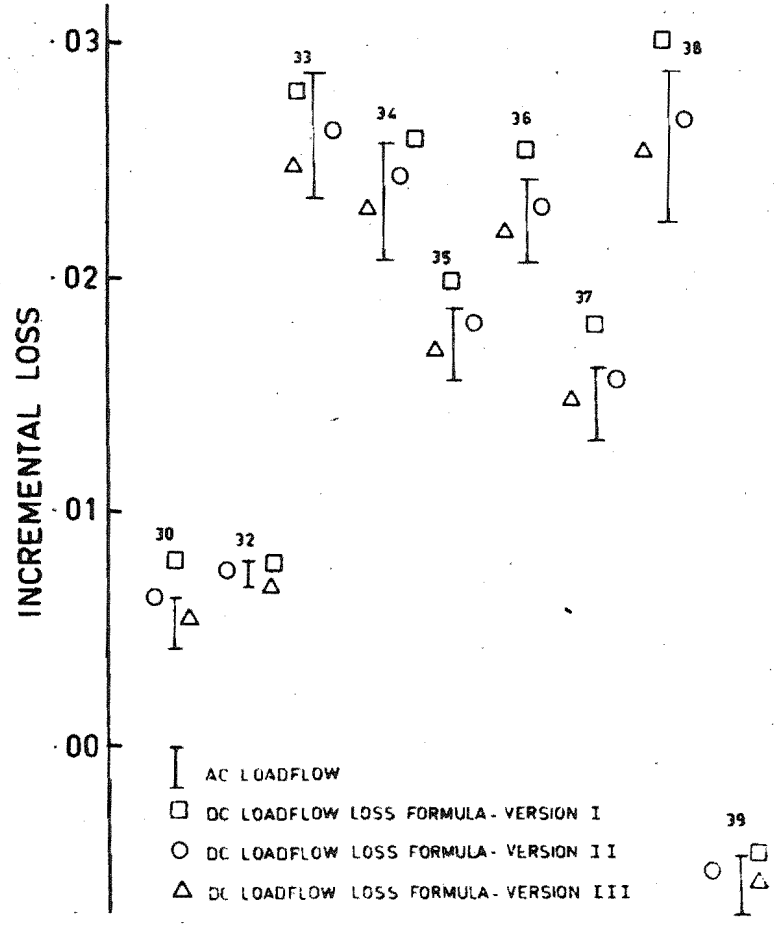

Fig. 7.10: 39 Bus System Incremental Losses

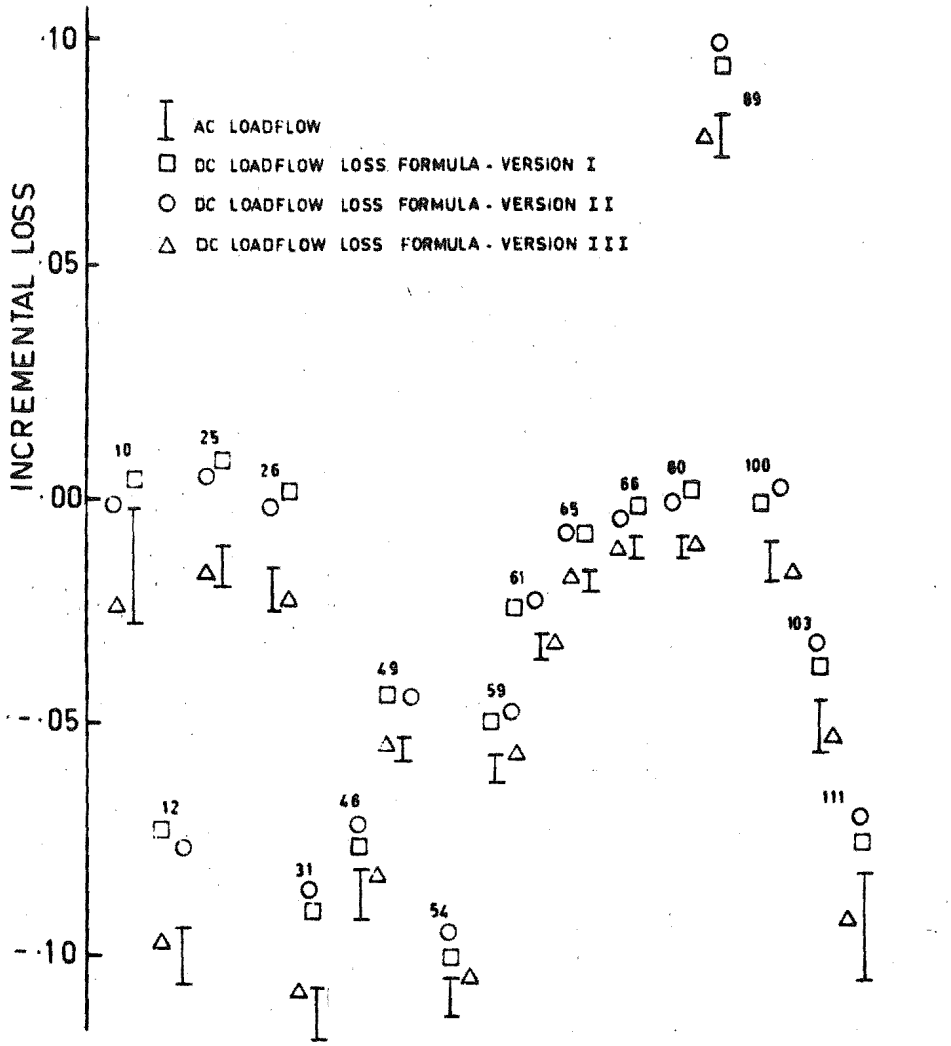

Figure 7.11: IEEE 118 Bus System Incremental Losses

System	DC Loadflow Loss Formula			
	V.I	V.II	V.III	B Coeff.
AGE	.050	.055	.035	.070
NZED-220	.012	.007	.0	-
NZED	.018	.010	.003	-
39 BUS	.004	.001	.001	-
IEEE	.025	.024	.010	-

Table 7.6: Maximum Incremental Loss Errors

The accuracy of the D.C. loadflow incremental losses is very satisfactory for economic dispatch. For the modern NZED-220, NZED and 39 Bus systems almost all the D.C. loadflow incremental losses lie within .01 of the exact values. This represents an error of only 1% in generator penalty factor $(1/1 - \frac{\partial P_L}{\partial P_{Gi}})$ and is better than the accuracy to which incremental production cost curves can be determined. The accuracy of version I is remarkable when one considers that the incremental losses are calculated solely from branch admittance and bus load data. Version II which also uses voltage magnitude data generally gives somewhat more accurate incremental losses than version I. However, the improvements in incremental loss accuracy are not as distinctive as the earlier improvements in loss accuracy. The version III results show the further improvements in accuracy which are obtained by also using generation data. For the modern systems with the high X/R ratios version III gives incremental losses which are practically exact.

A comparison of the accuracies of the D.C. loadflow loss formulas and the B coefficient loss formula has been made with

the AGE system. The B coefficients which were used for the incremental loss calculations are those calculated by Kirchmayer[1]. The results are shown in figure 7.7 and Tables 7.5 and 7.6. The accuracy of the D.C. loadflow incremental losses is generally better than the B coefficient incremental losses. The comparative accuracy of version I of the D.C. loadflow loss formula is enhanced by the fact that it is derived from a fraction of the network data used for the B coefficient loss formula.

For the NZED-220 system a study has been made of the incremental losses as the generator outputs have been swung with respect to the slack generator. Equation (37) shows that the incremental loss $\partial P_L/\partial P_{Gi}$ is a linear function of P_{Gi} with slope 2 x $E_{GG}(i,i)$. The corresponding graphs for the Aviemore, Benmore, Manapouri and Tekapo generators are shown in figures 7.12 to 7.15. Also shown are the exact incremental losses calculated by the A.C. loadflow method. The results clearly demonstrate the accuracy of the D.C. loadflow loss formulas. Version III provides an almost perfect linear fit to the variation of incremental losses with generator output. This is the ultimate performance which can be obtained from a quadratic loss formula.

7.4.5 Loss Formula Selection

In practice the most appropriate version of the D.C. loadflow loss formula will depend upon whether the more accurate versions enable significant extra cost savings. To illustrate, generation schedules have been calculated for the AGE system and the 39 bus system with each version of the D.C. loadflow loss formula and also without coordination of the incremental losses. These are shown in Tables 7.7 and 7.8.

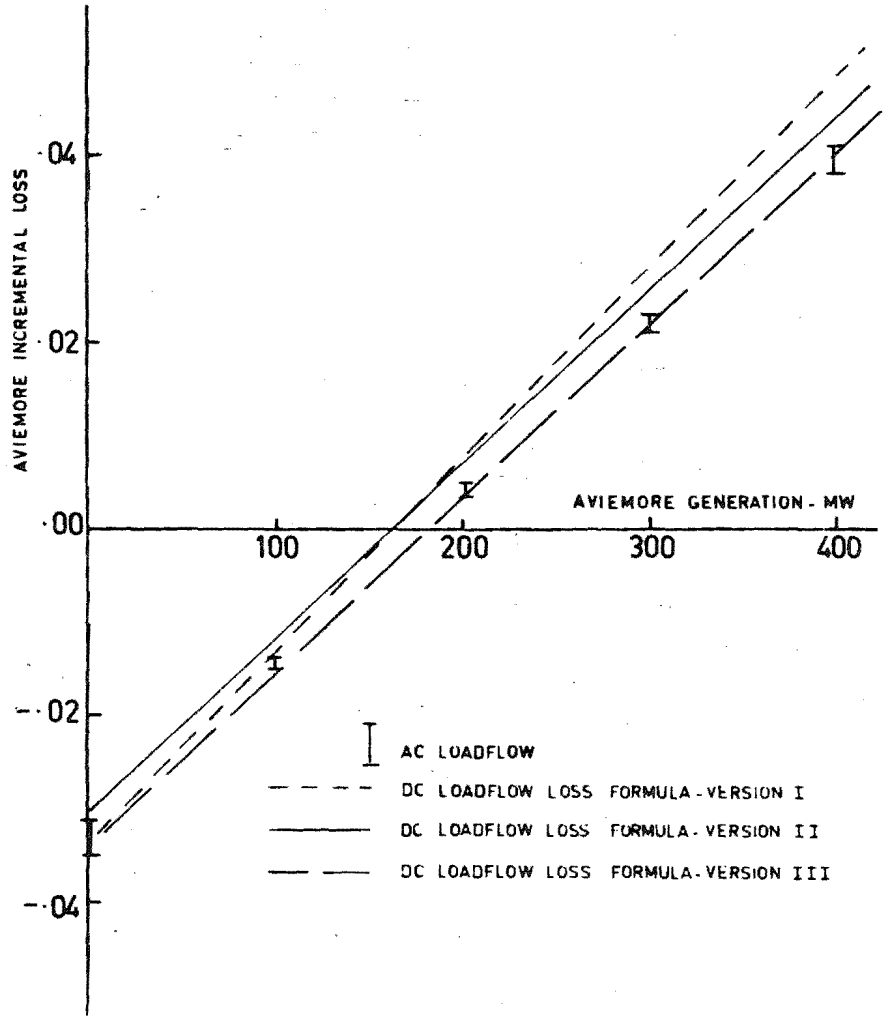

Figure 7.12: Incremental Loss Variation with Generation Swing Between Aviemore and Roxburgh

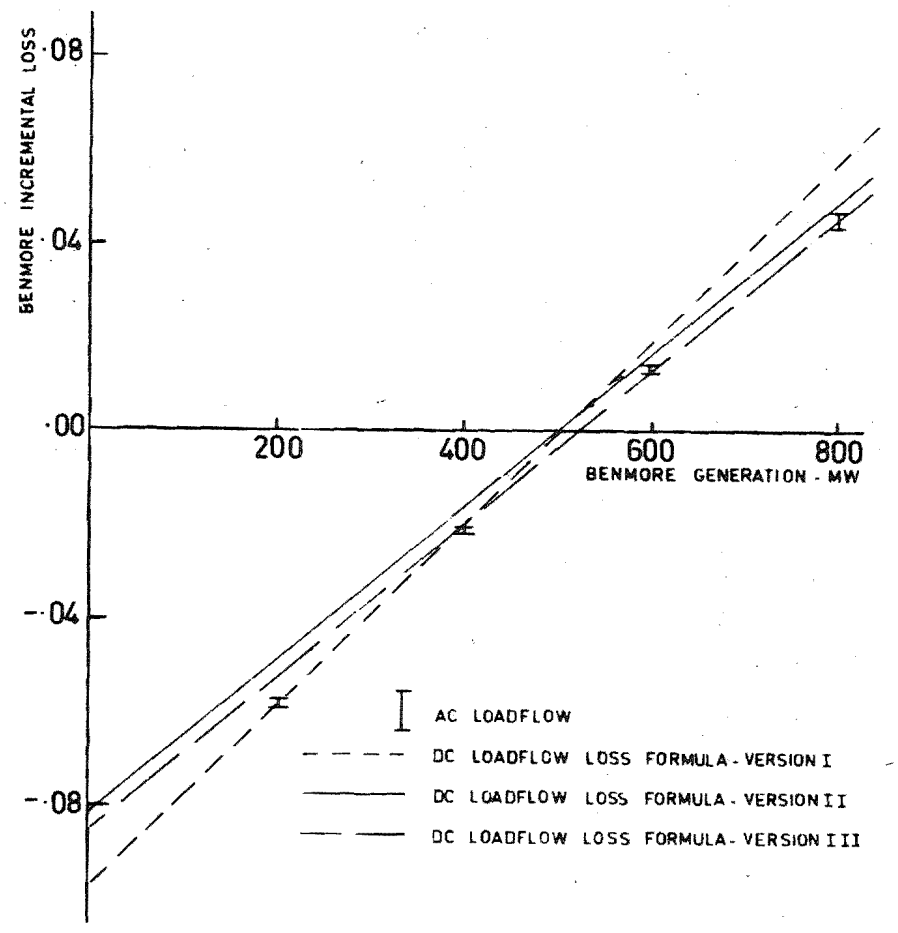

Figure 7.13: Incremental Loss Variation with Generation Swing Between Benmore and Roxburgh

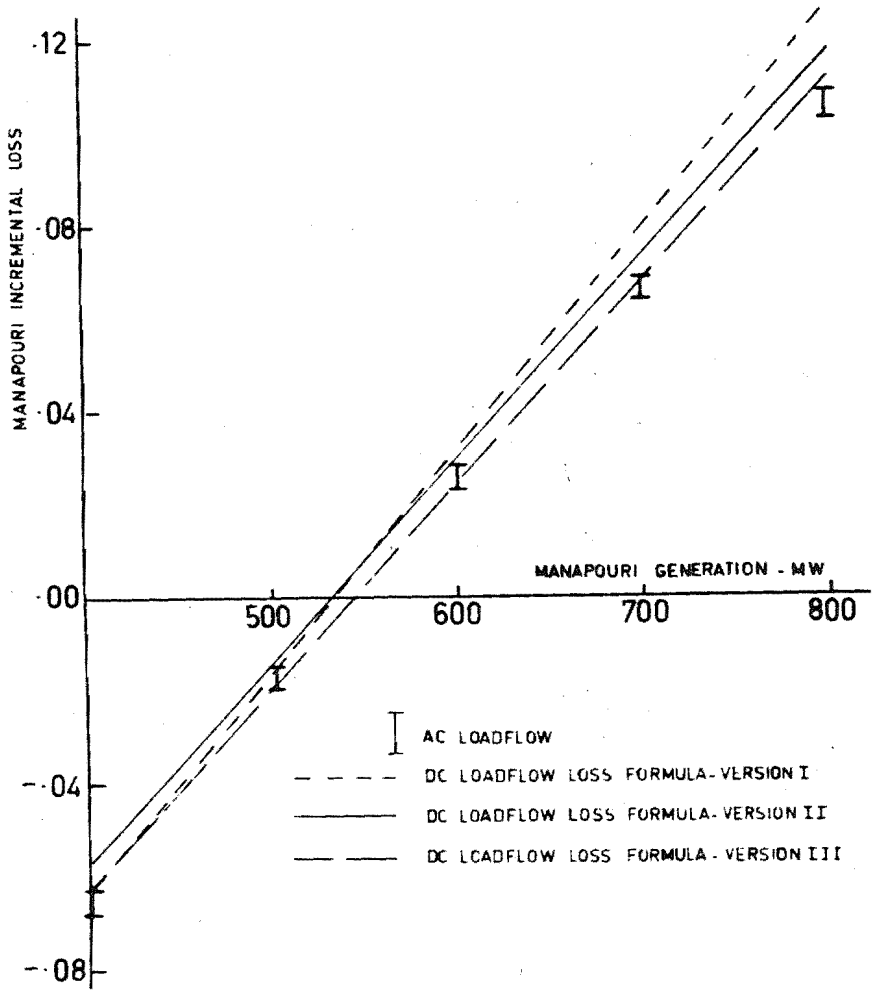

Figure 7.14: Incremental Loss Variation with Generation Swing Between Manapouri and Roxburgh

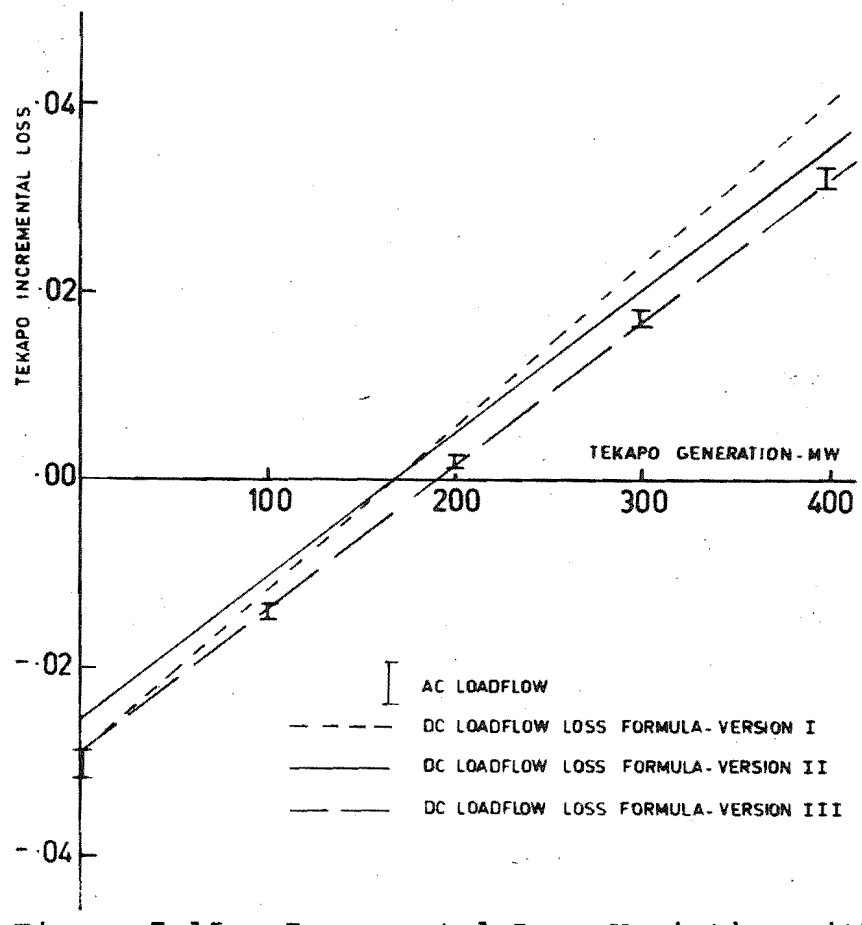

Figure 7.15: Incremental Loss Variation with Generation Swing Between Tekapo and Roxburgh

	DC Loadflow Loss Formula			No loss coordination
	V.I	V.II	V.III	
Load MW	1009.8	1009.8	1009.8	1009.8
Generation - MW				
Twin Branch	87.0	85.9	86.5	50.9
Tidd	185.1	182.4	182.0	204.8
Philo (Slack)	222.1	224.6	218.1	244.6
Sporn	292.1	295.7	299.2	310.0
Cabin Creek	114.5	114.1	115.1	116.4
Logan	54.1	53.5	54.1	51.1
Glen Lynn	96.6	95.9	96.8	88.5
Windsor	0.0	0.0	0.0	0.0
Loss from formula	41.4	39.5	41.6	53.8
Loss from AC loadflow	41.7	42.3	42.0	56.5
Generation cost - $/HR	1262.6	1262.6	1262.5	1277.4

Table 7.7: Generation Schedules for AGE System

	DC Loadflow Loss Formula			No loss Coordination
	V.I	V.II	V.III	
Load - MW	6165.7	6165.7	6165.7	6165.7
Generation - MW				
30	239.0	238.9	238.5	218.7
31 (Slack)	291.7	291.1	291.3	158.5
32	346.9	345.8	344.8	324.6
33	783.6	783.7	784.6	822.0
34	653.6	653.8	654.3	677.4
35	793.5	793.3	793.6	802.9
36	654.0	655.1	656.0	696.7
37	708.7	709.4	709.0	706.9
38	819.7	822.0	822.2	832.9
39	932.0	929.8	928.7	889.4
Loss from formula	58.9	58.5	56.8	66.0
Loss from AC loadflow	57.0	57.2	57.3	64.3
Generation cost - $/HR	5889.6	5889.6	5889.6	5895.1

Table 7.8: Generation Schedules for 39 Bus System

(Incremental cost data for the systems is given in Tables 8.2 and 8.3 of Chapter 8.) To enable the generation costs to be correctly compared the slack generation has been adjusted to satisfy the exact A.C. loadflow losses rather than the approximate loss formula value. The three versions of the D.C. loadflow loss formula give very similar schedules and the extra cost savings with the more accurate versions II and III are insignificant. Therefore, because of its minimal data requirements and extra simplicity, version I is most appropriate for both systems.

7.4.6 Program Performance

The D.C. loadflow loss coefficient program has been written in Fortran IV and executed on an IBM 360/44. The option is allowed for specifying which version of the D.C. loadflow loss coefficients are to be calculated.

The program is dimensioned for 250 buses, 400 lines and 50 generators. It uses 100k bytes of core memory. The execution time to calculate the loss coefficients for 17 generators in the IEEE system was 23s for a given network and load condition. For succeeding load conditions 1s was required to re-calculate the coefficients E_{G0} and E_{00}. Typically, in practice the period between network changes may be in the order of 1 hr and the generation dispatch may be performed for a new load condition every 5 m. The timing results clearly demonstrate the computational possibility of updating the D.C. loadflow loss coefficients according to the actual network and load conditions. In practice the appropriate rate for updating the loss coefficients can be determined primarily upon the basis of whether significant savings are obtained from a more up to date loss formula.

7.5 CONCLUSIONS

In conclusion some comparisons are made between the D.C. loadflow loss formula and Kron's B coefficient loss formula[1].

i) The D.C. loadflow loss formula is based upon the simple concepts of separating branch losses into voltage magnitude and angle dependent components and the use of the D.C. loadflow to relate bus powers and angles. On the other hand the B coefficient loss formula involves sophisticated mathematical manipulation and transformations and consequently the resulting loss coefficients cannot be easily related to the physical network.

ii) The B coefficient loss formula requires a linear relationship between the generator reactive and active outputs to be assigned. From the early days of B coefficients[16] until even recently[17] the validity and manner of determination of this relationship have been a point of contention. The D.C. loadflow loss formula does not depend upon assumed generator P/Q relationships. Instead, the easily identifiable assumption of constant bus voltage magnitudes is made.

iii) The B coefficient loss formula is dependent upon the solution of at least one and usually several A.C. loadflows. On the other hand, the D.C. loadflow loss formula can be directly calculated from branch impedances and load powers.

iv) Because the calculation of B coefficients has been a major task it is customary to calculate B coefficients for only a few standard load conditions. The computation requirements of the D.C. loadflow loss formula are reduced to the extent that loss coefficients can now be easily updated on-line according to actual network status and load conditions.

v) The D.C. loadflow loss formula enables losses and incremental losses to be calculated more accurately due to the ability to update the formula according to actual network conditions. When bus voltage magnitudes and generator powers are included in the D.C. loadflow loss formula highly accurate losses and incremental losses are obtained.

vi) In the B coefficient loss formula only the total losses in an equivalent network with a hypothetical load centre are represented and no information on the actual network solution is directly or indirectly available. Consequently, there is no guarantee that a generation schedule by the conventional coordination method will conform to line security limits. This limitation is a serious disadvantage of conventional coordination methods and it is a significant motive in the development of more sophisticated optimal loadflow programs[18]. However, in the D.C. loadflow loss formula development the actual network is retained throughout and it is a simple matter to check line power flows for a given network schedule. The method therefore offers the potential for recognizing line security limits in the economic schedule. Investigations along this line are described in the following chapter.

REFERENCES

*1. L.K. Kirchmayer, Economic Operation of Power Systems, Wiley, New York, 1958.

2. L.K. Kirchmayer, Economic Control of Interconnected Systems, Wiley, New York, 1959.

*3. E.E. George, "Intrasystem Transmission Losses", AIEE Trans., vol. 62, 1943, pp. 153-158.

4. J.B. Ward, J.R. Eaton, H.W. Hale, "Total and Incremental Losses in Power Transmission Networks", AIEE Trans., vol. 69, pt. I, 1950, pp. 626-632.

5. G. Kron, "Tensorial Analysis of Integrated Transmission Systems - Part I. The Six Basic Reference Frames", AIEE Trans., vol. 70, pt. II, 1951, pp. 1239-1248.

6. L.K. Kirchmayer, G.W. Stagg, "Analysis of Total and Incremental Losses in Transmission Systems", AIEE Trans., vol.70, pt.II, 1951, pp.1197-1205.

7. W.R. Brownlee, "Coordination of Incremental Fuel Costs and Incremental Transmission Losses by Functions of Voltage Phase Angles", AIEE Trans., vol. 73, pt. III, 1954, pp. 529-533.

8. E.D. Early, R.E. Watson, G.L. Smith, "A General Transmission Loss Equation", AIEE Trans., vol. 74, pt. III, 1955, pp. 510-520.

9. E.D. Early, R.E. Watson, "A New Method of Determining Constants for the General Transmission Loss Equation", AIEE Trans., vol. 74, Pt. III, pp. 1417-1423, 1955.

10. L.K. Kirchmayer, H.H. Happ, G.W. Stagg, J.F. Hohenstein, "Direct Calculation of Transmission Loss Formula - I", AIEE Trans., vol. 79, Pt. III, pp. 962-969, 1960.

11. J.R. Tudor, W.A. Lewis, "Transmission Losses and Economy Loading by Use of Admittance Constants", IEEE PAS-82, 1963, pp. 676-683.

12. H.H. Happ, J.F. Hohenstein, L.K. Kirchmayer, G.W. Stagg, "Direct Calculation of Transmission Loss Formula - II", IEEE PAS-83, pp. 702-707, 1964.

13. E.F. Hill, W.D. Stevenson, Jr., "An Improved Method of Determining Incremental Loss Factors from Power System Admittances and Voltages", IEEE PAS-87, 1968, pp. 1419-1425.

14. E.F. Hill, W.D. Stevenson, Jr., "A New Method of Determining Loss Coefficients", IEEE PAS-87, 1968, pp. 1548-1553.

15. W.S. Meyer, V.D. Albertson, "Improved Loss Formula Computation by Optimally Ordered Elimination Techniques", IEEE PAS-90, 1971, pp. 62-69.

16. P.L. Dandeno, Discussion of "Direct Calculation of Transmission Loss Formula - I", AIEE Trans., vol. 79, pt. III, p. 968, 1960.

17. W.R. Brownlee, Discussion of "Improved Loss Formula Computation by Optimally Ordered Elimination Techniques", IEEE PAS-90, 1971, p.67.

18. H.W. Dommel, W.F. Tinney, "Optimal Power Flow Solutions", IEEE PAS-87, pp. 1866-1876, 1968.

CHAPTER 8

ECONOMIC POWER DISPATCH WITH LINE SECURITY LIMITS

8.1 INTRODUCTION

This chapter presents a method for solving the economic dispatch of power systems while recognizing line security constraints. In the past, Kirchmayer's iterative method[1] has been well established as a fast simple and effective method for economic scheduling. However, a limitation of this method is that there is no guarantee that the schedules will not violate secure line limits. If such situations do arise it is necessary to reallocate the generation so that the line constraints are satisfied. In practice this operation is most commonly performed by manual intervention. With the demands upon power system reliability and the increasing size and complexity of networks more attention is being given to developing scheduling methods which automatically account for network security constraints[2-5]. A well known method which is representative of the state-of-the-art in these developments is the optimal power flow developed by Dommel and Tinney[2]. This method is based upon the Newton power flow solution and it is much more elaborate than the established method. It represents losses exactly, schedules real and reactive power and satisfies constraints on load voltages, reactive sources and tie line power angles. However, because the method is based upon explicit and exact solution of the network, it is computationally much more difficult than the established method. It also requires a greatly increased amount of system-state data as input which may create practical

difficulties[6]. The method will be beyond the range of many dispatch-office computer systems for some years.

The method which is presented effectively overcomes the major limitation of the established method to provide secure economic schedules without greatly increased computation or system-state data requirements. It is based upon the use of the D.C. loadflow to formulate the line security limits as linear inequality constraints on the generator outputs. In consequence the time consuming explicit solution of the network during the dispatch phase of computation is avoided. The method only requires the network condition and the power flow in the constrained lines as additional system-state data.

8.2 PROBLEM FORMULATION

List of Variables

In the following nomenclature upper case subscripts are used in a descriptive sense, e.g. P_G is the vector of generator powers. Lower case subscripts are used to denote an element of an array, e.g. P_{Gi} is the i^{th} element of the vector P_G. Alternatively the i^{th} element of P_G may also be written as $P_G(i)$.

P_L	system loss
P_G	vector of generator powers, P_G does not include the slack generation unless this is specifically stated
P_{GL}, P_{GU}	lower and upper limits on generation
E_{GG}, E_{G0}, E_{00}	DC loadflow loss coefficients
P_B	vector of branch power flows
P_{BL}, P_{BU}	lower and upper limits on branch power flows
P_N	vector of node powers

N	vector of node angles
B_{NN}	DC loadflow nodal susceptance matrix
δ_B	vector of branch angles
B_{BB}	diagonal matrix of branch susceptances
A_{BN}	branch-node transformation matrix
Z_{NN}	inverse of B_{NN}
Z_{NG}	generator node columns of Z_{NN}
P_{NL}	load powers
S_{BG}	branch-generator power matrix
R_B	load contribution of branch flows
F_T	total generation cost
F_{Gi}	cost of generator i
F_i	slope of incremental cost curve of generator i
P_D	total system load demand
P_L'	constant approximation to P_L

8.2.1 Unit Cost Characteristics

The economic scheduling of thermal generation is based upon the representation of the production cost characteristics of the units involved[7]. Figure 8.1 represents the performance curve of a typical thermal unit; fuel input in MBtu/hr is plotted against the output in MW. The incremental input curve, which is the slope of the input-output curve, is shown in figure 8.2. The fuel cost in $/h vs the MW output is obtained by scaling the input-output curve by the fuel cost in $/MBtu. Similarly, the incremental fuel cost in $/MWh vs the MW output is obtained by scaling the incremental input curve by the fuel cost in $/MWh. The incremental fuel cost curve is actually the one which is most often represented for computing generation schedules. Most commonly, this curve is approximated

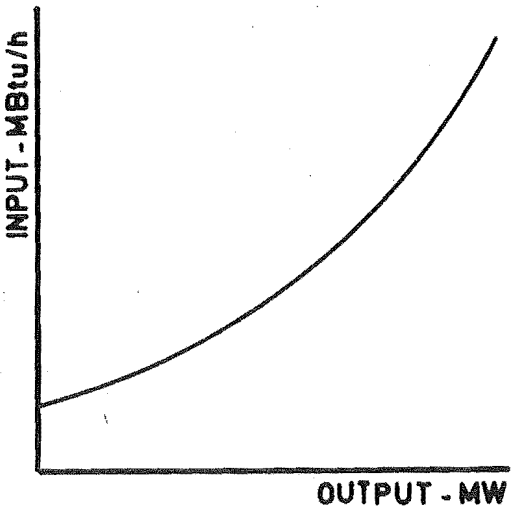

Figure 8.1: Thermal Unit Input-Output Curve

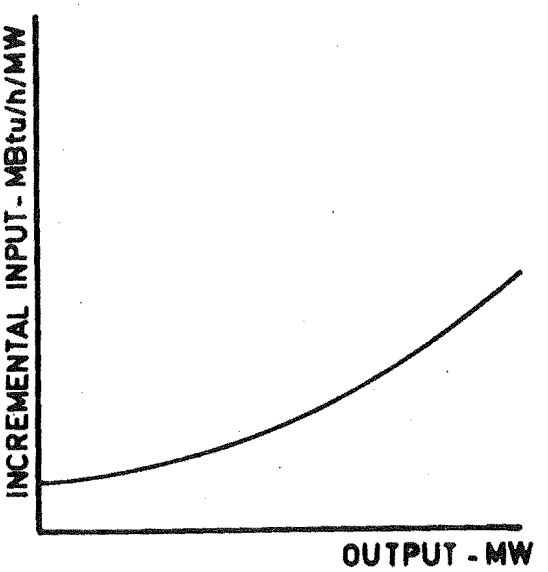

Figure 8.2: Thermal Unit Incremental Input Curve

by a number of piecewise linear segments, and this representation is used herein. Thus, it is implicit that the cost curves are represented by piecewise quadratic segments.

8.2.2 Representation of System Losses

The economic importance of representing transmission losses in the scheduling of generation has been well established[1] and this can be most easily achieved by the use of loss formulas. In the preceding chapter a simplified method for calculating a transmission system loss formula was developed and it can now be exploited. It was shown that the system losses could be expressed as:

$$(1) \qquad P_L = P_G{}^t E_{GG} P_G + P_G{}^t E_{G0} + E_{00}$$

For future reference, we note that this loss formula is dependent upon the system load condition (the load condition affects E_{G0} and E_{00}) and all the generator powers except that of the slack generator.

8.2.3 Line Security Limits

The line security limits take the form of constraints on the branch power flows. If we define the branch flow to be positive in a certain direction then we can express the constraints as:

$$(2) \qquad P_{BL} \leqslant P_B \leqslant P_{BU}$$

The branch powers can be expressed in terms of the generator powers by introducing the linearized D.C. loadflow.

$$(3) \qquad P_N = B_{NN}\ \delta_N$$

Solving for the node angles,

$$(4) \qquad \delta_N = Z_{NN}\ P_N$$

Therefore the branch angles are,

$$\delta_B = A_{BN}\, Z_{NN}\, P_N \tag{5}$$

and the branch powers are,

$$P_B = B_{BB}\, A_{BN}\, Z_{NN}\, P_N \tag{6}$$

Substituting for the load and generator components of P_N,

$$P_B = B_{BB}\, A_{BN}\, Z_{NG}\, P_G + B_{BB}\, A_{BN}\, Z_{NN}\, P_{NL} \tag{7}$$

Now let,

$$P_B = S_{BG}\, P_G + R_B \tag{8}$$

where we define branch-generator power matrix

$$S_{BG} = B_{BB}\, A_{BN}\, Z_{NG} \tag{9}$$

and

$$R_B = B_{BB}\, A_{BN}\, Z_{NN}\, P_{NL} \tag{10}$$

The vector R_B may be interpreted as the branch flows which would occur with $P_G = 0$, that is, with all the load supplied by the slack generator. If (8) is substituted into (2), the branch power constraints are transformed into linear inequality constraints on the independent generator powers,

$$P_{BL} \leqslant S_{BG}\, P_G + R_B \leqslant P_{BU} \tag{11}$$

Later, the linear form of (11) will have an important bearing on the approach chosen for the solution of the scheduling problem.

The total power flow in a group of lines is obtained by adding their flow equations as given by (8).

Thus, the general form of (11) also allows the net flow on a group of lines to be constrained and it can be used to constrain the interchange between system areas.

8.2.4 Mathematical Statement of the Problem

On the basis of the preceding sections the generation scheduling problem can now be mathematically stated. The objective of the problem is to minimize the total cost of generation given by,

$$(12) \qquad F_T = \Sigma_i \, F_{Gi}(P_{Gi})$$

with respect to the variables P_{Gi}. (The index i varies over all generators including the slack generator.)

The minimization of (12) is subject to several physical constraints.

i) The equality constraint of the specified load demand

$$(13) \qquad \Sigma_i \, P_{Gi} = P_D + P_L$$

ii) The upper and lower operating limits of the generation units,

$$(14) \qquad P_{GL} \leqslant P_G \leqslant P_{GU}$$

iii) The line security limits, which have been formulated as linear inequality constraints on the control variables P_G.

$$(15) \qquad P_{BL} \leqslant S_{BG} \, P_G + R_B \leqslant P_{BU}$$

Equations (12) to (15) are a basic mathematical statement of the generation scheduling problem. The effects of generation costs, system losses, generator operating limits and line security limits are all included.

8.2.5 Transformation of the Demand Constraint

To make the problem more tractable for optimization the non-linear demand constraint of (13) is removed by assigning the output of a certain generator as a dependent or slack variable. Solving (13) for the output of a slack generator s,

$$(16) \qquad P_{Gs} = P_D + P_L - \sum_{i \neq s} P_{Gi}$$

Now substituting for P_{Gs} into (12),

$$(17) \qquad F_T = \sum_{i \neq s} F_{Gi}(P_{Gi}) + F_{Gs}(P_D + P_L - \sum_{i \neq s} P_{Gi})$$

If s is the same slack generator that is defined for the calculation of the loss formula in (1), the slack generation P_{Gs} does not explicitly occur in the cost function F_T. The operating limits on the slack generator are changed from simple control constraints to functional constraints given by,

$$(18) \qquad P_{GLs} \leq P_D + P'_L - \sum_{i \neq s} P_{Gi} \leq P_{GUs}$$

By approximating the losses as being constant in (18), the slack generator operating constraints become linear and can be treated in the same way as the line security constraints. The approximation is quite acceptable since it has no effect other than causing a small tolerance in the operating limits of the slack generator. The transformation described does not affect the line security constraints since these are independent of the slack generation P_{Gs}.

In summary, the problem has been transformed so that we minimize,

$$(19) \qquad F_T = \sum_{i \neq s} F_{Gi}(P_{Gi}) + F_{Gs}(P_D + P_L - \sum_{i \neq s} P_{Gi})$$

Subject to the independent generator operating limits,

$$(20) \qquad P_{GLi} \leqslant P_{Gi} \leqslant P_{GUi} \qquad i \neq s$$

The slack generator limits,

$$(21) \qquad P_{GLs} \leqslant P_D - P'_L - \sum_{i \neq s} P_{Gi} \leqslant P_{GUs}$$

And the line security limits,

$$(22) \quad P_{BL} \leqslant S_{BG}P_G + R_B \leqslant P_{BU}.$$

The overall effect of the transformation is that the cost function in (19) is more complicated, but all the constraints are now linear. The gradients of the cost function in (19) are,

$$(23) \qquad \partial F_T/\partial P_{Gi} = dF_{Gi}/dP_{Gi} - dF_{Gs}/dP_{Gs}(1 - \partial P_L/\partial P_{Gi})$$

The gradient $\partial F_T/\partial P_{Gi}$ may be physically interpreted as the incremental cost of delivering a unit of power from generator i to the slack generator.

8.3 IMPLEMENTATION

8.3.1 Calculation of the Line Constraints

To achieve a high reliability, power system transmission systems are usually designed well within the capacity of system load and generation. A large proportion of the system lines will, for most of the time, have little possibility of becoming overloaded. Consequently, in calculating generation

schedules only the small proportion of the lines which are likely to be overloaded need to be directly incorporated. The loadings on the remaining lines can be checked either by load-flow or by actual measurement. If any of these lines do happen to approach overload then their constraints can be added to the scheduling program.

Because only a small proportion of the line constraints is represented the coefficients S_{BG} are calculated in a separate program and entered as input data to the dispatch program. The S_{BG} coefficients are determined by the network status and are only updated when major transmission changes occur. The triangularized D.C. loadflow matrix B_{NN}, which is also required for the calculation of the loss coefficients, is used to calculate the S_{BG} matrix. The columns of S_{BG} are calculated for each generator in turn by setting unity power on the generator in concern and all other generation and loads to zero. (We assume the generation is absorbed by the slack generator.) The solution for the branch flows in this situation then forms a column of the matrix S_{BG}.

The vector R_B which represents the combined effect of the system loads in the branch power equation (8) is updated for each new dispatch. This calculation may be performed with the triangularized B_{NN} matrix and the system loads. Alternatively, R_B may be calculated from the generation P_G^o and line powers P_B^o which exist prior to the economic dispatch. That is, we calculate,

$$R_B = P_B^o - S_{BG}\, P_G^o \qquad (24)$$

The latter approach has practical advantages, and is adopted . It requires less computation. It only requires the generator

outputs and the constrained line power flows as system-state data; whereas the first method requires data on all system loads. Further, the latter approach gives a more accurate representation of the line constraints.

8.3.2 The Dispatch Program

In section 8.2.5 the economic dispatch problem has been formulated as one of minimizing a non-linear cost function subject to linear inequality constraints. A method which is specifically designed for non-linear optimization with linear constraints is the gradient projection method[8]. This method has been well established and its characteristics and limitations are well documented[8,9]. Further, it has been extensively tested and has solved problems with up to 69 variables and 168 linear constraints in approximately 4m on an IBM 7090[9]. Consequently, from the outset it has appeared to be well suited to the problem in hand. An alternative approach would have been to use penalty functions to represent the line constraints and to use an unconstrained minimization technique. However, this would not have taken advantage of the linear form of the constraints.

The gradient projection method is basically an extension of the method of steepest descent. It proceeds in the same manner as the method of steepest descent until the linear constraints are encountered. Then, a feasible direction for decreasing the cost function is obtained by projecting the direction of steepest descent along the constraints. A typical gradient projection trajectory for a two dimensional problem is shown in figure 8.16.

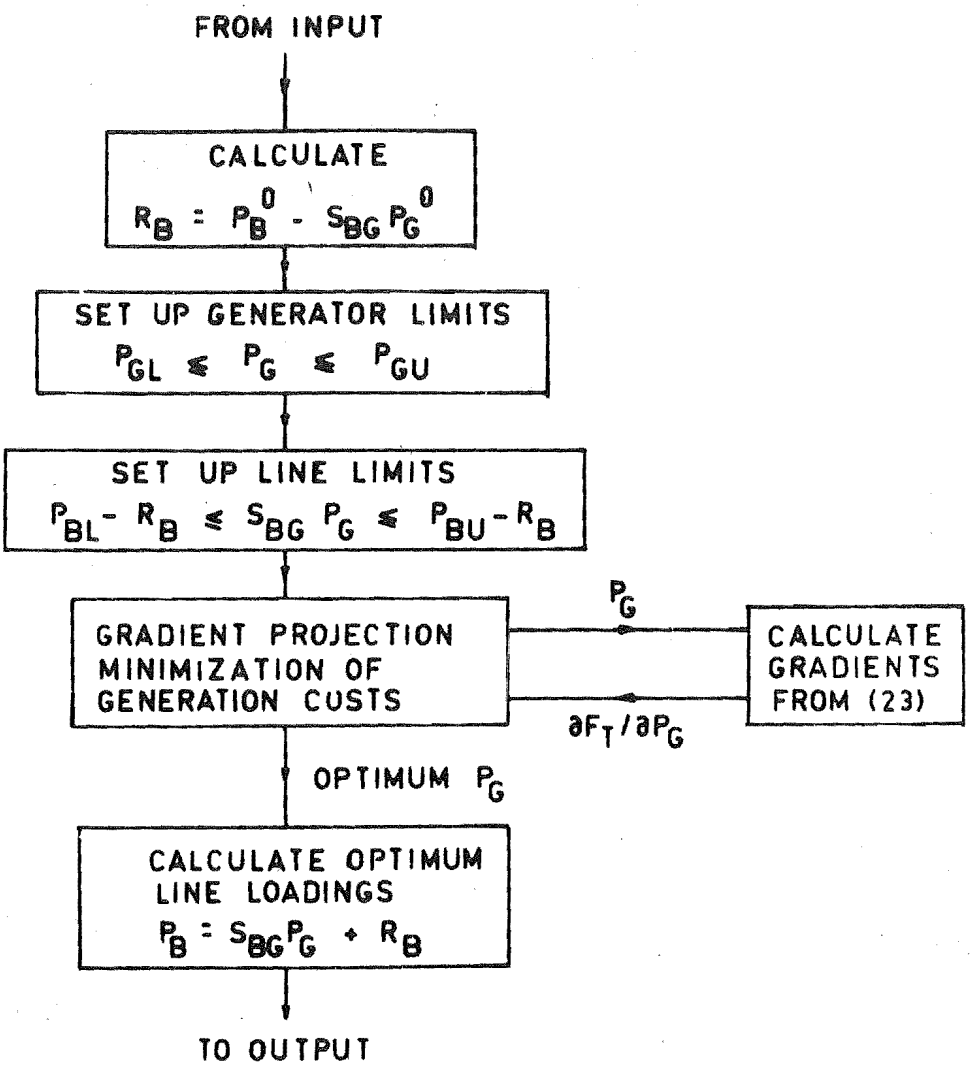

Figure 8.3: Flow Diagram of Dispatch Program with Line Security Limits

A flow diagram of the dispatch program is shown in figure 8.3. The gradient projection optimization is programmed as a subroutine and its procedure is fully described in section 8.6. The input for the dispatch program consists of the following data,

i) loss coefficients E_{GG}, E_{G0}, E_{00}

ii) branch-generator power matrix S_{BG}

iii) generator incremental cost data

iv) branch power limits P_{BL}, P_{BU}

v) generator power limits P_{GL}, P_{GU}

vi) total load P_D

vii) initial generation P_G^o and initial line flows P_B^o

8.4 EVALUATION

8.4.1 Test Systems

A summary of the data on the three test systems which are used for evaluating the gradient projection dispatch method is given in Table 8.1.

	BUSES	GENERATORS	LINES	AVERAGE X/R	LOAD MW
AGE system	28	8	35	3	1100
39 Bus system	39	10	46	10	6166
IEEE system	118	18	179	3	4000

Table 8.1: Summary of System Data

AGE System

This system is based upon the representation of the American Gas and Electric System developed by Kirchmayer[1]. It was also used as a test example in Chapter 4 for calculating

loss coefficients and these are used in this chapter for coordinating the losses. The generator incremental cost characteristics are represented by single straight lines and their data is given in Table 8.2. Previous studies on this system[1] have shown that the optimum generation schedules in this system are considerably influenced by the system losses. This system is therefore ideal for testing the ability of the gradient projection method to efficiently and correctly account for the effects of losses.

i	F_i	f_i	$P_{max.}$
1	.00820	1.280	170
2	.00440	.795	210
3	.00222	.889	310
4	.01200	.300	180
5	.02080	.635	100
6	.01270	.572	140
7	.00190	1.809	140
8	.00429	.657	370

Table 8.2: AGE System Incremental Cost Data

39 Bus System

This system was also studied in Chapter 7 for developing loss coefficients. The generator incremental cost curves for this system are represented by single segment straight lines. (Table 8.3.) This system is a convenient size to allow a detailed study of the effects of line security limits on the distribution of the generation. It also has an advantage in that because of its higher X/R ratio it is easier to create

reasonable situations in which the conventional schedules (i.e. ones with equal incremental cost of power delivered to the load) violate line limits. On the other hand, in the older AGE system the X/R ratio is smaller, the line losses are more significant, and this factor in itself tends to keep line loadings to within reasonable limits[1].

i	F_i	f_i	P_{max}
1	.00108	1.12	1000
2	.00160	0.94	1000
3	.00196	0.72	1000
4	.00092	0.60	1000
5	.00150	0.34	1000
6	.00144	0.20	1000
7	.00054	0.98	1000
8	.00090	0.72	1000
9	.00110	0.44	1000
10	.00130	0.20	1000

Table 8.3: 39 Bus System Incremental Cost Data

IEEE 118 Bus System

This system represents a moderately large scheduling problem and it has been convenient to use for computer timing studies of the gradient projection method. The generator incremental cost curves for this system are represented by two linear segments (Table 8.4). The data intentionally includes a wide range in the slopes of the incremental cost segments to be a difficult test case for the gradient projection method.

The loss coefficients for the 18 major generators in this system have been calculated using the DC loadflow method in Chapter 7.

i	LOWER SEGMENT			UPPER SEGMENT		
	F_i	f_i	$P_{max.}$	F_i	f_i	$P_{max.}$
1	.00100	1.0	400	.00600	1.4	500
2	.00750	0.4	80	.04000	1.0	100
3	.00125	0.3	240	.00667	0.6	300
4	.00437	0.6	320	.00750	2.0	400
5	.01250	0.6	80	.06000	1.6	100
6	.01375	0.7	80	.02000	1.8	100
7	.00167	0.4	240	.02667	0.8	300
8	.00625	0.5	80	.05500	1.0	100
9	.00188	0.6	160	.03750	0.9	200
10	.00188	0.7	160	.03250	1.0	200
11	.00094	0.8	320	.01620	1.1	400
12	.00156	0.9	320	.01250	1.4	400
13	.00075	1.0	400	.00600	1.3	500
14	.00107	0.5	560	.00429	1.1	700
15	.00292	0.6	240	.00667	1.3	300
16	.01250	0.8	80	.04000	1.8	100
17	.00500	0.4	80	.02000	0.8	100
18	.00292	0.4	480	.00500	1.8	600

Table 8.4: IEEE System Incremental Cost Data

8.4.2 Convergence

8.4.2.1 Convergence Characteristics

Since the gradient projection method is basically an extension of the method of steepest descent it also has the characteristic limitations of slow convergence near the optimum and oscillation along a steep sided valley. Graphs showing the convergence of the total generation cost in the three test systems are shown in figures 8.4, 8.5 and 8.6. The nature of the generation cost function is mainly determined by the range in the slopes of the generator incremental cost curves. Because, if the loss term in (19) is neglected the second derivatives of the total generation cost are,

$$\partial^2 F_T / \partial P_{Gi}^2 = F_i + F_s \tag{25}$$

$$\partial^2 F_T / \partial P_{Gi} \partial P_{Gj} = F_s . \tag{26}$$

We can therefore expect the limitations of the gradient projection method to be most apparent when there is a large range in the slopes of the incremental cost curves. This is the case for the IEEE System and as shown by Table 8.5 a fairly large number of iterations is required to obtain convergence in this system. Nevertheless, because very little calculation is required on each iteration the actual computation time is still very low. Consequently, the limitations of the gradient projection method have little practical significance in the generation dispatch problem. Further, they are well compensated for by the relative simplicity of the method in comparison to the more elaborate second order methods.

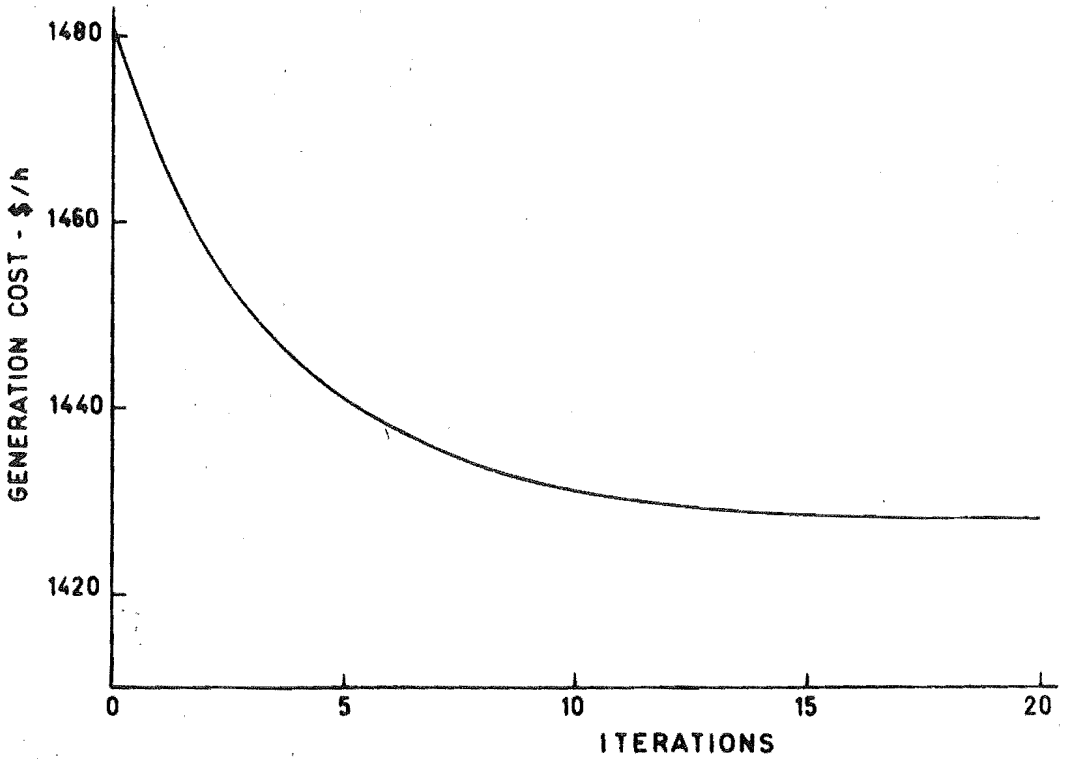

Figure 8.4: Convergence of Generation Cost in AGE System

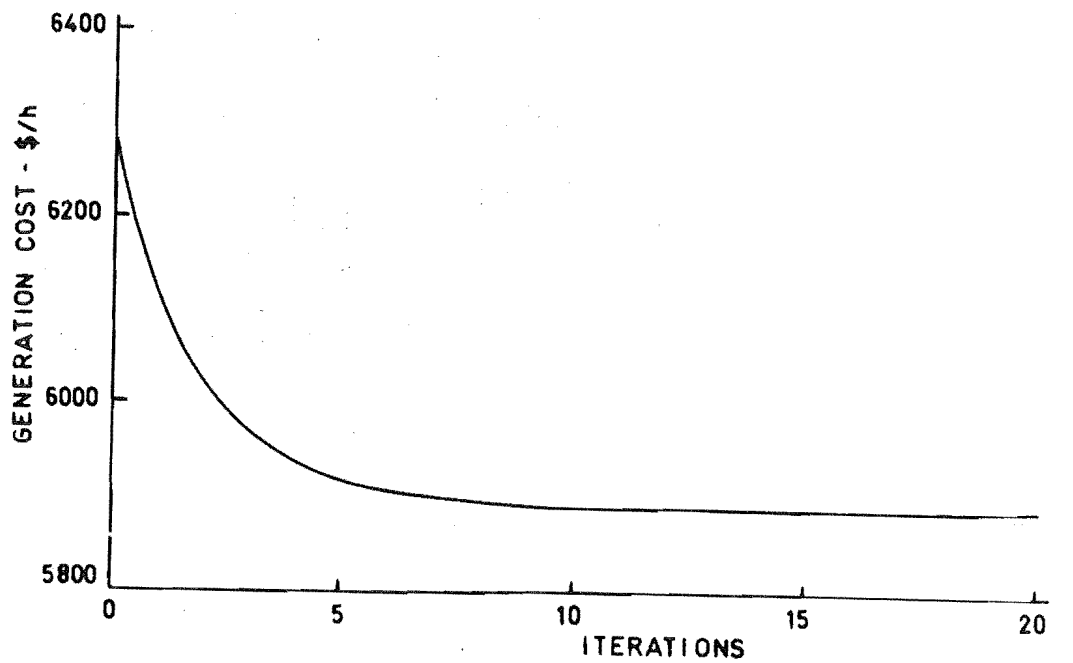

Figure 8.5: Convergence of Generation Cost in 39 Bus System

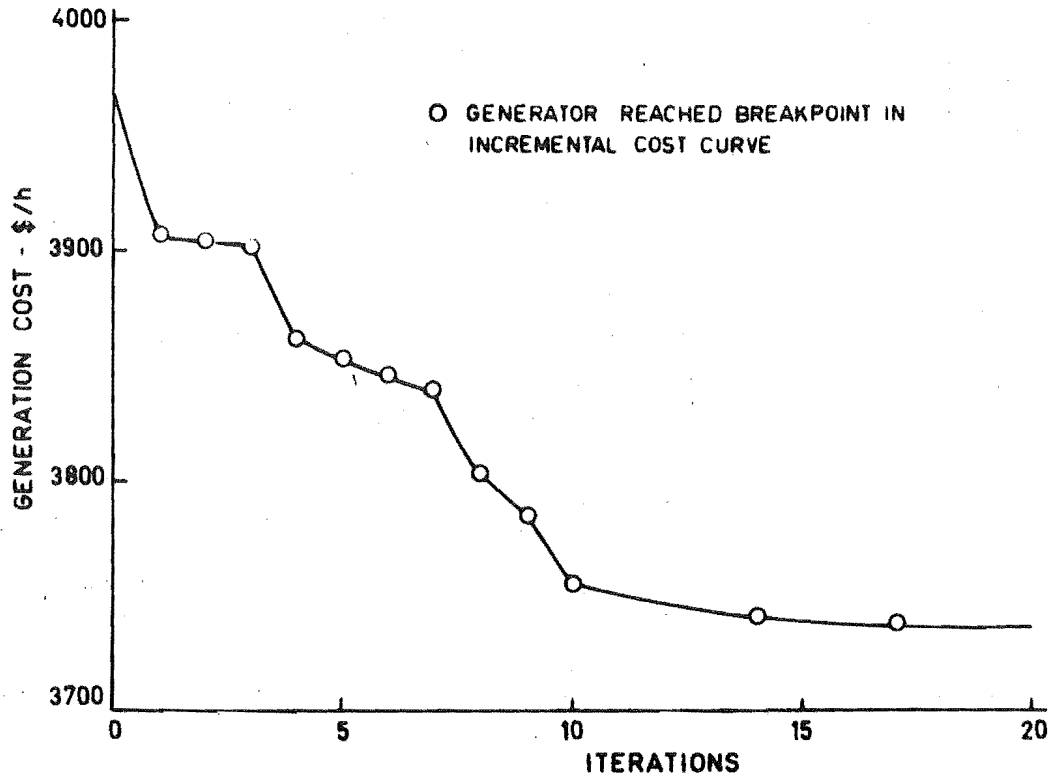

Figure 8.6: Convergence of Generation Cost in IEEE 118 Bus System

SYSTEM	GRADIENT PROJECTION Cost $/hr	Iterations	KIRCHMAYER Cost $/hr	G-S Iterations
AGE	1427.58	29	1427.66	21
39 BUS	5892.35	17	5892.29	28
IEEE	3736.00	35	3735.91	60

Gradient projection tolerance = .01 $/MWHR

Kirchmayer's G-S iteration tolerance = 1 MW

Kirchmayer's lamda iteration tolerance = 0.1 MW

Table 8.5: Summary of Convergence Data.

8.4.2.2 Convergence Tolerance

The gradient projection conditions for an optimum are that the projection of the gradient onto the active constraints should be a null vector, and that none of the active constraints should be able to be deactivated. In practice it is necessary to terminate the iterative procedure when the components of the projected gradient become less than a certain tolerance.

For situations without line constraints Kirchmayer's iterative method has also been applied and the schedules obtained have been compared with those of the gradient projection method (Table 8.5). With a gradient tolerance of .01 $/MW.hr the generator outputs usually agree to within a MW except for isolated instances in which larger errors occur on generators which operate on very flat incremental cost segments. However, the actual total cost of generation invariably agrees to within 0.1 $/hr and this is quite satisfactory for practical purposes.

8.4.2.3 Effect of Multi-Segment Incremental Cost Curves

It is important that the convergence of the gradient projection method should not be significantly impaired by multi-segment representation of the generator incremental cost curves. In the gradient projection method the calculation of the optimum step length assumes a constant quadratic cost function (section 8.6.3). Thus, on each iteration the break points in the generator incremental cost segments are temporarily imposed as generation limits.

The effects of multi-segment representation of the generator incremental cost curves are shown by the convergence of the total generation cost in the IEEE system in figure 8.6. In the early iterations the changes in the generator powers are frequently limited by the break points in the generator incremental cost curves. As a result the total generation cost does not decrease as smoothly as it did for the AGE and 39 Bus systems. (These systems have only single segment representation.) However, the multi-segment representation does not cause a significant increase in the calculation per iteration or in the iterations for convergence and this is a definite advantage of the gradient projection method. On the other hand a second order method would suffer quite seriously if multi-segment representation were used, since the matrix of second derivatives would change with the segments.

8.4.3 Illustrative Examples

Some example gradient projection schedules for the 39 bus system are described to illustrate the effects of line limitations on the distribution of generation and line flows. For this study we consider the 39 bus system separated into

two areas A and B as shown in figure 8.10. The generation in area A is lower cost than area B and if no line constraints are imposed (Case I) an economic schedule results in a net flow of 1246 MW from area A to area B.

The effects of a single constraint on a line interconnecting the two areas have been studied by varying the upper limit of line 16-15 from 500 MW (Case II) to 640 MW. A situation with two constraints imposed is also demonstrated. The upper limit on line 16-15 is set at 500 MW and simultaneously a lower limit of 1200 MW is set on the total interchange from area A to area B (Case III).

8.4.3.1 Variation of the Line Limit

The effect of the variation of the MW limit of line 16-15 on the total cost of generation and the generator outputs are shown in figures 8.7 and 8.8. When the constraint is active the total generation cost varies closely as the square of the difference between the constrained line flow and its unconstrained value. Further, while the line constraint is active, the generator outputs vary linearly with the imposed limit. (The graphs for the generators besides those shown were also linear.) The relationships can be explained by considering an example with two independent generators and a single line constraint, as illustrated in figure 8.9. The variation of the line MW limit corresponds to shifting the constraint in figure 8.9 parallel to itself. As this is done the optimum point follows the locus of the point at which the constraint is tangential to a contour. Now, if the losses are neglected the contours are elliptic and the locus described is a straight line. If this argument is extended to include an arbitrary number of generators then we can generally expect the

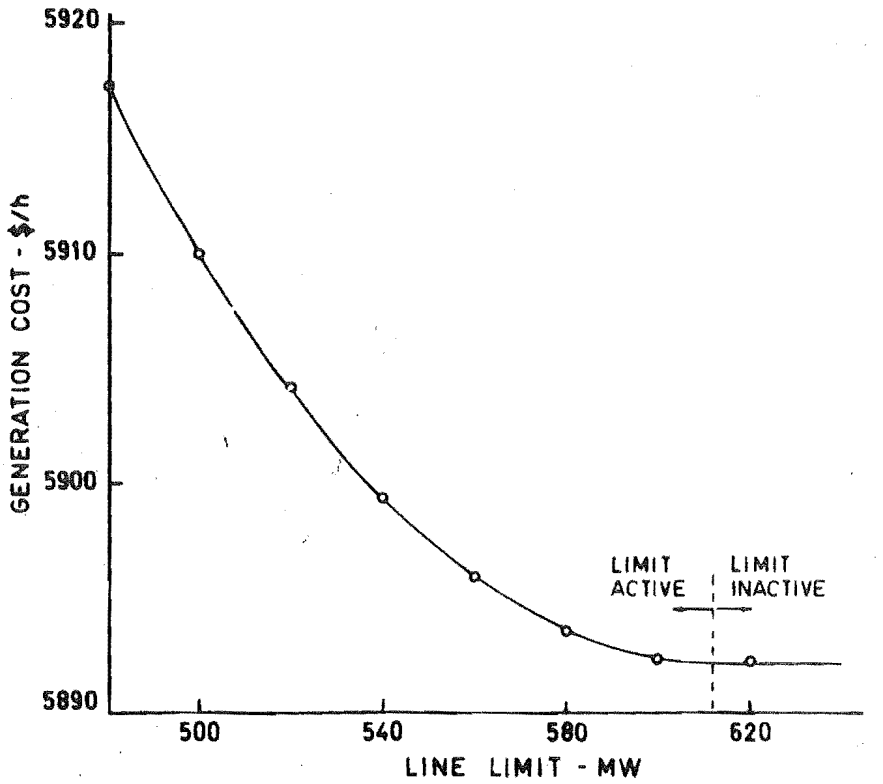

Figure 8.7: Variation of Generation Cost with Loading Limit of Line 16-15 in 39 Bus System

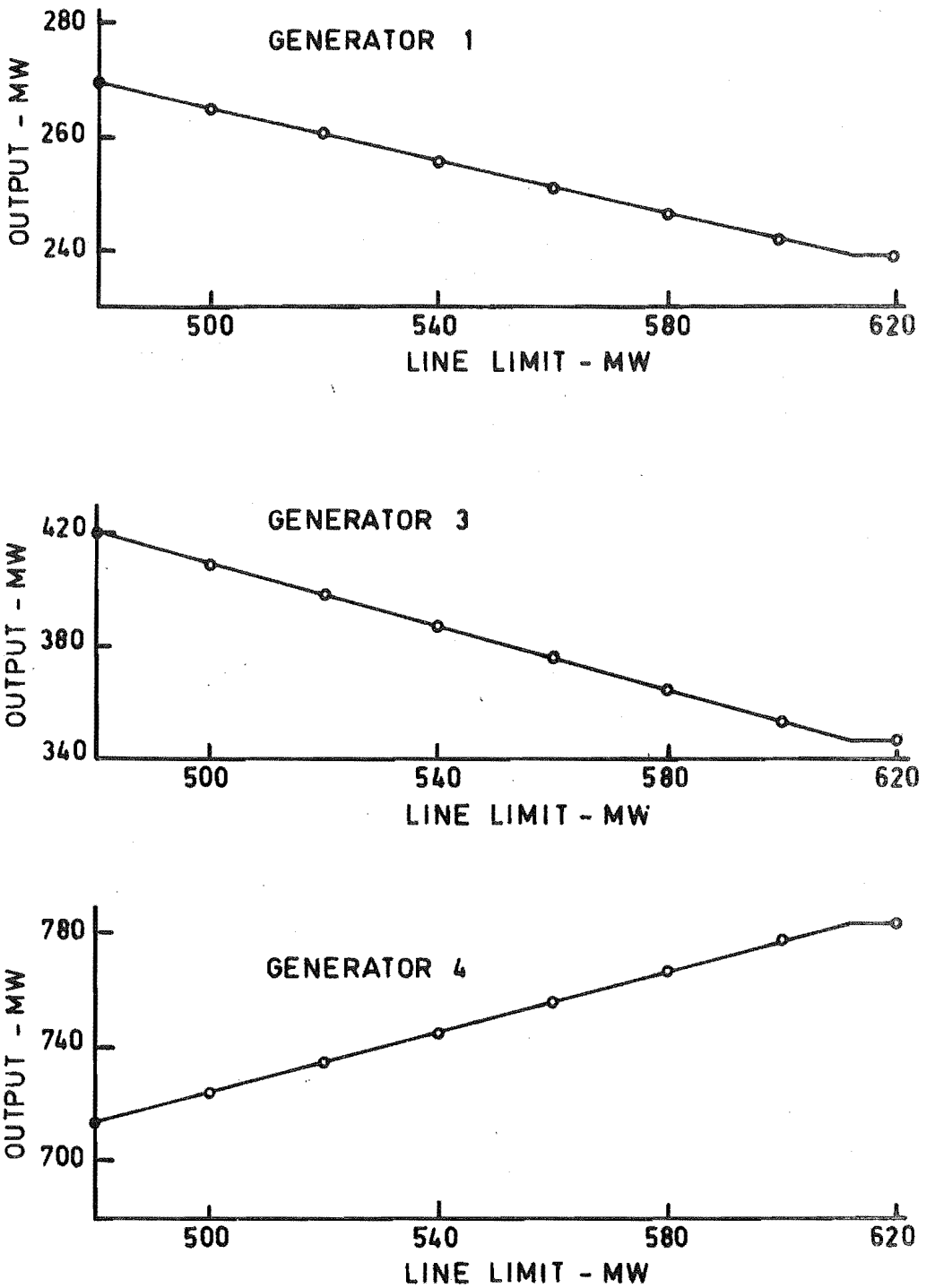

Figure 8.8: Variation of Generator Outputs with Loading Limit of Line 16-15 in 39 Bus System

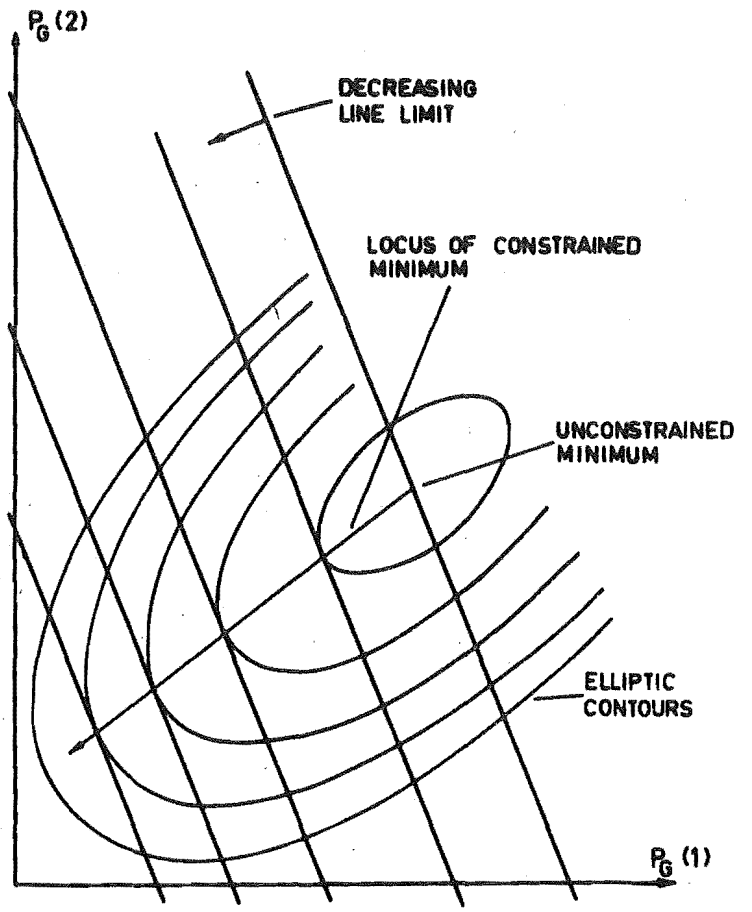

Figure 8.9: Locus of Minimum as Line Limit is Varied

total generation cost to vary as the square and the generation outputs to vary in proportion to an active line limit.

8.4.3.2 Redistribution of Generation and Line Flows

In figure 8.10 the generation and line flows with the unconstrained schedule and the schedule with line 16-15 limited at 500 MW are compared on the system line diagram. It is noticeable that in order to obtain the minimum cost schedule the changes in generation are well distributed throughout the network. The 112 MW reduction in the flow of line 16-15 is only achieved by a considerably larger overall swing in generation, e.g. a combined decrease of 235 MW occurs on generators 4, 5, 6 and 7. The relationship between the generation changes and the branch flows can be obtained for the lines interconnecting area A and area B from the coefficients given in Table 8.6. To calculate the change in line flow for a swing between two generators, the amount of the swing is multiplied by the difference in the generator coefficients. For example, a swing of 100 MW from generator 4 to generator 3 decreases the flow of line 16-15 by:

$$(.543 - (-.04)) \times 100 \text{ MW} = 58.3 \text{ MW}.$$

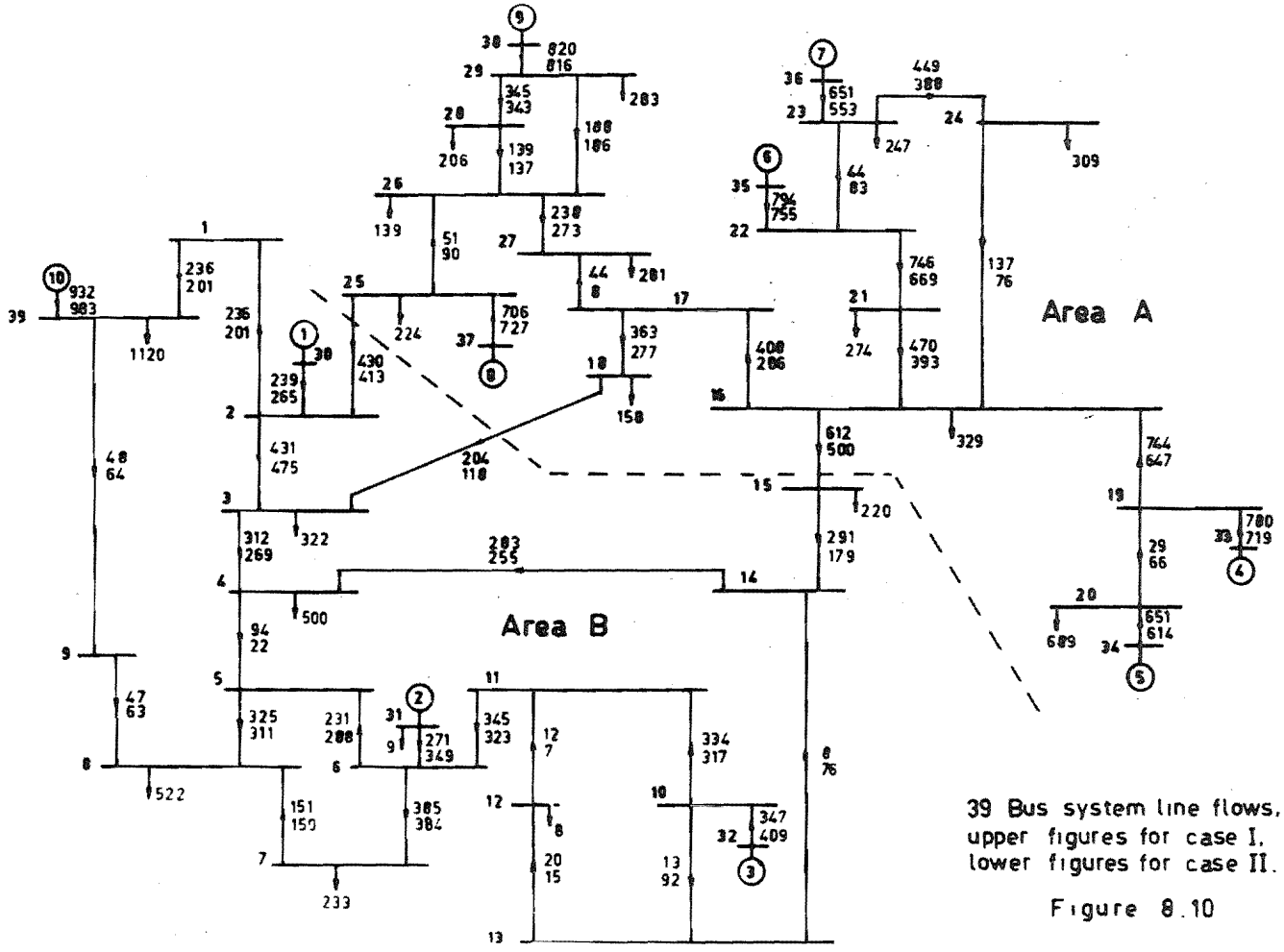
Area A
Area B
39 Bus system line flows,
upper figures for case I,
lower figures for case II.

Figure 8.10

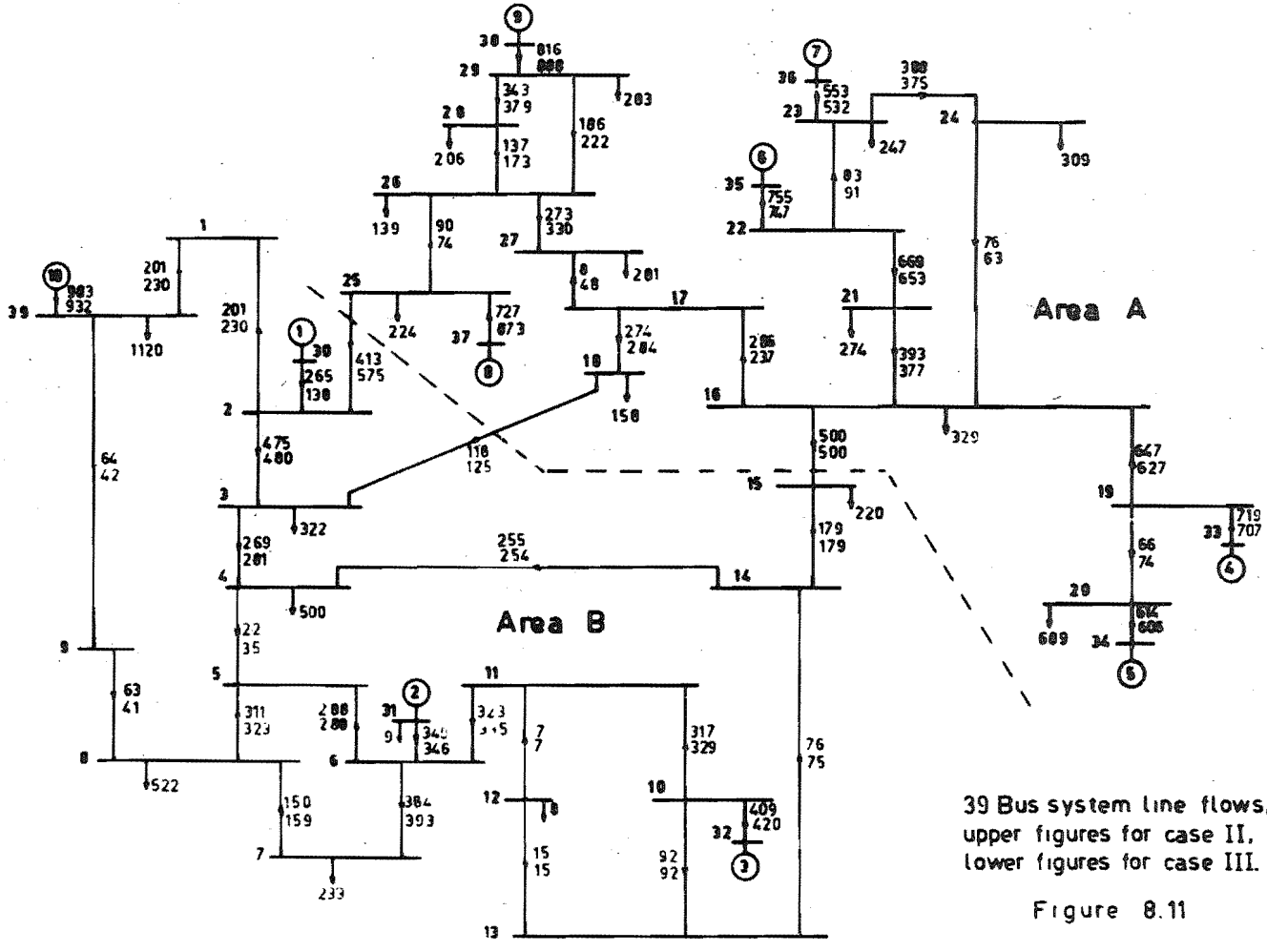

39 Bus system line flows,
upper figures for case II,
lower figures for case III.

Figure 8.11

GENERATOR	LINE 16-15	18-3	25-2
1	.249	-.091	-.157
2	.0	.0	.0
3	-.04	.029	.011
4	.543	.352	.104
5	.543	.352	.104
6	.543	.352	.104
7	.543	.352	.104
8	.271	-.029	.758
9	.355	.204	.441
10	.127	-.047	-.080

Table 8.6: Coefficients of Branch-Generator Power Matrix - S_{BG}

8.4.3.3 Example with Two Constraining Line Limits

When line 16-15 is limited at 500 MW the interchange from Area A to Area B drops from 1246 MW to 1031 MW. The effect of keeping the 500 MW limit on line 16-15 and placing a lower limit of 1200 MW on the total interchange from area A to area B is shown in figure 8.11. In this case the major swing occurs from generators 1 and 10 onto generators 8 and 9. The limit on line 16-15 keeps the remaining generators almost constant. Because line 18-3 has a similar generation dependence to line 16-15 (Table 8.6) it is not able to significantly share in increasing the interchange.

8.4.3.4 Accuracy of the Linearized Line Constraints

The accuracy of the linearized line constraints is examined by comparison with accurate A.C. loadflow results. Figures 8.12, 8.13 and 8.14 compare the A.C. lineflows with

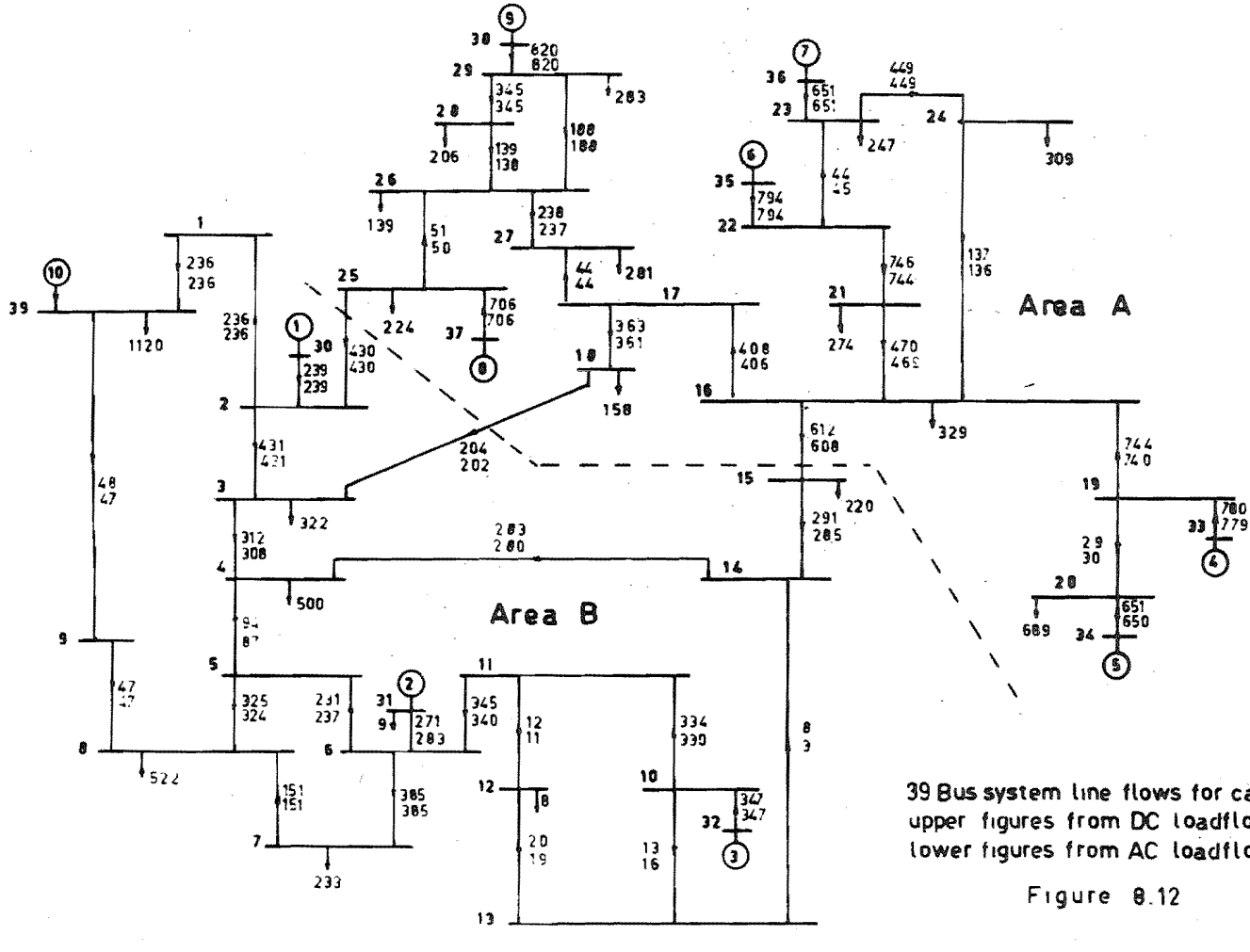

39 Bus system line flows for case I.
upper figures from DC loadflow,
lower figures from AC loadflow.

Figure 8.12

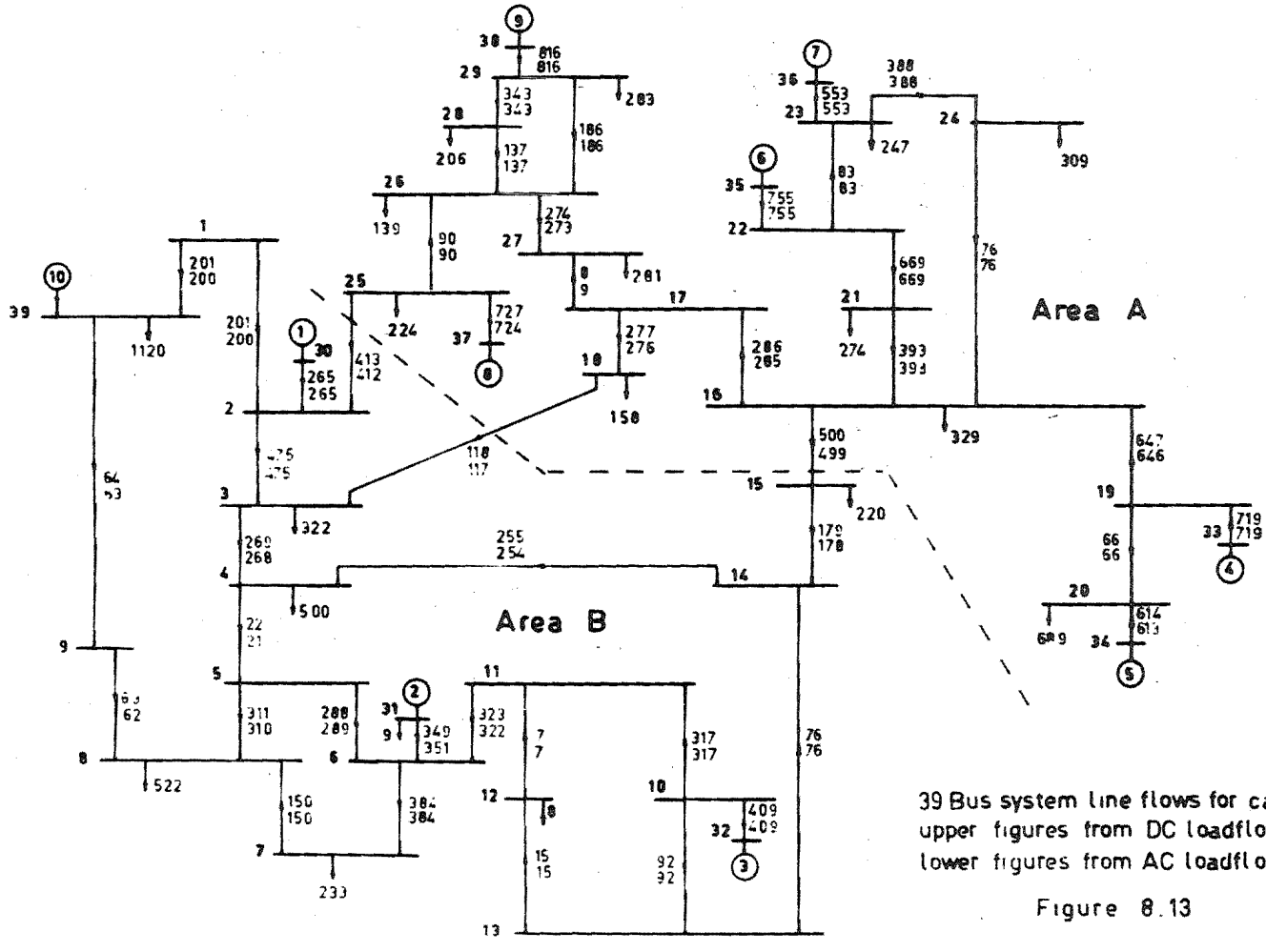

39 Bus system line flows for case II.
upper figures from DC loadflow,
lower figures from AC loadflow.

Figure 8.13

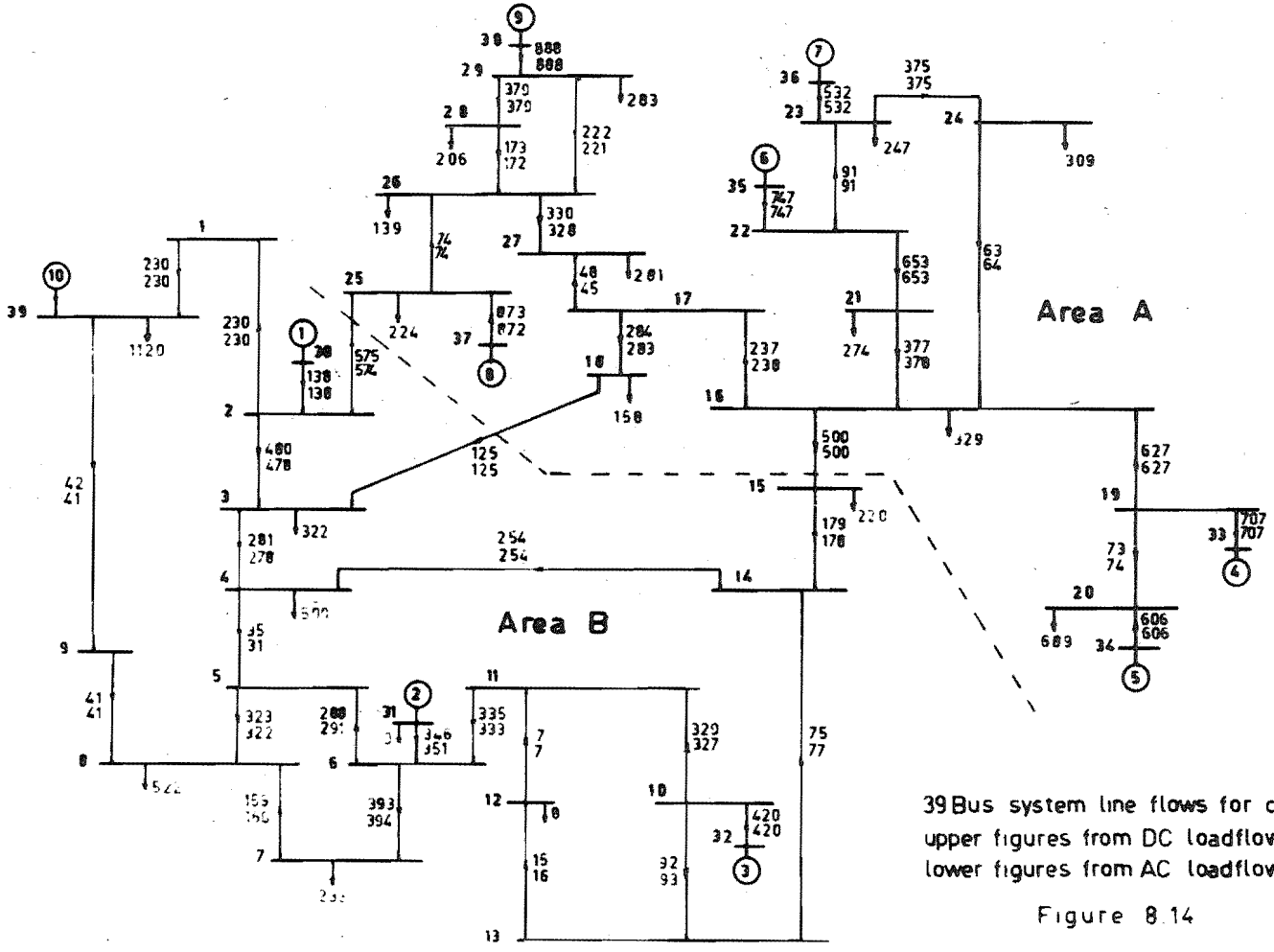

39 Bus system line flows for case III,
upper figures from DC loadflow,
lower figures from AC loadflow.

Figure 8.14

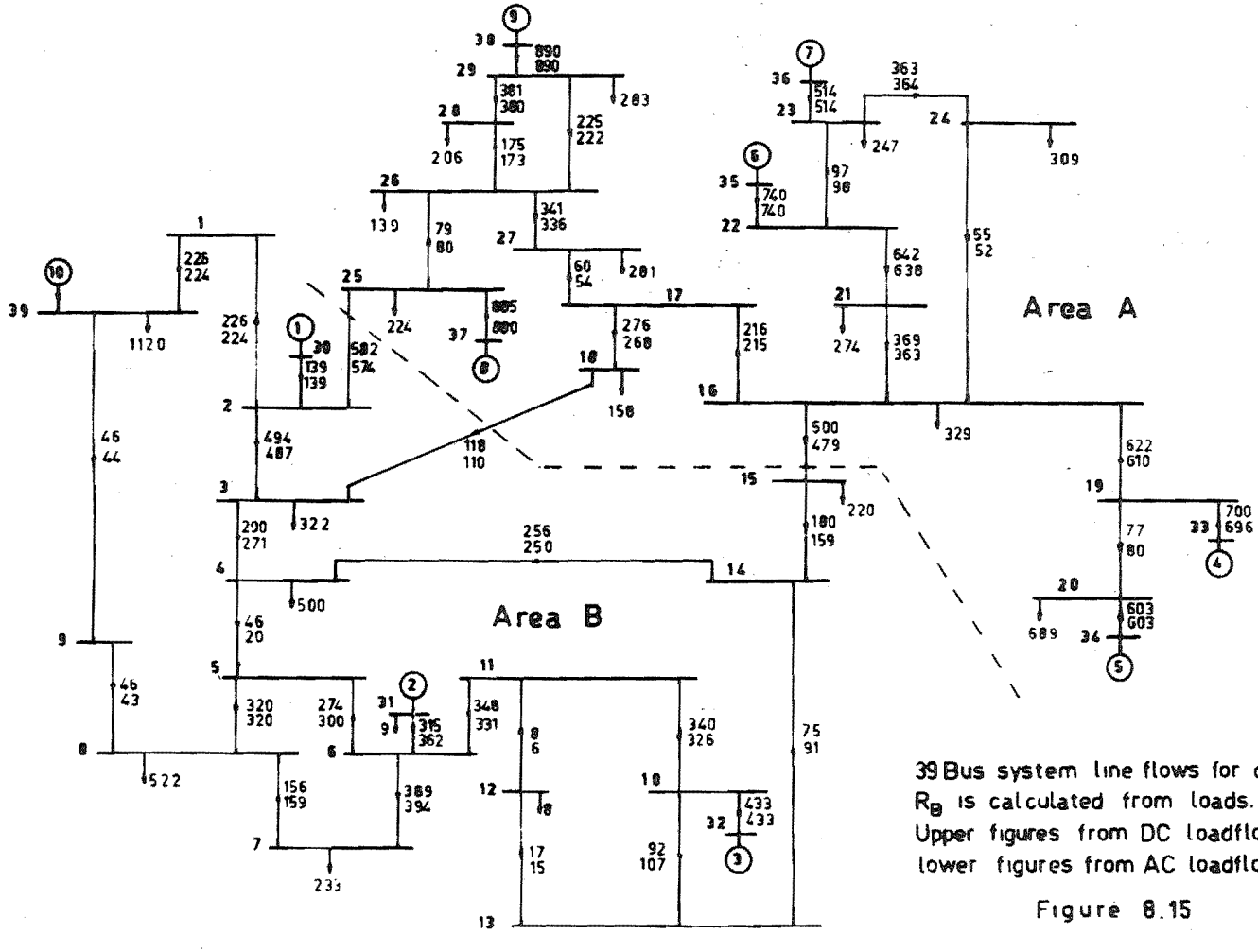

39 Bus system line flows for case III.
R_B is calculated from loads.
Upper figures from DC loadflow,
lower figures from AC loadflow.

Figure 8.15

the lineflows obtained by the linearized expressions. The agreement is very good, usually to within 1 MW. The constant term R_B in the linearized line power equation was calculated from equation (24). The branch flows P_B^0 were obtained from an A.C. loadflow on a manual generation schedule set up for constraint case II. This simulates the on-line measurement of the actual line flows prior to the schedule. Table 8.7 shows the manual schedule and the schedules obtained by the gradient projection method. The gradient projection schedules are significantly different from the case II manual schedule so that a good test of the accuracy of the linearization is obtained.

Generation MW	GRADIENT PROJECTION SCHEDULES				MANUAL SCHEDULES	
	Case I	Case II	Case III	Case III*	CaseII	Case III
1	239	265	138	139	240	240
2 Slack**	292	360	361	373	404	437
3	347	409	420	432	471	405
4	784	723	711	700	721	671
5	654	617	610	603	592	592
6	794	755	747	739	731	701
7	653	554	534	514	593	593
8	709	730	876	885	708	998
9	820	816	888	890	820	820
10	932	983	932	940	932	762
Cost $/hr	5890	5908	5932	5941	5926	5987

* R_B is calculated from the load powers.

** The slack generation is adjusted to meet the exact losses.

Table 8.7: Schedules for the 39 Bus System with Line Constraints

As previously explained, the term R_B may alternatively be calculated directly from the load powers. This has been done for constraint case II I. The resulting schedule is also shown in Table 8.7 and the exact and approximate line flows are compared in figure 8.15. In this case the agreement with the exact line powers is not so good. Further, Table 8.7 shows that a significant increase in generation cost, 9 $/MW.hr, is incurred due to the inaccurate constraint representation. Thus, even though accurate representation of the constraints may not be necessary from a security standpoint, it is necessary if optimum economy is to be obtained.

8.4.3.5 Cost Savings

In current practice it is usual to compute schedules which disregard the line security constraints and to manually adjust the generation if any line constraints happen to be violated. There is no defined procedure for this adjustment. Therefore, it is difficult to assess the savings which would be obtained if the method proposed were used as an alternative. However, as the number of constraints to be satisfied increases it becomes exceedingly more difficult to manually obtain a schedule which satisfies all the constraints, let alone one which is also near to the minimum cost. The savings from the gradient projection method would be greatest in these situations. This remark is illustrated by considering the manual schedules obtained for the 39 Bus system (Table 8.7). When only the constraint of line 16-15 had to be satisfied (case II) the first manual schedule satisfied the constraint and the gradient projection schedule resulted in a saving of 18 $/hr. However, when the interchange constraint was also included (case III) several attempts were required to obtain

an allowable schedule and the gradient projection schedule then gave a saving of 55 $/hr. The savings are substantial when accumulated over the year. For example, if the 18 $/hr was saved for a load condition which typically lasted for 4 hrs per day this would represent a yearly saving of about $26,300.

8.4.4 Computation Requirements

Timing studies have been made on a gradient projection dispatch program written in Fortran IV and executed on an IBM 360/44. For the studies the IEEE system has been considered and the limits of 20 lines have been represented. The line flows have been constrained to lie within a certain MW range of the initial flows. The variation of this allowable range has enabled the effects of the number of active line constraints to be studied. The results are summarized in Table 8.8.

	NO. ACTIVE CONSTRAINTS		ITERATIONS	TIME	TIME/ ITERATION
	GENERATOR	LINE			
Gradient Projection					
100 MW line limits	2	0	36	7.8	.21
50 MW line limits	1	3	34	7.4	.22
10 MW line limits	0	8	26	8.1	.31
Kirchmayer's Method	2	0	60	1.7	.03

Table 8.8: Timing Data for Schedules on IEEE System

There is a beneficial tendency for the number of iterations to decrease when more branch constraints are active since there is also a decrease in the number of degrees of freedom. On the other hand, when more branch constraints are active the average time per iteration is increased due to the increased size of the matrix (N^tN) (Section 8.6.2).

To appreciate the extra computer time which is introduced by the representation of line security constraints, timing studies have also been made using the conventional method to schedule the IEEE system without line constraints. In the conventional method the incremental cost of received power is iterated and starting values must be specified. These starting values were arbitrarily set to 1.0 and 2.0 since in both methods it was assumed that no prior information on the solution was available. The timing results are included in Table 8.8. For Kirchmayer's method the number of iterations shown is the total number of Gauss-Seidel iterations which are performed within the iterations on the incremental cost of received power. When line security constraints are included, the gradient projection method requires 4-5 times longer than the conventional method.

The storage requirement of the gradient projection dispatch program is quite compatible with its use on a small dispatch computer. The dispatch program is dimensioned to handle 20 dispatchable generators and 50 line constraints. It requires less than 28k bytes of core storage.

Very little computation is required to update the S_{BG} coefficients according to the network status. The execution time to calculate the S_{BG} coefficients for the 18 generators in the IEEE system was less than 10s. The program which calculates S_{BG} handles networks with up to 300 nodes and uses less than 40k bytes of core storage.

8.4.5 Further Program Developments

The program which has been developed to date includes a basic version of the gradient projection method which was most appropriate for the immediate task of evaluating its application to generation scheduling. Now that the method has been successfully evaluated the relevant refinements which can be added to further improve the performance of the method have been illuminated. In all, three possible extensions are proposed and these are outlined under separate headings.

8.4.5.1 Automatic Procedure for Finding a Feasible Solution

When line constraints are incorporated, it is necessary to have an initial feasible schedule to start the gradient projection iterative procedure. The present version of the gradient projection program requires that an initial feasible solution be specified in the input data. In the off-line situation this initial solution can be obtained by established procedures such as manual adjustment of the generator outputs along with DC loadflows. However, in the on-line application it would be essential to have some automatic procedure for obtaining the initial feasible schedule. A simple and effective starting procedure for the basic gradient projection method is described in the original paper by Rosen[5]. The inclusion of this extra facility into the present gradient projection program is therefore an extension which would greatly increase its potential for on line application.

8.4.5.2 Recursion Relations to Form the Projection Matrix

In the present version of the program the matrix (N^tN) (Section 8.6) is rebuilt and inverted each time a constraint is activated or deactivated. As shown by the results in section 8.4.4 this process requires a major proportion of

computation time when the number of active constraints increases. It is possible to make a large saving in computation by using recursion relations to derive the new inverse matrix in terms of the old inverse matrix when a constraint is activated or deactivated. Instead of requiring approximately $q^2m/2$ multiplications for the formation of N^tN and $q^3/2$ multiplications for its inversion, the recursion relations allow a constraint to be dropped from $(N^tN)^{-1}$ with approximately q^2 multiplications and a constraint to be added with approximately $3qm$ multiplications. (q = number of active constraints, m = number of constraints.) Full details for including the recursion relations into the method are given in Rosen[5].

8.4.5.3 Linearly Dependent Constraints

For the inverse of N^tN to exist the active constraints which form the columns of N must be linearly independent. In the generation scheduling problem a set of active constraints will be linearly dependent if the constraints on all the branches connected to a single bus, or if the constraints on parallel branches are simultaneously activated. To extend the present program to deal with such situations it is necessary to ensure before a constraint is added to N that it is linearly independent of the existing constraints. In Rosen[5] it is shown that this will be so if:

$$P_i \, n_{i+1} \neq 0 \tag{27}$$

where

P_i is the projection matrix on iteration i

n_{i+1} is a column vector of the constraint to be added at iteration i+1.

It should be a straightforward matter to include this test so that the present program can be extended to deal with the situation of linearly dependent constraints.

8.5 CONCLUSIONS

A method for the economic dispatch of power has been developed and evaluated. The main advantage of the method is its ability to account for line security limits. This facility may lead to improved reliability and economy in system operation. The proposed method of dispatch does not require a great deal more computation or system-state data than the established method of dispatch. Thus, the method should be within the capability of many existing dispatch-office computer systems.

The present study has been limited to a single system. Further work is required to develop methods for the dispatch of interconnected systems[10,11] with line security constraints represented.

8.6 APPENDIX - THE GRADIENT PROJECTION METHOD

In the following description of the gradient projection method we are mainly concerned with explaining how the algorithm works. Therefore, the important theoretical results which form the basis of the algorithm are stated and explained but they are not mathematically proven. The mathematical proofs are given in the original paper by Rosen[5]

The method was originally described as a maximization method and for continuity this convention is retained. To apply the method to the generation scheduling problem we simply maximize the negative of the cost function.

8.6.1 Geometrical Problem Formulation

The maximization of a function with m control variables, $f(x_j)$, $j = 1,2,\ldots,m$, is considered. Geometrically, $f(x)$ exists in an m dimensional Euclidean space of the variables x, which is denoted by E_m. We assume that the variables x are subject to k linear inequalities of the form,

$$n_i^T x \leqslant b_i \qquad (i = 1,2,\ldots,k) \tag{28}$$

where the m dimensional vector n_i has been normalized, so that,

$$|n_i|^2 = n_i^T n_i = 1 \tag{29}$$

The constraints in (28) form a convex region R in E_m which is assumed to be bounded, therefore, $k \geqslant m+1$. The m-1 dimensional manifold defined by $n_i^T x = b_i$ is a hyperplane which is denoted by H_i. The unit vector n_i is orthogonal to H_i and is directed so that if it originates in H_i it points out of the region R (see figure 8.16).

8.6.2 Projection of the Gradient

The gradient projection method is based upon the projection of the gradient $g(x)$ on a subspace of E_m given by the intersection of the hyperplanes which contain the point x.

Consider, at the point x, that q constraints are active, i.e. we have,

$$n_i^T x = b_i \qquad (i = 1,2,\ldots,q) \tag{30}$$

Define the m x q matrix,

$$N_q = (n_1, n_2, \ldots, n_q) \tag{31}$$

Assuming the unit vectors $n_1, n_2, \ldots, n_q$ are linearly independent, then the q x q symmetric matrix $(N_q^T N_q)$ is

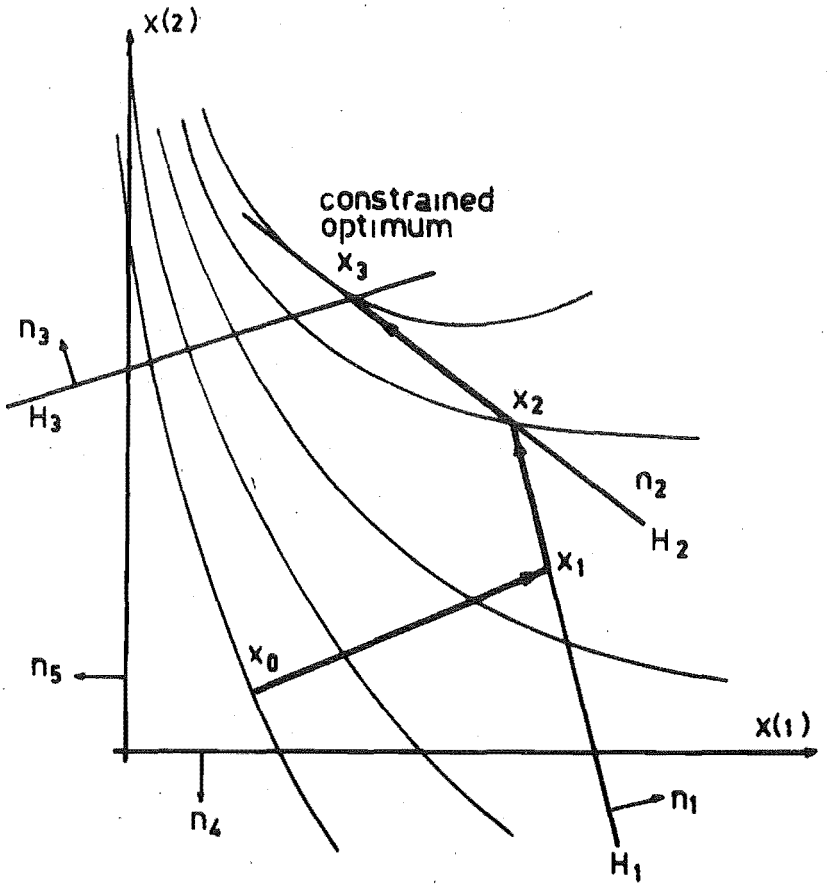

Figure 8.16: Two Dimensional Example of Gradient Projection Trajectory

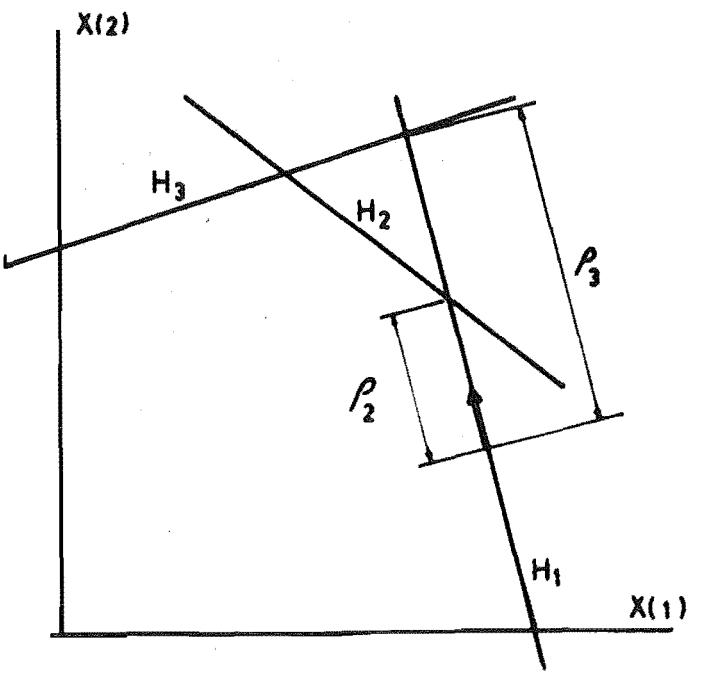

Figure 8.17: Determination of Optimum Step Length

non-singular and its inverse exists. An important theorem of the gradient projection method is; the projection matrix,

$$P_q = (I - N_q(N_q^T N_q)^{-1} N_q^T) \tag{32}$$

takes any vector, which originates at x, into the intersection of the q hyperplanes defined by x and N_q. (The hyperplane H_i is uniquely defined by the point x and its normal n_i.)

The significance of this result is that by projecting the gradient at x according to,

$$z = P_q\, g(x)/|P_q g(x)| \tag{33}$$

then a feasible direction for increasing f(x) is given by z.

8.6.3 Determination of Optimum Step Length

Once the projected gradient z is determined as a feasible direction for increasing f(x) we have to find the step length for which f(x) is a maximum. That is, we require the value of τ which maximizes $f(x+\tau z)$.

The upper limit on τ is the distance along z to the closest inactive hyperplane, and it is determined as follows (see figure 8.17). Let ρ_i be the distance along z to the inactive hyperplane H_i. From (28),

$$n_i^T(x_i + \rho_i z) = b_i \qquad (i = q+1, q+2, \ldots, k) \tag{34}$$

and therefore,

$$\rho_i = (b_i - n_i^T x)/n_i^T z \tag{35}$$

Let H_b be the closest inactive hyperplane in the direction z, then,

(36) $$\rho_b = \min\{\rho_i\} \quad \text{for} \quad \rho_i \geqslant 0$$

The maximization of $f(x+\tau z)$ is therefore constrained by,

(37) $$0 \leqslant \tau \leqslant \rho_b$$

It now remains to find the actual value of τ for which $f(x+\tau z)$ is maximized. Let the point at which z intersects H_b be given by,

(38) $$x_b = x + \rho_b z$$

If the gradient along z at x_b is positive, i.e.

(39) $$g(x_b).z > 0$$

$f(x+\tau z)$ has a maximum at the intersection of H_b and the optimum step length is,

(40) $$\tau_m = \rho_b$$

In this case the variables x are updated by,

(41) $$x_{NEW} = x + \rho_b z$$

and the hyperplane H_b is added to the constraint basis.

Alternatively, if the gradient at x_b is negative, i.e.

(42) $$g(x_b).z < 0$$

$f(x+\tau z)$ has a maximum between x and the intersection of z with h_b. If we assume that $f(x+\tau z)$ is quadratic the gradient varies linearly along z and the maximum occurs at,

(43) $$\tau_m = \rho_b.g(x).z/(g(x).z - g(x_b).z)$$

In this case the variables x are updated by,

$$x_{NEW} = x + \tau_m z \tag{44}$$

and the constraint basis is unchanged.

8.6.4 Conditions for an Optimum

The conditions are given for the global maximum of a concave function f(x). The region R will have an interior global maximum of f(x) at the point x_0 if, and only if,

$$g(x_0) = 0. \tag{45}$$

If g(x) does not vanish in the interior of R then a constrained global maximum lies on the boundary of R. In this case the following conditions apply.

Let x_0 be a boundary point of R which lies exactly on q, $1 \leqslant q \leqslant m$, linearly independent hyperplanes. The point x_0 is a constrained global maximum of f(x) if, and only if,

$$P_q g(x_0) = 0 \tag{46}$$

and

$$r = (N_q^T N_q)^{-1} N_q^T g(x_0) \geqslant 0. \tag{47}$$

If the condition in (46) is true, f(x) cannot be increased while x is confined to the intersection of the hyperplanes H_i, i = 1,2,...,q. The condition in (47) ensures against the situation in which a further increase in f(x) may be obtained by dropping a hyperplane from the constraint basis. The vector r has elements r_i, i + 1,2,...,q, and can be interpreted as follows.

If (32) and (47) are substituted into (46) we obtain,

$$g(x_0) = N_q r \tag{48}$$

This can be expanded as,

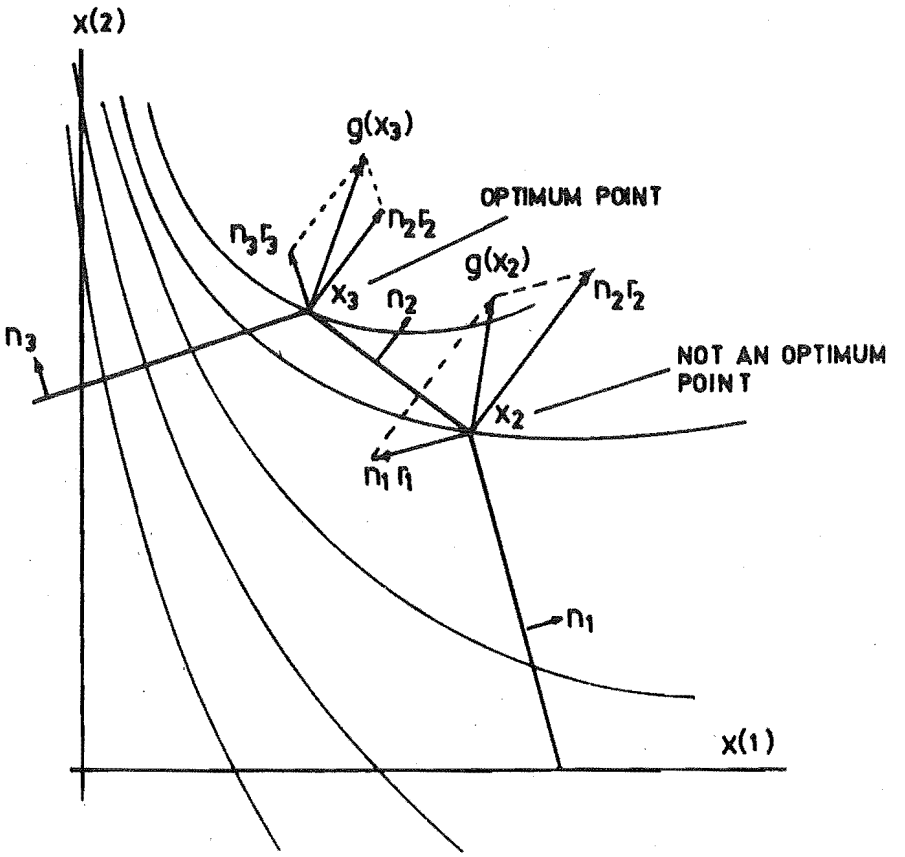

Figure 8.18: Two Dimensional Example Illustrating Conditions for a Constrained Optimum

$$g(x_0) = n_1 r_1 + n_1 r_2 \ldots n_q r_q \tag{49}$$

Equation (49) shows that when x_0 satisfies the condition in (46) the gradient $g(x_0)$ is generated by the normals n_i, $i = 1,2,\ldots,q$, according to the elements of r. For the two dimensional example of figure 8.16 the geometrical interpretation of r at the points x_2 and x_3 is shown in figure 8.18. If $r_i > 0$ the vector $n_i r_i$ points out of the feasible region but if $r_i < 0$ $n_i r_i$ points into the feasible region. The geometrical interpretation of the condition in (47) is that it requires all the vectors $n_i r_i$ to point out of the feasible region, otherwise, if there is any one vector which points into the feasible region a further increase in f(x) can be obtained by dropping the hyperplane corresponding to this vector from the constraint basis.

8.6.5 The Gradient Projection Algorithm

The procedure of the gradient projection algorithm is as follows.

1. An initial feasible solution of x is accepted.
2. The initial constraint basis is set up.
3. The gradient g(x) is calculated.
4. The projected gradient is calculated, i.e. $P_q g(x)$. If $P_q g(x) \neq 0$ step 5 is skipped.
5. The optimum is reached if no active constraint can be dropped from the basis. Otherwise, a constraint is dropped from the basis and a new projection of the gradient is made.
6. The projected gradient is normalized,

$$z = P_q g(x) / |P_q g(x)| .$$

7. The distance ρ_b to the nearest inactive hyperplane, H_b is calculated.

8. The optimum step length τ_m is calculated. The hyperplane H_b is added to the constraint basis if $\tau_m = \rho_b$.

9. A new value of x is calculated from,

$$x_{NEW} = x + \tau_m z.$$

10. Step 3 is returned to.

REFERENCES

*1. L.K. Kirchmayer, Economic Operation of Power Systems , Wiley, New York, 1958.

*2. H.W. Dommel, W.F. Tinney, "Optimal Power Flow Solutions", IEEE, PAS 87, 1968, pp. 1866-1876.

3. C.M. Shen, M.A. Laughton, "Determination of Optimum Power System Operating Conditions under Constraints", Proc. IEE, vol. 116, 1969, pp. 225-239.

4. C.M. Shen, M.A. Laughton, "Power System Load Scheduling with Security Constraints using Dual Linear Programming", Proc. IEE, vol. 117, 1970, pp. 2117-2127.

5. D.W. Wells, "Method for Economic Secure Loading of a Power System", Proc. IEE, vol. 115, 1968, pp. 1190-1194.

*6. J.M. Undrill, "Power-system Dispatch-office Automation Functions", N.Z. Eng., 1972, pp. 164-170.

7. IEEE Committee Report, "Present Practices in Economic Operation of Power Systems", IEEE, PAS 90, 1971, pp. 1768-1775.

8. J.B. Rosen, "The Gradient Projection Method for Non-linear Programming. Part I. Linear Constraints", J. Soc. Indust. Appl. Math., vol. 8, 1960, pp. 181-217.

9. R.P. Merrill, "Gradient Projection 7090", Shell Development Co., Emeryville, Calif., Tech. Rept. 219-62, 1962.

*10. L.K. Kirchmayer, Economic Control of Interconnected Systems , Wiley, New York, 1959.

11. J.F. Aldrich, H.H. Happ, J.F. Leuer, "Multi Area Dispatch", IEEE, PAS 90, 1971, pp. 2661-2670.

C H A P T E R 9

SUMMARY AND CONCLUSIONS

The increasing size and complexity of problems in the planning, design and operations of power systems have necessitated an evolutionary development and improvement of methods for power system network analysis. The major contributions which have been made by the thesis in this area are summarized as follows:

i) Computational Techniques for Network Representation and Solution.

The LINKNET structure has been developed as a general purpose technique for efficient computer representation of networks (Chapter 2). It has been a valuable tool for the programming of a wide variety of network algorithms in this thesis.

An efficient program for solving large sets of network equations has been constructed using ordered triangularization techniques (Chapter 3). The program has been developed primarily as a tool for network developments within the thesis. However, a novel feature of the program which is of general interest is the use of the LINKNET structure as a simple and effective way for storing and processing only the non-zero matrix elements.

ii) General Method for Unbalanced Fault Analysis.

A highly effective piecewise method for analyzing general types of unbalanced fault has been developed (Chapter 4). The method uses considerably less computer time and storage than methods previously presented. With the piecewise method simultaneous faults and line open unbalances can now

be handled with the same computational ease as the standard single phase short circuit.

iii) Improvement in the Convergence of the Nodal Iterative Loadflow.

A modification for improving the convergence of the nodal iterative loadflow has been developed (Chapters 5 and 6). The modification supplements the normal or "primary" bus adjustments with "secondary" adjustments on adjacent buses. It gives significant reductions in computation time and improved reliability in the presence of series branches with low or capacitive impedance. The modification can be included into existing nodal iterative loadflow programs with little increase in complexity or storage.

iv) Simplified Methods for Economic Dispatch.

A simplified and improved method has been developed for calculating transmission loss coefficients (Chapter 7). The method is based upon the separation of losses into magnitude and angle dependent components and the use of the D.C. loadflow to relate bus angles to generator outputs. An extensive evaluation with practical systems has shown that the D.C. loadflow loss formula gives losses and incremental losses which are well within the accuracy required for economic dispatch. The computational requirements of the method are low enough to enable the loss formula to be updated on-line according to actual network conditions.

The D.C. loadflow approximation has also been applied to develop an economic dispatch method which recognizes line security constraints (Chapter 8). The method effectively overcomes the major limitation of the classical method with only a small increase in computation and system-state data

requirement. The proposed method gives power control centers with only moderate sized dispatch computers the potential for recognizing line security limits in their economic dispatch and thereby obtaining improved security and economy in system operation.

The developments which have just been summarized contribute a valuable overall improvement in the practical network methods which are used for power system analysis. In other words, the basic aim of the thesis (section 1.3) has been achieved.